Dissertation
submitted to the
Combined Faculties for the Natural Sciences and for Mathematics
of the Ruperto-Carola University of Heidelberg, Germany
for the degree of
Doctor of Natural Sciences

presented by
Nadine Hertrich, M.Sc. Molecular Biosciences
born in Bad Friedrichshall, Germany
Oral examination on 12.12.2014

Proteolytic processing of the merozoite surface protein 1 from *Plasmodium falciparum*: Implications on its structure and function during invasion

Referees: Prof. Dr. Michael Lanzer
Prof. Dr. Hermann Bujard

„S' Lebe isch koi Schlotzr“

Schwäbisches Grundgesetz §4

Abstract

The most virulent form of malaria is caused by the apicomplexan parasite *Plasmodium falciparum*, which invades and replicates within erythrocytes. The most abundant surface protein of merozoites and a prime vaccine candidate is the merozoite surface protein 1 (MSP-1). In the course of merozoite maturation and invasion, MSP-1 is proteolytically processed several times. The parasite's subtilisin-like protease PfSUB1 converts the MSP-1 precursor into MSP-1_{83}, MSP-1_{30}, MSP-1_{38} and MSP-1_{42}. This primary processing may be essential for priming the malaria parasites for erythrocyte invasion and thus merozoite infectivity.

The aim of this study was to unravel the biological significance of primary processing for MSP-1 function using a number of approaches. PfSUB1 cleavage sites within MSP-1 were identified *in silico*. Recombinant proteins with mutations in the respective sites were generated to investigate their *in vitro* cleavage susceptibility by exposure to recombinant PfSUB1. Some cleavage sites, in particular between MSP-1_{38} and MSP-1_{42}, revealed redundant PfSUB1 recognition sequences, suggesting an important role of processed MSP-1. Mutation of all PfSUB1 cleavage sites rendered the protein entirely refractory to processing by the protease.

To study the direct effect of primary processing on invasion, the binding of the MSP-1 precursor as well as its processed fragments to erythrocytes was investigated. Only PfSUB1-cleaved MSP-1 bound to fresh erythrocytes via the MSP-1_{83} and MSP-1_{38} fragments. This attachment was inhibited by MSP-1 specific antibodies but not by heparin or enzymatic treatment of erythrocytes, indicating MSP-1 to be a common receptor for invasion.

In another approach, the effect of non-cleavable MSP-1 on parasite viability was investigated. Various cleavage-deficient versions of full length *msp-1f* (FCB1 strain) were expressed in *P. falciparum* 3D7 parasites which were analysed for their growth and MSP-1 expression. Dose-dependent regulation of the latter was

accomplished via the blasticidin co-selection system. Indeed, transgenic MSP-1F correctly localised to the merozoite surface. However, primary processing of MSP-1 was only observed for wildtype MSP-1F, while the mutant versions remained as refractory to cleavage *in vivo* as previously found *in vitro*. Although only low levels of non-cleavable MSP-1F were tolerated in transgenic parasites, they displayed a significant growth defect.

In summary, this study shows that PfSUB1 cleavage of MSP-1 is vital for merozoite maturation and infectivity and thus for parasite viability. A key function of processed MSP-1 is the direct binding to erythrocytes, thereby providing a prerequisite for merozoite invasion and replication.

Zusammenfassung

Die virulenteste Form der Malaria wird durch den Apicomplexa-Parasiten *Plasmodium falciparum* hervorgerufen, die Erythrozyten invadieren und sich dort vermehren. Ihr häufigstes Oberflächenprotein und einer der wichtigsten Impfstoffkandidaten ist das Merozoitenoberflächenprotein 1 (MSP-1). Im Laufe der Merozoitenreifung und Invasion wird MSP-1 mehrfach geschnitten. Die parasitische subtilisin-ähnliche Protease PfSUB1 wandelt das MSP-1-Vorläuferprotein in MSP-1_{83} MSP-1_{30}, MSP-1_{38} und MSP-1_{42} um. Diese primäre Prozessierung trägt potenziell zur Vorbereitung der Malaria-Parasiten für die Erythrozyten-Invasion und damit zur Infektiosität der Merozoiten bei.

Ziel dieser Studie war die Entschlüsselung der biologischen Bedeutung der primären Prozessierung für die Funktion von MSP-1. PfSUB1-Schnittstellen innerhalb von MSP-1 wurden *in silico* identifiziert. Rekombinante Proteine mit Mutationen an den entsprechenden Stellen wurden generiert, um deren Prozessierbarkeit durch PfSUB1 *in vitro* zu untersuchen. Interessanterweise verfügen einige Schnittstellen, insbesondere jene zwischen MSP-1_{38} und MSP-1_{42}, über redundante PfSUB1 Erkennungssequenzen, was auf eine wichtige Rolle von prozessiertem MSP-1 deutet. Die Mutation aller PfSUB1-Schnittstellen machte das Protein resistent gegen jegliche PfSUB1-Prozessierung.

Zur Aufklärung der direkten Wirkung der primären Prozessierung auf die Invasion wurde die Bindung des MSP-1-Vorläuferproteins sowie der prozessierten Fragmente an Erythrozyten untersucht. Nur PfSUB1-prozessierte MSP-1 Fragmente konnten an frische Erythrozyten binden und zwar über MSP-1_{83} und MSP-1_{38}. Diese Bindung konnte durch MSP-1-spezifische Antikörper gehemmt werden, nicht aber durch Heparin oder enzymatische Behandlung von Erythrozyten, was auf MSP-1 als gängigen Rezeptor für die Invasion hinweist.

Des Weiteren wurde die Wirkung von nicht-schneidbarem MSP-1 auf die Lebensfähigkeit der Parasiten untersucht. Verschiedene nicht-prozessierbare Versionen von MSP-1 wurden in *P. falciparum* Parasiten exprimiert und deren

Auswirkungen auf Wachstum und MSP-1-Expression analysiert. Die Dosis-abhängige Regulation der Expression wurde mit Hilfe des Blasticidin Co-Selektionssystems erreicht. Die transgenen MSP-1F-Versionen lokalisierten ordnungsgemäß zur Merozoitenoberfläche. Jedoch wurde die primäre Prozessierung von MSP-1 nur bei Wildtyp-MSP-1F beobachtet, während die mutierten Versionen *in vivo* ebenso ungeschnitten blieben wie *in vitro*. Obwohl nur geringe Mengen an nicht-prozessierbarem MSP-1 in den transgenen Parasiten toleriert wurden, zeigten diese einen signifikanten Wachstumsdefekt.

Die vorliegende Studie zeigt, dass die primäre Prozessierung von MSP-1 durch PfSUB1 für die Reifung und Infektiosität von Merozoiten notwendig ist und damit für deren Lebensfähigkeit. Eine Schlüsselfunktion des prozessierten MSP-1 spielt dabei die direkte Bindung an Erythrozyten, die eine Voraussetzung für Invasion und Replikation der Merozoiten darstellt.

Acknowledgements

I would like to thank **Prof. Michael Lanzer** for being my first examiner and giving me the opportunity to work in his laboratory in the Centre for Infectious Diseases. Furthermore, I would like to express my gratitude to **Prof. Herman Bujard** for being the second examiner of this thesis, an excellent TAC member always keen to discuss all kinds of topics, and for funding my work.

Additionally, I would like to thank **Dr. Ann Kristin Müller** and **Dr. Marcel Deponte** for being my examiners, but most of all for their fruitful discussions and support throughout my thesis. Likewise, I appreciate the help and support from **Prof. Friedrich Frischknecht**.

Particular thanks go to **Dr. Christian Epp** for giving me the opportunity to work on this project, his patience with me in countless discussions and the chance to work independently.

I would also like to thank our collaboration partners **Prof. Michael Blackman** and **Sujaan Das** for their helpful input to our shared project.

I would like to acknowledge all members of the Epp and Lanzer group, who gave me a good and inspiring time throughout my thesis: **Kristin Fürle** especially for her help with the ÄKTA system, **Tanja Marzluf, Karl Heinonen, Anja Jäschke, Elisa Kless, Alessia Valdarno, Yvonne Maier, Nicole Kilian, Carolin Geiger, Sebastiano Bellanca, Sonia Molliner, Martin Dittmer, Hani Kartini Agustar, Sirikamol Srismith, Carine Djuika, Felix Müller, Marvin Haag, Eike Pfefferkorn,** and former members of the lab that are not mentioned here.

Many thanks go to **Miriam Griesheimer** for her excellent help in organising my thesis and always having an open ear! In addition, I would like to thank **Stefan Prior** and **Marina Müller** who always had an open ear for me over many coffees and maintained a cheerful atmosphere in the cell culture. I enjoyed it a lot!

Thank you **Katharina Ehrhard** and **Sophia Deil** for being the 'sunshines' in the lab, the endless discussions about PhD projects and for being friends beyond

the lab. The same is true for all the people from the Müller lab, especially **Britta Nyboer** and **Julia Sattler** who helped in any ways they could.

Lots of thanks to all of my friends who have stayed with me throughout my whole thesis and who are hopefully going to stay with me for years to come!

Thank you **Julia Klermund** for making life so much fun during the last couple of years!

I immensely appreciate **Kathrin Leppek's** help with her enormous knowledge, for proofreading my thesis, but moreover for being a dear friend since the start of our studies. In this course, I would like to thank **Dr. Georg Stoecklin** who allowed me to work in his lab. Thank you very much!

I would like to thank my dearest friend **Christian Hüber** for his support, although he has been almost a thousand kilometres away. Thank you for giving me shelter when I needed to get out of Heidelberg, lots of fun in the stadiums and our regular Christmas dinners. I hope we are going to continue this way.

Special thanks go to **Stephanie Hoppe** for accompanying me on countless runs through the forest and half marathons when I needed to clear my mind, for her open ear at any time of the day and night, for sharing the nicest and the worst days of my life and for reminding me that there is indeed a life outside the lab. Thank you!

My greatest thanks go to my dear **Thomas** who helped me through all the hardship by cheering me up, for proofreading this thesis, his creative skills, his patience with me and most of all his unconditional love. I know the last couple of years have not been easy, but we have managed to get through and we will have a better time now!

Finally, I can hardly express how incredibly thankful I am to my entire **family**, especially my parents **Martin** and **Tina,** my brother **Heiko**, and my grandmother **Erna** for their love and perpetual support in all the matters of life, for their encouragement, patience and interest, for listening and, frankly, for always being there for me. - Thank you so much!

Table of Contents

Abstract I
Zusammenfassung III
Acknowledgements V
Table of Contents VII
List of Abbreviations XI
List of Figures XVI
List of Tables XVIII
1 Introduction 1
1.1 Malaria – a general overview 1
1.2 The malaria parasite *Plasmodium falciparum* and its vector *Anopheles* 2
1.3 Plasmodium life cycle 4
1.4 Clinical manifestation and immunity 6
1.5 Intervention strategies and resistance 7
1.6 Invasion and egress 10
1.6.1 Invasion 10
1.6.2 Egress 13
1.7 MSP-1 and PfSUB1 17
1.7.1 The merozoite surface protein 1 17
1.7.2 Erythrocyte binding of MSP-1 20
1.7.3 The subtilisin-like protease PfSUB1 22
1.8 Molecular genetic tools in *Plasmodium falciparum* 24
1.8.1 Blasticidin co-selection system 26
1.8.2 Blasticidin resistance 27
1.9 Aim of thesis 29
2 Materials and Methods 31
2.1 Material 31
2.1.1 Laboratory Equipment 31
2.1.2 Software 32
2.1.3 Disposables/Consumables 33
2.1.4 Chromatography media 34

2.1.5 Chemicals 34
2.1.6 Enzymes 36
2.1.7 Markers 37
2.1.8 Molecular Biology Kits 37
2.1.9 Antibodies 38
2.1.10 Plasmids 38
2.1.11 Oligonucleotides 40
2.1.12 Bacteria strains 43
2.1.13 Parasite strains 43
2.1.14 Antibiotics & Drugs 44
2.1.15 Common solutions 44
2.1.16 Recombinant protein expression and renaturation 45
2.1.17 Chromatographic purification of recombinant proteins 45
2.1.18 Analysis of proteins 47
2.1.19 *In vitro* processing assay 48
2.1.20 Cell culture of *Plasmodium falciparum* 48
2.2 Molecular Biological Methods 50
2.2.1 Isolation of plasmid DNA from *E. coli* 50
2.2.2 Determination of concentration and purity of DNA and RNA 50
2.2.3 Precipitation of DNA 51
2.2.4 Agarose gel electrophoresis of DNA 51
2.2.5 Primer design 51
2.2.6 Polymerase Chain Reaction (PCR) 52
2.2.7 TOPO and pGEM-T cloning 55
2.2.8 DNA restriction 55
2.2.9 DNA dephosphorylation 55
2.2.10 Ligation 56
2.2.11 Isolation of total parasitic RNA 56
2.2.12 DNase digestion 57
2.2.13 Reverse Transcription PCR (RT-PCR) 57
2.2.14 Quantitative Real time PCR (qRT-PCR) 58
2.2.15 Standard curve and absolute quantification 60

2.3 Biochemical Methods 60
2.3.1 Enzymatic treatment of RBCs 60
2.3.2 Erythrocyte Binding Assay 61
2.3.3 *In vitro* processing assay 61
2.3.4 SDS polyacrylamide gel electrophoresis (SDS-PAGE) 62
2.3.5 Western Blot analysis 63
2.3.6 Mass Spectrometry 65
2.3.7 Indirect Immunofluorescence analysis (IFA) 65
2.4 Microbiological Methods 66
2.4.1 Liquid culture of *E. coli* 66
2.4.2 Recombinant protein expression and renaturation 66
2.4.3 Chromatographic purification of recombinant proteins 69
2.4.4 Preparation of competent *E. coli* cells 72
2.4.5 Transformation of self-made competent cells 72
2.4.6 Preparation of Cryopreservation stocks 73
2.5 *Plasmodium falciparum* experimental methods 73
2.5.1 Microscopic demonstration of *P. falciparum* using Giemsa staining 73
2.5.2 Determination of parasitemia by blood smear 74
2.5.3 Determination of parasitemia by flow cytometry 74
2.5.4 *Plasmodium falciparum* transfection 76
2.5.5 DNA loading of erythrocytes 76
2.5.6 Purification of mature schizont-stage parasites 77
2.5.7 Protein extraction 78
2.5.8 Cryopreservation of *P. falciparum* 78
3 Results 81
3.1 *In silico* identification of novel putative PfSUB1 cleavage sites 81
3.2 Mutagenic analysis of predicted PfSUB1 processing sites 83
3.3 Identification of PfSUB1 cleavage sites by LC-MS 88
3.4 Expression of mutant MSP-1F variants in *P. falciparum* 91
3.4.1 Generation of *P. falciparum* expression vectors 91
3.4.2 Generation of transgenic parasite lines 92
3.4.3 Proteolytic processing of MSP-1in transgenic parasite lines 93

3.4.4 Co-localisation of MSP-1D and MSP-1F in transgenic parasites 97
3.4.5 Regulation of episome copy number by blasticidin concentrations 99
3.4.6 Regulation of *msp-1f* expression by altering blasticidin concentration 100
3.4.7 Parasite growth is affected by expression of cleavage-deficient *msp-1f* 103
3.4.8 Nutrient uptake of transgenic parasite lines is not impaired 105
3.4.9 Knockout attempts on *Pfmsp-1d* via double homologous crossover recombination 107
3.4.10 Processed MSP-1 binds to erythrocytes 110
4 Discussion 115
4.1 Cleavage analysis of mutant MSP-1F proteins 115
4.2 Co-expression of *msp-1f* in *Pf*3D7 117
4.3 Are the MSP-1F versions cleaved *in vivo*? 119
4.4 Immunofluorescence analysis 120
4.5 Growth analysis and *clag* gene expression 121
4.6 Knockout of *msp-1d* 122
4.7 Erythrocyte binding of MSP-1 124
4.8 Outlook 127
4.9 Conclusion and Model 131
References 133
Appendix XX
A1 Mutation of cleavage junctions in MSP-1F XX
A2 MSP-1 and its fragments XXIII
A3 Loading control for protein extracts from transgenic parasites XXVIII
A4 Absolute quantification of copy number and transcription XXIX
A5 Knockout of *msp-1d* XXXI
A6 Surface coverage with MSP-1 XXXII
A7 Vector maps XXXIII

List of Abbreviations

5-FC	5-fluorocytosine
α	anti
aa	amino acids
ACT	artemisinin-based combination therapy
AMA-1	apical membrane antigen 1
Amp	ampicillin
AP	alkaline phosphatase
APS	ammonium persulfate
ATP	adenosine triphosphate
B.C.	Before Christ
BCIP	5-Bromo-4-chloro-3-indolyl phosphate
bp	base pairs
BSA	bovine serum albumin
BSD	blasticidin S deaminase
°C	degree Celsius
Ca^{2+}	calcium
$CaCl_2$	calcium chloride
CD	cytosine deaminase
cDNA	complementary DNA
CDUP	cytosine deaminase/uracil phosphoribosyl transferase
CHO	Chinese hamster ovary (cells)
cm	centimetre
CO_2	carbon dioxide
CR1	complement receptor 1
CRISPR	clustered, regularly interspaced, short palindromic repeat
CSA	chondroitin sulphate A
CSP	circumsporozoite protein
Ct	threshold cycle
C-terminus	carboxyl-terminus
CV	column volumes
Da	dalton
DAG	diacylglycerol
dATP	deoxyadenosine triphosphate
DBL	duffy-binding like
dCTP	deoxycytosine triphosphate
DD	destabilisation domain
ddH_2O	double distilled water
DHFR/TS	dihydrofolate reductase/thymidylate synthetase
DHOD	dihydroorotate dehydrogenase

DHPS	dihydropteroate synthase
dGTP	deoxyguanosine triphosphate
DIC	differential interference contrast
DICo	Diversity-Covering
DMSO	dimethylsulfoxide
DNA	deoxyribonucleic acid
DNAse	deoxyribonuclease
dNTP	deoxynucleoside triphosphate
DPAP3	dipeptidyl peptidase 3
dsDNA	double-stranded DNA
DTT	dithiothreitol
dTTP	deoxythymidine triphosphate
E64	Epoxysuccinyl-leucylamido(4-guanidino)butane
EBA	erythrocyte binding antigen
EBL	erythrocyte binding-like
E. coli	*Escherichia coli*
ED_{50}	median effective dose
EDTA	ethylene-diamine-tetra-acetic acid
EGF	epidermal growth factor-like domain
EGTA	ethylene-glycol-tetra-acetic acid
ER	endoplasmatic reticulum
F	farad
For	forward
FSC	forward scatter
g	gram
G6PD	glucose-6-phosphate-dehydrogenase deficiency
gDNA	genomic DNA
GIA	growth inhibition assay
GLURP	glutamate-rich protein
GMAP	Roll Back Malaria Action Plan
GMP	good manufacturing practice
GPI	glycosylphosphatidylinositol
GSH	reduced glutathione
GX	glutathione-S-transferase (GST)-tag
h	hour
H	histidine(His)-tag
HCl	hydrochloric acid
hDHFR	human dihydrofolate reductase
HeLa	Henrietta Lacks (cells)
HEPES	4-(2-hydroxyethyl)-1-piperazineethanesulfonic acid
h.p.i.	hours post invasion

HIV	human immunodeficiency virus
HRP	horseradish peroxidase
HTPBS	human tenacity phosphate buffered saline
IB	inclusion body
IC_{50}	half maximal inhibitory concentration
IFA	immunofluorescence analysis
IMC	inner membrane complex
IP_3	inositol 1,4,5-trisphosphate
IPTG	isopropyl-β-thiogalactopyranosid
IPTp	intermittent preventive treatment in pregnancy
IRS	indoor residual spraying
ITNs	insecticide-treated bed nets
k	kilo
KCl	potassium chloride
KH_2PO_4	monopotassium phosphate
l	litre
LB	Luria broth
LC-MS	liquid chromatography-mass spectrometry
mA	milli Ampère
malERA	Malaria Eradication Research Agenda
µg	microgram
$MgCl_2$	Magnesium chloride
µl	microliter
µm	micrometre
M	mol
MCS	multiple cloning site
$MgCl_2$	magnesium chloride
mg	milligram
min	minutes
ml	millilitre
mm	millimetre
mM	millimolar
mRNA	messenger ribonucleic acid
MSP-1	merozoite surface protein-1
MTBST	Tris-buffered saline with milk powder
MVA	modified vaccinia Ankara (virus)
N_2	liquid nitrogen
NaCl	sodium chloride
NaH_2PO_4	monosodium phosphate
Na_2HPO_4	disodium hydrogen phosphate
NaOH	sodium hydroxide

Na-P	sodium phosphate
NBT	nitro blue tetrazolium chloride
NEO	neomycin phosphotransferase II
nm	nanometre
Ni^{2+}	nickel (II)
NIMR	National Institute for Medical Research
N-terminus	amino-terminus
O_2	oxygen
OD	optical density
oligo(dT)	oligo-tyrosine
o/n	overnight
Pf	*Plasmodium falciparum*
PAA	polyacrylamide
PAGE	polyacrylamide gel electrophoresis
PALM	photoactivated localization microscopy
PBS	phosphate buffered saline
PCR	polymerase chain reaction
PfCDPK1	*P. falciparum* calcium-dependent protein kinase 1
PfCRT	*P. falciparum* chloroquine resistance transporter
PfEMP1	*P. falciparum* erythrocyte membrane protein 1
Pfmdr1	*P. falciparum* multidrug resistance transporter 1
PfPLP1	*P. falciparum* perforin-like protein 1
PfRH	*P. falciparum* reticulocyte-binding protein homologue
PfROM4	*P. falciparum* rhomboid protease 4
PfSUB	*P. falciparum* subtilisin-like protease
pH	*potentia hydrogenii*
pI	isoelectric point
PIP_2	phosphatidylinositol 4,5-bisphosphate
PLC	phospholipase C
PMSF	phenylmethanesulfonylfluoride
pN	pico Newton
PSAC	plasmodial surface anion channel
PV	parasitophorous vacuole
PVDF	polyvinylidene fluoride
PVM	parasitophorous vacuole membrane
qRT-PCR	quantitative real time PCR
r	recombinant
RAP-1	rhoptry-associated protein 1
RBC	red blood cell
Rev	reverse
RNA	ribonucleic acid

RNAse	ribonuclease
RON	rhoptry neck protein
rpm	rounds per minute
RPMI	Roswell Park Memorial Institute medium
RT	room temperature or reverse transcriptase
-RT	without reverse transcriptase
+RT	with reverse transcriptase
RT-PCR	reverse transcriptase PCR
SAO	Southeast Asian ovalocytosis
s	second
SERA	serine repeat antigen
SDS	sodium dodecyl sulfate
SP	signal peptide
SP	sulfadoxine-pyrimethamine
SPAM	secreted polymorphic antigen associated with merozoites
SSC	side scatter
STED	stimulated emission depletion
STORM	stochastic optical reconstruction microscopy
TAE	Tris-acetate-EDTA
Taq	*Thermus aquaticus*
TBS	Tris-buffered saline
TBST	Tris-buffered saline/tween
TEMED	tetramethylethylenediamine
TK	thymidine kinase
TM	transmembrane domain
TNF-α	tumour necrosis factor α
TRAP	thrombospndin related adhesive protein
Tris	Tris-[hydroxymethyl] aminoethan
U	unit
UTR	untranslated region
UV	ultraviolet
V	Volt
v/v	volume to volume
Vol	volume
WHO	World Health Organization
w/o	without
WR99210	1,6-Dihydro-6,6-dimethyl-1-[3-(2,4,5-trichlorophenoxy)propoxy]-1,3,5-triazine-2,4-diamine
wt	wildtype
w/v	weight to volume
ZMBH	Zentrum für Molekulare Biologie

List of Figures

Figure 1 | Worldwide malaria distribution and burden stages of countries (Alonso and Tanner, 2013). 2
Figure 2 | Life cycle of *Plasmodium falciparum* (Boddey and Cowman, 2013). 6
Figure 3 | The host-parasite interactions during erythrocyte invasion by *P. falciparum* (Harvey et al., 2012)....14
Figure 4 | Egress of malaria parasites from erythrocytes (Glushakova et al., 2005). 17
Figure 5 | Maturation of MSP-1 and allelic dimorphism. 18
Figure 6 | Blasticidin co-selection system....26
Figure 7 | Schematic representation of the assembly of the Western Blot. 65
Figure 8 | Predicted PfSUB1 cleavage sites within MSP-1 and mutations introduced....82
Figure 9 | PfSUB1-mediated proteolytic processing of MSP-1F. 85
Figure 10 | PfSUB1-mediated proteolytic processing of MSP-1F....87
Figure 11 | LC-MS analysis of MSP-1Fmut38/42. 90
Figure 12 | Generation of *msp-1f* expressing parasite lines. 93
Figure 13 | Protein expression and cleavage by PfSUB1. 96
Figure 14 | Immunofluorescence analysis of parental and transgenic parasite lines. 98
Figure 15 | DNA copy number of episomes using variable blasticidin concentrations....100
Figure 16 | Regulated transgene expression via variable blasticidin concentrations. 102
Figure 17 | Growth analysis of transgenic parasites. 104
Figure 18 | Growth phenotypes of transgenic parasite lines are not associated with changes in *clag3* expression. 106
Figure 19 | Knockout strategy for *PfMSP-1D* using the pCC1/pHTK vector system and analysis of transgenic parasites by PCR. 109
Figure 20 | Binding of MSP-1D to erythrocytes....111

Figure 21 | Erythrocyte binding of MSP-1D is not affected by heparin or enzymatic treatment of red blood cells.....112
Figure 22 | Working model of MSP-1 function.....132
Figure 23 | Western Blot analysis of transgenic parasites via anti-AMA1 antibody.....XXVIII
Figure 24 | qRT-PCR standard curves for absolute quantification of DNA copy numbers and transcript numbers.....XXX
Figure 25 | *E. coli* expression vectors.....XXXIII
Figure 26 | *P. falciparum* expression vector.....XXXIV
Figure 27 | *P. falciparum* knockout vectors.....XXXIV
Figure 28 | *P. falciparum* knockdown vectors.....XXXV

List of Tables

Table 1 | Overview of malaria forms and causative agents. 3
Table 2 | Molecular genetic tools in *P. falciparum*. 25
Table 3 | Laboratory equipment overview. 31
Table 4 | Software overview 32
Table 5 | Overview of disposables and consumables. 33
Table 6 | Overview of chromatography media. 34
Table 7 | Overview of chemicals 34
Table 8 | Enzyme overview. 36
Table 9 | Macromolecular marker overview. 37
Table 10 | Molecular biology kit overview. 37
Table 11 | Antibody overview. 38
Table 12 | Bacterial expression vector overview. 38
Table 13 | *Plasmodium* vectors overview. 39
Table 14 | Oligonucleotide overview 40
Table 15 | Bacteria strain overview 43
Table 16 | Parasite strain overview. 43
Table 17 | Overview of antibiotics used for *E. coli* cultivation. 44
Table 18 | Overview of antibiotics and drugs used for *P. falciparum* cultivation. 44
Table 19 | Composition of common solutions. 44
Table 20 | Composition of solutions for recombinant protein expression and renaturation. 45
Table 21 | Composition of solutions for chromatographic purification of MSP-1 heterodimers using Q Sepharose column. 45
Table 22 | Composition of solutions for chromatographic purification of full length MSP-1F using GST column 46
Table 23 | Composition of solutions for chromatographic purification of full length MSP-1F using NTA column. 46
Table 24 | Composition of solutions for biochemical protein analysis 47
Table 25 | Composition of solutions for *in vitro* protein processing 48
Table 26 | Composition of solutions for cultivating *Plasmodium falciparum* 48

Table 27 | PCR composition and conditions for Taq DNA Polymerase. 52
Table 28 | PCR composition and conditions for Phusion High-Fidelity DNA Polymerase.....53
Table 29 | PCR composition and conditions for Platinum Pfx DNA Polymerase. 54
Table 30 | RT-PCR composition. 58
Table 31 | qRT-PCR composition. 59
Table 32 | Programme for Real-time PCR in ABI 7500.....59
Table 33 | Chemical volumes for preparation of SDS polyacrylamide gels. 63
Table 34 | FACSCalibur settings for parasitemia determination. 75
Table 35 | Overview of mutations of cleavage sites within MSP-1F XX
Table 36 | Fragment weights of MSP-1 before and after processing by PfSUB1. XXIII
Table 37 | List of protein fragments identified by LC-MS in MSP-1Fmut38/42_1_KK and PfSUB1-digested MSP-$1F_{42}$ fragment after dimethyl labelling according to (Boersema et al., 2009).....XXIV
Table 38 | List of protein fragments identified by LC/MS in MSP-1Fmut38/42_2_KK and PfSUB1-digested MSP-$1_{42^{**}}$ after dimethyl labelling according to Boersema et al. (2009). XXV
Table 39 | Primers and DNA template used for standard curves. XXIX
Table 40 | Calculation of copy numbers and DNA concentrations used for standard curves.....XXIX
Table 41 | Cycling of transfectants to acquire knockout of *PfMSP-1D* via double crossover recombination.....XXXI
Table 42 | Calculation of MSP-1 molecule number on the merozoite surface. XXXII

1 Introduction

1.1 Malaria – a general overview

Malaria, a vector-borne infectious disease caused by protozoan parasites of the genus *Plasmodium*, threatens half of the world's population. According to the World Health Organisation (WHO, 2013) malaria is endemic in 104 countries, including Africa, Southeast Asia, Oceania, the Indian Subcontinent as well as Central and South America (Figure 1). Approximately 287 million cases of malaria were reported in the year 2012, killing about 789,000 people, 77 % of whom are children below the age of five (WHO, 2013). The majority of infections (85 %) and deaths (80 %) occurred in sub-Saharan Africa rendering malaria one of the major causes of death in this part of the world. Malaria does not only pose a major health problem, it also has a great economic impact, lowering the annual economic growth by 1.3 % (WHO, 2009). Thus, the disease is estimated to cost African countries more than $12 billion annually (Tuteja, 2007).

Malaria was known throughout history, described already in recordings from 2700 Before Christ (B.C.) (Cox, 2010). As early as 2000 years ago, Chinese healers used the quinghao plant, which contains the antimalarial drug artemisinin, to treat fever and malaria. Among others, the Greek physician Hippocrates formulated a detailed description of the malarial disease 400 B.C. (Cox, 2002; Dhingra et al., 1999; van Agtmael et al.). The term malaria originates from the Italian 'mal' aria', which literally means "bad air". Throughout the 19th century, the so-called miasmic theory persisted, attributing the causative agent of the feverish disease to gases rising from swamps and floodplains (Guillemin, 2001; Retief and Cilliers, 2006). In contradiction to this theory, Charles Louis Alphonse Laveran noticed parasites in the blood of a patient suffering from malaria in 1880. Seventeen years later, Dr. Ronald Ross discovered that mosquitoes transmit malaria. This finding was complemented by Giovanni Battista Grassi, Amico Bignami and Guiseppe Bastianelli who showed that human malaria could indeed only be transmitted by *Anopheles* mosquitoes. Finally, in 1948, Henry Shortt and

Cyril Garnham discovered that malaria parasites develop in the liver before entering the blood stream (Cox, 2010; Tuteja, 2007).

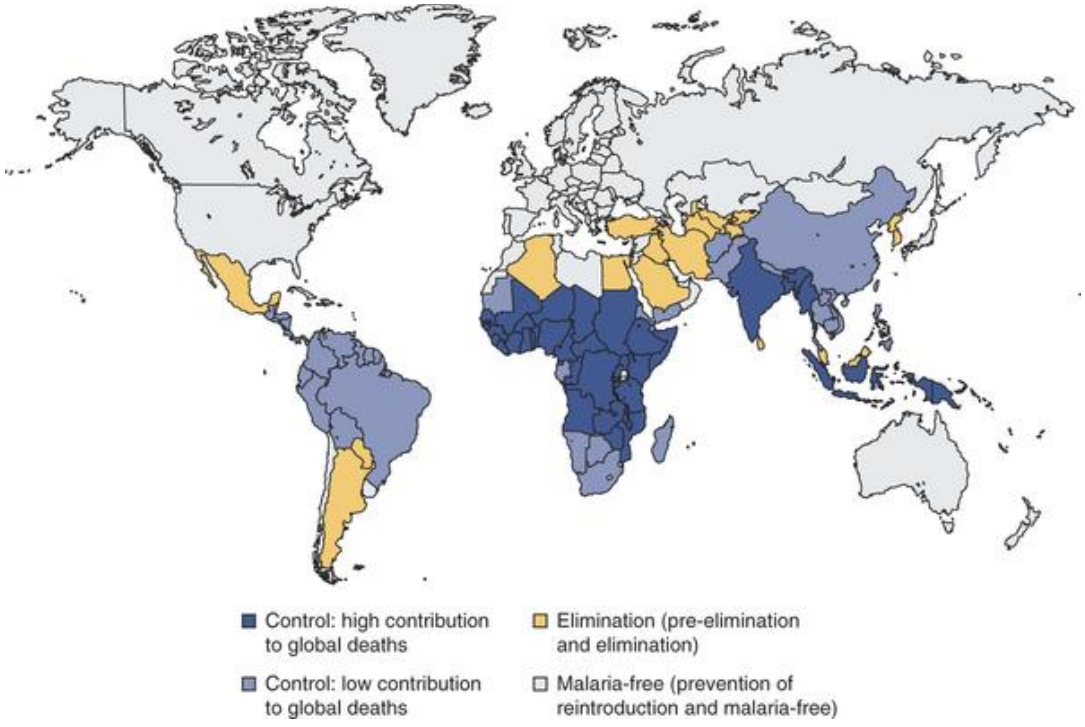

Figure 1 | Worldwide malaria distribution and burden stages of countries (Alonso and Tanner, 2013).

1.2 The malaria parasite *Plasmodium falciparum* and its vector *Anopheles*

Malaria parasites are eukaryotic single-cell microorganisms belonging to the genus *Plasmodium* of the phylum *Apicomplexa* (Class: *Sporozoa*, Order: *Coccidia*, Suborder: *Haemsporidiae*, Family: *Plasmodiidae*). Apicomplexa are a versatile phylum of more than 5000 protozoan parasites with many major human and animal pathogens such as *Toxoplasma gondii*, *Eimeria spec.* or *Theileria spec.* Apicomplexa possess unique specialized organelles. One of these is the apicoplast, a chloroplast-like product of secondary endosymbiosis (Vaishnava and Striepen, 2006). Eponymous is the apical complex which has an essential role in gliding motility, host cell invasion and establishment of the parasitophorous vacuole (PV) (Hakansson et al., 2001). It consists of the roptries, micronemes, subpellicular microtubules, the apical polar ring and the conoid (Morrissette and

Sibley, 2002). Another unique feature of Apicomplexa is the three-layered pellicle consisting of the plasma membrane and the inner membrane complex (IMC) with the gliding machinery located in between (Keeley and Soldati, 2004).

Of the more than 100 species of *Plasmodium* parasitising on vertebrate species such as reptiles, birds and various mammals, only five can infect humans: *P. falciparum*, *P. vivax*, *P. ovale*, *P. malariae* and *P. knowlesi* (Greenwood et al., 2005; Singh et al., 2004; Tuteja, 2007). Infection with one of these species is associated with different manifestations of malaria as summarised in Table 1.

Table 1 | Overview of malaria forms and causative agents.

species	name	fever periods	persistence
P. falciparum	Malaria tropica	non-periodic	6-12 months
P. malariae	Malaria quartana	72 h	20-30 years
P. ovale	Malaria tertiana	48 h	2-3 years (hypmozoites)
P. vivax	Malaria tertiana	48 h	4-5 years (hypnozoites)
P. knowlesi		24 h	

The distribution of the different *Plasmodium* species mainly depends on the ecology of the arthropod-vector *Anopheles* (phylum: *Arthropoda*, Class: *Insecta*, Order: *Diptera*, Suborder*: Nematocera,* Family: *Culicidae,* Subfamily: *Anophelinae*). Among approximately 400 *Anopheles* species worldwide, about 60 are malaria vectors under natural conditions (Tuteja, 2007). Of major importance for the transmission of human malaria are *Anopheles gambiae* and *A. funestus.* In scientific research, the rodent and human malaria parasites are often transmitted by *Anopheles stephensi* (Killick-Kendrick, 1978; Sinden, 1997) due to unfavourable breeding and low infection rates of other *Anopheles* species under laboratory conditions (Sinden, 1997).

1.3 Plasmodium life cycle

The life cycle of the obligate intracellular parasite *Plasmodium* is extremely complex, alternating between the insect primary (definite) host and the vertebrate secondary host (Figure 2). During its life cycle, *Plasmodium* parasites invade different cell types, undergo ten morphological transitions in five different host tissues, proliferate both sexually and asexually within them and adapt to a variety of environmental conditions e.g. variable temperature or host metabolism (Enserink, 2010). In addition, the parasites escape immune responses by antigenic variation (Tuteja, 2007). While sexual reproduction (gamogony) occurs in the anopheline mosquito vector, asexual reproduction (schizogony) takes place in the mammalian host. Here, the parasites proliferate and differentiate first in hepatocytes (exo-erythrocytic phase) and later in erythrocytes (erythrocytic phase) (Yamauchi et al., 2007).

Malaria infection is initiated by the bite of a female *Anopheles* mosquito. *Plasmodium* sporozoites are injected from the salivary glands of the mosquito along with anticoagulant-containing saliva into the mammalian host. During a blood meal, approximately 15-123 sporozoites are deposited within the mammalian skin (Frischknecht et al., 2004). The majority of them remain at the injection site for hours and are only slowly released into the bloodstream (Yamauchi et al., 2007). Via the bloodstream, the sporozoites rapidly home to the liver where they enter liver sinosoids. The sporozoites cross the sinusoidal layer via Kupffer cells (Pradel and Frevert, 2001; Pradel et al., 2002, 2004) and migrate through several hepatocytes in a process called transmigration before they productively invade the final hepatocyte (Mota and Rodriguez, 2004).

The invasion is mediated by invagination of the host cell plasma membrane forming a parasitophorous vacuole (PV). It surrounds the invading sporozoite and builds up a physical barrier between the parasite and the host (Lingelbach and Joiner, 1998). Within the hepatocyte, asexual replication, the so-called exo-erythrocytic schizogony, takes place. There, sporozoites transform into round-shaped early liver stages and develop into a metabolically very active trophozoite

which rapidly increases in size and matures into a liver-stage schizont. Multiple rounds of DNA replication and nuclear division without mitosis result in a multinuclear syncytium containing up to 30,000 nuclei.

After 2-15 days, depending on the parasite strain, individual merozoites are formed by invaginations of the parasite plasma membrane which are then released into the bloodstream as merosomes, parasite-filled vesicles (Baer et al., 2007; Sturm et al., 2006; Sturm et al., 2009). *P. vivax* and *P. ovale* additionally develop hypnozoites in the liver, latent forms that can remain dormant for years until they are reactivated and cause a relapse of the malarial disease (Cogswell, 1992). The prepatency varies among the different *Plasmodium* species between 8-30 days (Tuteja, 2007).

After the release of thousands of merozoites into the blood stream, they invade erythrocytes to undergo further replication in the so-called erythrocytic schizogony. Once inside the red blood cells, the merozoite develops within a parasitophorous vacuole from the ring stage parasite, followed by the metabolically very active trophozoite, into the schizont which in turn contains 8-32 merozoites, depending on the parasite strain (Bannister et al., 2000). Upon erythrocyte rupture, released merozoites can directly invade new erythrocytes, starting a new cycle of schizogony.

Some merozoites differentiate within red blood cells into sexual parasite stages, gametocytes, which can be taken up by a female *Anopheles* mosquito upon a blood meal. In the mosquito midgut, gametocytes undergo further development triggered by a shift of temperature between vertebrate (37°C) and invertebrate host (20°C), change of pH, and presence of xanthurenic acid (Billker et al., 1998). In a process called exflagellation, the nucleus of each male gametocyte divides into 4-8 nuclei giving rise to microgametes. After exflagellation, microgametes are able to fertilise mature female gametocytes, so-called macrogametes, forming a zygote which subsequently transforms into an ookinete. The motile ookinete crosses the mosquito midgut wall, rounds up and forms an oocyst between the epithelial lining and the basal lamina (Sinden and Billingsley, 2001).

During subsequent sporogony, midgut sporozoites are formed that break through the oocyst wall and are released into the hemolymph. Finally, sporozoites migrate to the salivary glands for onward transmission into another vertebrate host (Tuteja, 2007).

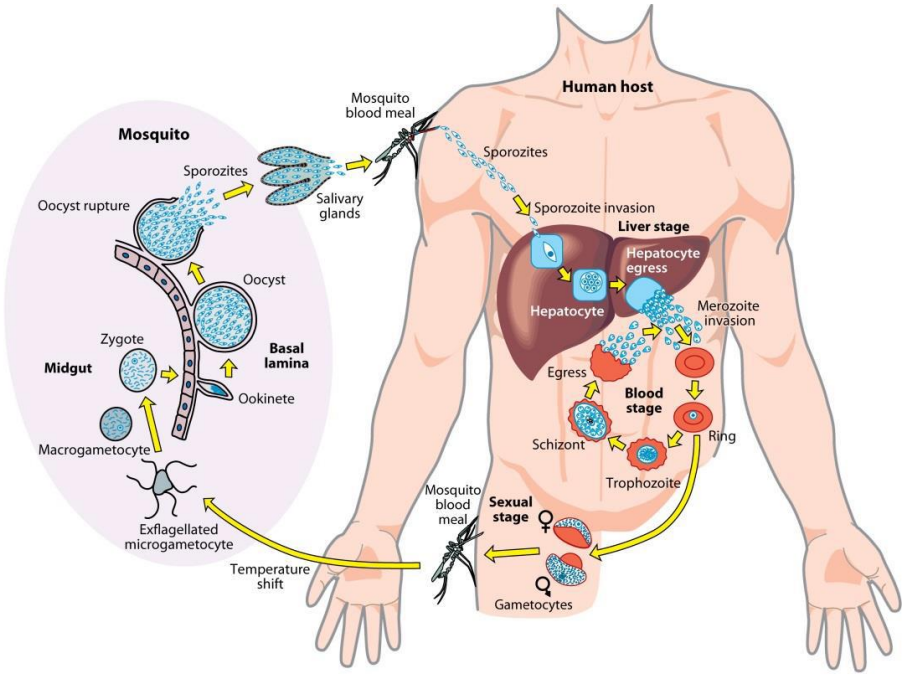

Figure 2 | Life cycle of *Plasmodium falciparum* (Boddey and Cowman, 2013).

1.4 Clinical manifestation and immunity

Initial symptoms of malaria infections are rather unspecific including tiredness, diarrhoea, nausea, sweat periods, chills and dizziness. Since these symptoms are also found during viral or bacterial infections, rapid malaria diagnosis tests are required to discriminate between those diseases. In the course of the malarial disease, recurrent periods of a cold stage (sensation of cold, chills), a hot stage (fever, vomiting, headaches, and seizures) and a sweating stage (sweats, tiredness) are characteristic. This is due to the massive simultaneous release of merozoites into the blood stream which coincides with a sharp incline in body temperature during the typical feverish periods. In particular, this reaction is caused by the activation of the immune system upon contact with hemozoin, parasite antigens

such as shed merozoite surface proteins, and erythrocytic cell debris (Shio et al., 2010). Consequently, innate as well as adaptive immune responses are activated such as the release of pro-inflammatory cytokines and antibodies (Engwerda and Good, 2005; Ramasamy, 1998). High parasitemia and severe anaemia resulting from the destruction of erythrocytes are characteristic for severe malaria. As a consequence, hemoglobinuria and hepatosplenomegaly occur. Sequestration of infected erythrocytes (rosetting) leads to the blockage of blood flow, oxygen deprivation and inflammation in the capillaries which in turn can induce multi-organ failure. If localised to the microvasculature of the brain, severe cerebral malaria is established coinciding with impaired vision, coordination and movement, as well as coma usually leading to death after a short period of time (White, 2014). Primigravidae are particularly threatened as sequestration in placental capillaries caused by the binding of the *P. falciparum* erythrocyte membrane protein 1 (PfEMP1) to chondroitin sulphate A (CSA) can lead to miscarriage, premature delivery, low birth weight and increased mortality in the new-born, as well as severe anaemia or death of the mother (Tuteja, 2007).

Individuals living in endemic areas can usually acquire semi-immunity after multiple infections, which protects them from severe consequences of recurrent malaria infections (Ramasamy, 1998). Additionally, a number of genetic polymorphisms confer resistance to malaria. These fall into four groups: hemoglobinopathies e.g. haemoglobin S, altered erythrocyte membrane proteins e.g. Duffy Antigen, altered red blood cell enzymes e.g. glucose-6-phosphate-dehydrogenase deficiency (G6PD) and modifications of immunity-related genes e.g. TNF-α (Lopez et al., 2010; Williams, 2006).

1.5 Intervention strategies and resistance

According to the World Malaria Report in 2013, the estimated number of malaria cases has decreased from 226 million in 2000 to 207 million in 2012. Interlinked with the decrease of cases is the mortality rate which fell by 42 % in all age groups and by 48 % in children under 5 years of age (WHO, 2013).

This reduction is attributed to successful intervention campaigns such as the 'Roll Back Malaria Action Plan' (GMAP) and the 'Malaria Eradication Research Agenda' (malERA) (Alonso et al., 2011). Malaria control is carried out on different levels including vector control interventions through the use of insecticide-treated bed nets (ITNs), indoor residual spraying (IRS), and larval control. In addition, preventive therapies e.g. intermittent preventive treatment in pregnancy (IPTp) with sulfadoxine-pyrimethamine (SP), diagnostic testing, treatment with anti-malarials such as artemisinin-based combination therapies and strong surveillance are important cornerstones of malaria control (WHO, 2013). Despite these improvements, 627,000 people still died from malaria worldwide in 2012, with the majority of deaths occurring in sub-Saharan Africa (WHO, 2013). Therefore, further initiatives are required on governmental, financial, public, medical and scientific levels to defeat malaria. Up to now, there are no licensed malaria vaccines with only one candidate, RTS,S/AS01, being currently assessed in phase III clinical trials. So far RTS,S/AS01, a hybrid of the *P. falciparum* circumsporozoite protein (CSP) and the hepatitis B antigen (Stoute et al., 1997), has proven to be less efficient than originally assumed (Goldstein and Shapiro, 1997; Salvador et al., 2012). About 20 other vaccine candidates are in phase I or II clinical trials such as AMA1, TRAP, EBA175, and MSP-3. Besides, many other antigenic targets are under evaluation e.g. MSP-1, Rh5, and Var2-CSA (Chilengi and Gitaka, 2010; Schwartz et al., 2012; WHO, 2014). Additionally, approaches for next-generation vaccines include whole sporozoite vaccines that are either attenuated by radiation or genetically or given under drug cover (Borrmann and Matuschewski, 2011; Hoffman et al., 2002).

Nonetheless, malaria can effectively be treated, if drugs are administered appropriately. However, emerging parasite resistances towards nearly all effective anti-malarial drugs pose a serious threat (Mendis et al., 2009; Turschner and Efferth, 2009). Anti-malarials can be classified into four groups: aminoquinolines, antifolates, artemisinin derivates and other antibiotics (Schrader et al., 2012). The most well-known aminoquinoline drug against malaria is chinin from the

bark of the Cinchona tree (*Cinchona pubescens*). Already in the 16th century, Chinese people were using the bark for its antipyretic effect (Webb 2009).

Nowadays, chinin is widely replaced by chloroquine, another important aminoquinoline that interferes with the haemoglobin metabolism of the parasite (Hempelmann, 2007). It was widely used from the 1940's until the 1960's due to its low prize, effectiveness and safety even in pregnant women. Yet, resistances emerged with respective parasites being able to tolerate 4-10 times more chloroquine than susceptible strains (Sanchez et al., 2003). This resistance is attributed to mutations in the *P. falciparum* chloroquine resistance transporter (PfCRT) and the multidrug resistance transporter 1 (Pfmdr1) (Fidock et al., 2000).

Belonging to the antifolates, pyrimethamine, sulphadoxin and proguanil target the folate biosynthetic pathway of the parasite by inhibiting either the enzyme dihydrofolate reductase (DHFR) or dihydropteroate synthase (DHPS) and thus inhibiting DNA replication as well as metabolism of some amino acids (Petersen et al., 2011). Still, resistances rapidly occurred after introduction of these drugs which were probably conferred by mutations in the genes encoding for these enzymes (Baird, 2005). Nevertheless, sulphadoxin-pyrimethamine is still the method of choice for preventive treatment for pregnant women (IPTp) and non-immune travellers (Nakato et al., 2007).

As resistances to the above mentioned drugs rapidly evolved, artemisinin-derivatives were increasingly used. Artemisinin from the Chinese herb quinghao and its derivatives arthemeter and artesunate rapidly eliminate malaria parasites. However, they have a very short half-life of approximately 0.5-1.4 hours which increases the risk of the development of resistance when used in monotherapy. Therefore, they are administered together with a second drug in so-called artemisinin-based combination therapy (ACT). By June 2008, all but four countries with high burden of malaria had adopted ACTs as the first-line treatment for malaria tropica (WHO, 2009). Notwithstanding this progress, monotherapies are still applied and illegal drug trafficking as well as fake drugs

pose a major problem. Moreover, even parasite resistance to artemisinin has recently been detected in Southeast Asia at the borders of Cambodia and Thailand (Fairhurst et al., 2012). Due to the rapid rise of resistances, the identification of new drugs is urgently needed. Hence, in order to combat malaria, current efforts in all areas of malaria control and elimination need to be intensified.

1.6 Invasion and egress

Central to malaria pathogenesis is the asexual replication within erythrocytes. From one parasite, 16-32 daughter merozoites capable of invading new red blood cells result upon schizogony and lysis. Invasion and egress of erythrocytes are highly regulated events including molecular interactions and signal transduction events that are similar among all *Plasmodium* species.

1.6.1 Invasion

Invasion of erythrocytes is a multi-step process that occurs within minutes to minimise the exposure to the host immune system. Earliest observations of invasion were made in *Plasmodium knowlesi* in 1975 (Dvorak et al., 1975) and recently developed imaging techniques have greatly enhanced the insights into these events (Harvey et al., 2012). The invasion process can be divided into four steps. Upon receptor binding (attachment), apical reorientation takes place, followed by the formation of the tight junction and active invasion (Figure 3) (Aikawa et al., 1978; Chitnis, 2001; Dvorak et al., 1975).

Initial, reversible low affinity interaction of merozoites with red blood cells is most likely mediated by merozoite surface proteins with unknown erythrocyte receptors (Lin et al., 2014; Miller et al., 1979). The force needed to detach them was measured by optical tweezers and calculated to be 40 pN which corresponds to typical receptor-ligand interactions (Crick et al., 2014). Merozoite surface

proteins involved in this initial attachment are elucidated in more detail below. The initial contact elicits waves of dynamic deformation in the erythrocyte (echinocytosis), tumbling the merozoite over the surface and allowing it to reorientate to its apical end (Dvorak et al., 1975; Harvey et al., 2012) which is the energetically most favourable contact region of the curved parasite membrane (Farrow et al., 2011). This process takes only about 6 seconds (Harvey et al., 2012). Following reorientation, an apical "resting phase" of 5 seconds marks the irreversible contact and commits the parasite to invasion as an electron-dense tight junction is formed (Aikawa et al., 1981). Reorientation and tight junction formation involve many proteins, namely AMA1, RONs, Rhs, EBAs and so far unidentified factors, all of whose exact timing and function are not fully understood yet.

The low potassium level in the blood plasma activates phospholipase C (PLC) to hydrolyse phosphatidylinositol 4,5-bisphosphate (PIP_2) into inositol 1,4,5-trisphosphate (IP_3) and diacylglycerol (DAG). In turn, IP_3 activates IP_3 receptor to release Ca^{2+} from the endoplasmatic reticulum (ER). Rise in cytosolic Ca^{2+} levels activates calcium-dependent protein kinase 1 (CDPK1) leading to microneme discharge onto the merozoite surface (Sharma and Chitnis, 2013) which are involved in the reorientation process and tight junction formation. In addition, the binding of PfRh1 to the erythrocyte was proposed to trigger Ca^{2+} release which in turns leads to microneme release (Gao et al., 2013). Micronemal proteins such as EBA-175 bind to glycophorin A on erythrocytes leading to the restoration of basal cytosolic Ca^{2+} levels and release of rhoptry proteins such as PfRh2a/b.

Multiple redundant invasion pathways have been described in which distinct receptor-ligand combinations can operate independently and mediate invasion with equal efficiency (Harvey et al., 2012). These ligands belong to the erythrocyte binding-like (EBL) and reticulocyte binding-like (PfRh) protein families. The redundancy of these ligands confers a broad host range and adaptability to red blood cell polymorphisms as well as immune evasion mechanisms. Among the EBLs are EBA-175, EBA-140, EBA-181, and EBL-1

which are released onto the merozoite surface from the micronemes likewise due to the low potassium level in the serum. The receptor of EBA-175 was the first to be discovered and shown to be the highly abundant sialogylcoprotein glycorphorin A on the erythrocyte surface (Orlandi et al., 1992). Unlike EBA-175, EBA-181 binds to a trypsin-resistant and chymotrypsin-sensitive, unknown receptor. In contrast, the receptors of EBA-140 and EBL-1 are identified as glycophorin C and B, respectively (Maier et al., 2003; Mayer et al., 2009). A very recent publication showed another parasitic binding partner for glycophorin C, namely a variant of the STEVOR gene family, which was formerly only shown to be involved in erythrocyte cytoadherence and rosetting (Niang et al., 2014).

The PfRh family compromises five members with one, Rh5, being completely atypical. These proteins are stored in the rhoptry neck from where they are secreted onto the merozoite surface. PfRh1 binds to an unknown sialiated receptor Y, while PfRh2a and PfRh2b bind to trypsin-resistant receptor Z. The complement receptor 1 (CR1) was recently identified as the receptor for PfRh4 (Tham et al., 2012). The atypical PfRh5 binds to basigin and is supposed to be essential for parasite growth as demonstrated by a knockdown of basigin which inhibited invasion by the parasite (Crosnier et al., 2011). It is still not known in detail how many alternative pathways exist and which ligands are needed by the parasite for invasion. However, the ability of the parasite to switch between the use of receptor-ligand pairs might be a reason why *Plasmodium* parasites are so successful.

The apical membrane antigen 1 (AMA1) is one of the best characterised invasion ligands and a central facilitator of invasion. Nevertheless, its role is quite debated lately and several paralogues might take over redundant functions (Lamarque et al., 2014). While some reports suggested both AMA1 and RONs as key molecules for invasion (Lamarque et al., 2011; Richard et al., 2010), others claimed that they were not necessary for invasion (Andenmatten et al., 2012; Lamarque et al., 2014). Upon its discharge from the micronemes, the type 1 integral membrane protein AMA1 associates with a complex of rhoptry neck proteins (RONs) consisting of RON 2, 4, 5 and 8 that have been translocated into the host

beforehand. Both interactions of EBL/Rhs with receptors and AMA1-RON2 interaction trigger rhoptry release and the formation of the moving junction, thus the next step in erythrocyte invasion.

During actual penetration of the erythrocyte, the tight junction transforms into a ring-like structure, the moving junction, through which the parasite actively passes by using its actin-myosin motor. In addition, rhoptry organelles secret their contents into the host cell to be incorporated into the growing parasitophorous vacuole membrane (PVM) completely encapsulating the parasite. Internalisation takes approximately 17 seconds. Disengagement of host-parasite interactions carried out by parasite encoded sheddases is also very crucial for successful invasion (O'Donnell and Blackman, 2005). While the micronemal subtilisin-like protease PfSUB2 is responsible for the shedding of AMA1 as well as MSP-1 (Harris et al., 2005), rhomboid proteases such as PfROM4, are responsible for the cleavage of EBA-175 (O'Donnell et al., 2006).

1.6.2 Egress

The malaria blood stage life cycle is initiated by the invasion of an erythrocyte by a parasite. Approximately 40-48 hours later, 16-32 daughter merozoites are released completing the intracellular life cycle. These two space-time coupled events, parasite release and invasion, are termed cycle transition and form the shortest stage of the plasmodial erythrocyte cycle as they only last seconds (egress) to a few minutes (invasion) (Glushakova et al., 2007).

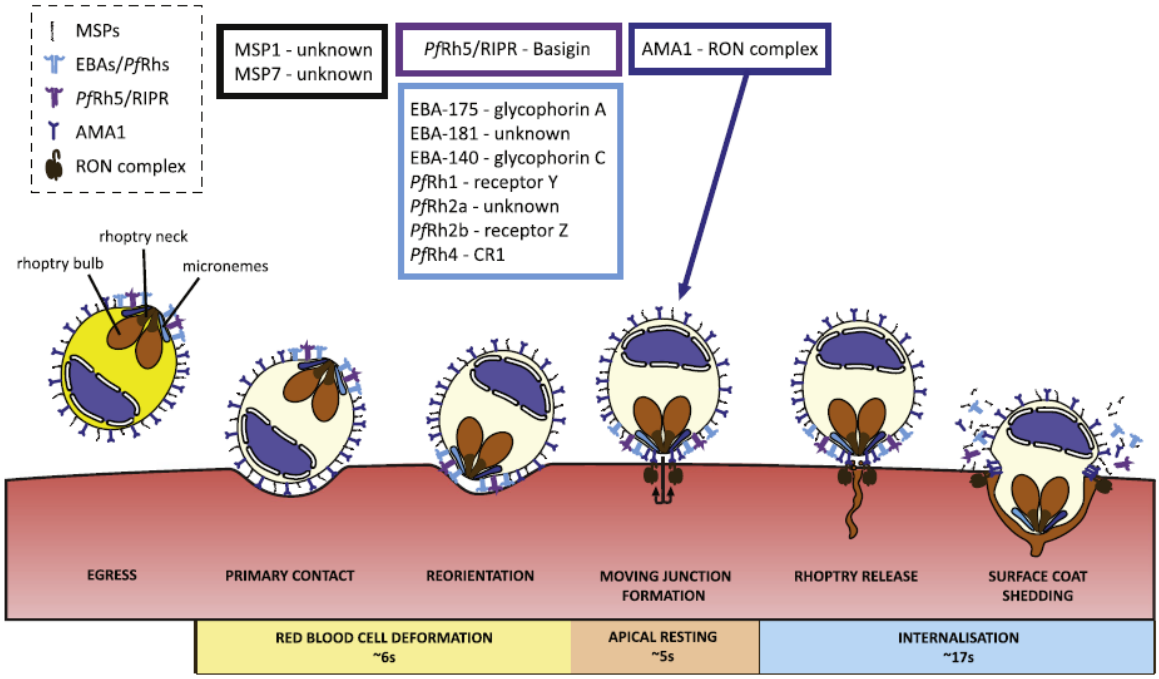

Figure 3 | The host-parasite interactions during erythrocyte invasion by *P. falciparum* (Harvey et al., 2012).
Receptor–ligand pairs build up during invasion are listed in boxes. Egress: low environmental potassium levels trigger release of calcium into the cytosol (yellow) leading to release of microneme content on the merozoite surface. Primary contact: merozoites reversibly attach to an erythrocyte possibly via merozoite surface proteins and their associated partners (black). Reorientation: primary contact induces echinocytosis in the red blood cell, resulting in reorientation of the parasite. This is most likely accompanied by a concentration of apical adhesins such as the erythrocyte binding-like and reticulocyte binding-like (EBA/PfRh) ligands (light blue) or PfRh5/Rh5 interacting protein (RIPR) (purple) that in turn bind to the host cell. Moving junction formation: Apical attachment of parasites allows for translocation of the rhoptry neck protein complex (brown) into the erythrocyte and formation of AMA1–RON complex (dark blue), thus the apposition of the moving junction through which the parasite invades. Invasion: During active host penetration surface ligands are shed and the parasite invades into the nascent parasitophorous vacuole created by secretion of the rhoptries into the host cell.

The exact mechanism of parasite egress was long debated. Three opposing pathways were proposed: First, coordinated rupture of the two membranes surrounding mature parasites (Dvorak et al., 1975; Lew, 2001), second, fusion of erythrocyte membrane and parasitophorous vacuole membrane (PVM) (Winograd et al., 1999) and, third, liberation of vacuole-enclosed parasites from erythrocytes followed by disintegration of the PVM (Salmon et al., 2001). In 2005, it was conclusively demonstrated that parasite egress occurs via sequential rupture of

PVM and host cell membrane (Glushakova et al., 2005). Two morphological stages precede the convulsive rupture of membranes and rapid radial discharge of separated merozoites, leaving behind membrane fragments and plasma membrane blebs at the site of parasite egress. Figure 4 summarises parasite egress. Prior to parasite release, an "irregular" schizont can be observed due to its anisotropy. This schizont occupies only a fraction of the infected red blood cell and exists for hours before release. A few minutes before release, it transforms into a "flower", which is characterised by the approximation of the RBC and the parasite membranes as well as tightly-packed merozoites surrounding the centrally positioned digestive vacuole with its hemozoin. The parasites initiate water influx into the vacuole from the erythrocyte cytosol for expansion and ultimately rupture. Thereby, the separated parasites leave the red blood cell by breaching its membrane which has been weakened by the proteolytic digestion of the erythrocyte cytoskeleton (Glushakova et al., 2010).

Using high-speed differential interference contrast (DIC) video microscopy and epifluorescence, it was demonstrated that the release occurs within 400 milliseconds (Abkarian et al., 2011). After osmotic swelling, a pore opens, ejecting 1-2 merozoites propelled by the hydrostatic pressure gradient that occurs after terminal swelling. Immediately thereafter, the membrane around the opening first curls outward to form a circular toroid around the opening, and then rapidly curls further backwards, buckles, and turns inside out (eversion), pushing the remaining parasites forward and vesiculates (Abkarian et al., 2011; Crick et al., 2013). Released parasites are immediately capable of invasion (Glushakova et al., 2005).

Parasite proteases may mediate the cascade of final cycle events. Indeed, the cycle can be blocked by the broad-spectrum cysteine protease inhibitor E64 as well as by the cysteine and serine inhibitors leupeptin and calpeptin which inhibit the final step in parasite release – the breaching of the erythrocyte membrane. On the other hand, the breakdown of the PV is not blocked (Glushakova et al., 2009).

Similarly to invasion, Ca^{2+} is an important second messenger during the release of parasites from red blood cells. A steady increase in cytoplasmic Ca^{2+} is found to precede parasite egress (Glushakova et al., 2013) with a multitude of intracellular targets. In particular, it initiates cell swelling and activates both host and parasitic proteases. However, the identification of specific proteases has been challenging and the exact timing and spacing has not been resolved yet.

P. falciparum parasites were shown to hijack host cell calpain 1 protease for destabilisation of the erythrocyte cytoskeleton and thus facilitate parasite egress. This protease is activated by elevated Ca^{2+} levels (Chandramohanadas et al., 2009). Besides, the calcium-dependent protein kinase 5 (PfCDPK5) was shown to be induced upon binding Ca^{2+} and might contribute to parasite egress by activation of perforin-like proteins, membrane channels and/or proteases (Dvorin et al., 2010). One perforin-like protein was identified as PfPLP1 which localises to the micronemes of merozoites. Ca^{2+} triggers the discharge of PfPLP1 from micronemes and these in turn bind to membranes, oligomerise and create pores. Pore formation by PfPLP1 may directly destabilise membranes leading to egress or act as gateways for additional effector proteins already present in the PV or released during egress (Garg et al., 2013).

In a forward chemical genetic screen, specific serine and cysteine protease inhibitors that block host cell rupture by *P. falciparum* were identified (Arastu-Kapur et al., 2008). Using hits from the library screen, the serine protease subtilisin-like protease 1 (PfSUB1) and the cysteine protease dipeptidyl peptidase 3 (DPAP3) were found as primary regulators of this process. It was proposed that the PfSUB1 precursor is transferred to the exonemes in vesicles along the secretory pathway. On their way, these vesicles pass vesicles containing DPAP3 which converts PfSUB1 into its active form. Before egress, PfSUB1 is released into the PV where it mediates processing of the serine repeat antigen 5 (SERA5) and other SERAs which promote egress.

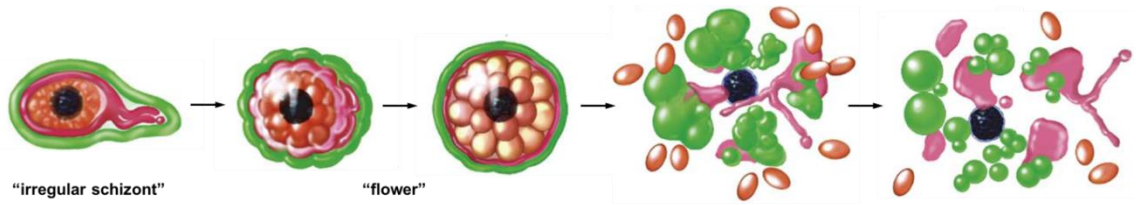

Figure 4 | Egress of malaria parasites from erythrocytes (Glushakova et al., 2005).
Sequential morphological changes of the "irregular schizont" to the "flower" followed by rupture of parasite-enclosed membranes and vesiculation of the RBC membrane. Color code: green, RBC membrane; red, PVM or TVN; orange, merozoites; black, digestive vacuole.

1.7 MSP-1 and PfSUB1

1.7.1 The merozoite surface protein 1

Covering the whole merozoite, the merozoite surface protein 1 (MSP-1) is the parasite's most abundant surface protein (Freeman and Holder, 1983; Holder et al., 1985) and implicated in the ligand-receptor interactions leading to invasion (Boyle et al., 2010; Goel et al., 2003). The 185-200 kDa precursor protein is a product of the approximately 5000 bp *msp-1* gene on chromosome 9 that is expressed during late blood stages and attached to the parasite plasma membrane via a glycosylphosphatidylinositol (GPI)-anchor. During merozoite maturation, MSP-1 is modified by the subtilisin-like protease PfSUB1 which cleaves MSP-1 into four major fragments MSP-1_{83}, MSP-1_{30}, MSP-1_{38} and MSP-1_{42}, which are named according to their molecular weight. These fragments remain non-covalently attached to each other and, together with MSP-6_{36} and MSP-7_{22}, form the merozoite surface protein 1 complex (Kauth et al., 2006; McBride and Heidrich, 1987; Pachebat et al., 2001; Stafford et al., 1994; Stafford et al., 1996; Trucco et al., 2001). Just prior or during erythrocyte invasion, PfSUB2 is released from the micronemes onto the merozoite surface and processes the most C-terminal part of MSP-1, MSP-1_{42}, yielding the MSP-1_{33} and MSP-1_{19} fragment. While MSP-1_{33} is shed off together with the remaining MSP-1 complex during invasion, MSP-1_{19} is dispatched into the red blood cells where it remains for up to 24 hours (Figure 5) (Blackman et al., 1991).

MSP-1 is ubiquitous among all *Plasmodium* species. Since the first cloning and sequencing of the protein from *P. falciparum* in 1985 (Holder et al.), several *msp-1* sequences from different field isolates were determined and revealed variable, conserved and semi-conserved regions (Figure 5) (Chang et al., 1988; Holder et al., 1985; Hope et al., 1985; McBride et al., 1982; Tanabe et al., 1987; Weber et al., 1986). Accordingly, the *msp-1* sequence is partitioned into 17 blocks (Tanabe et al., 1987). Despite the variability of some parts, all *msp-1* sequences can be assigned to two allelic isoforms, either the MAD20 or K1 allelic variants, named after field isolates from Papua New Guinea and Thailand, respectively (Hope et al., 1985; McBride et al., 1982).

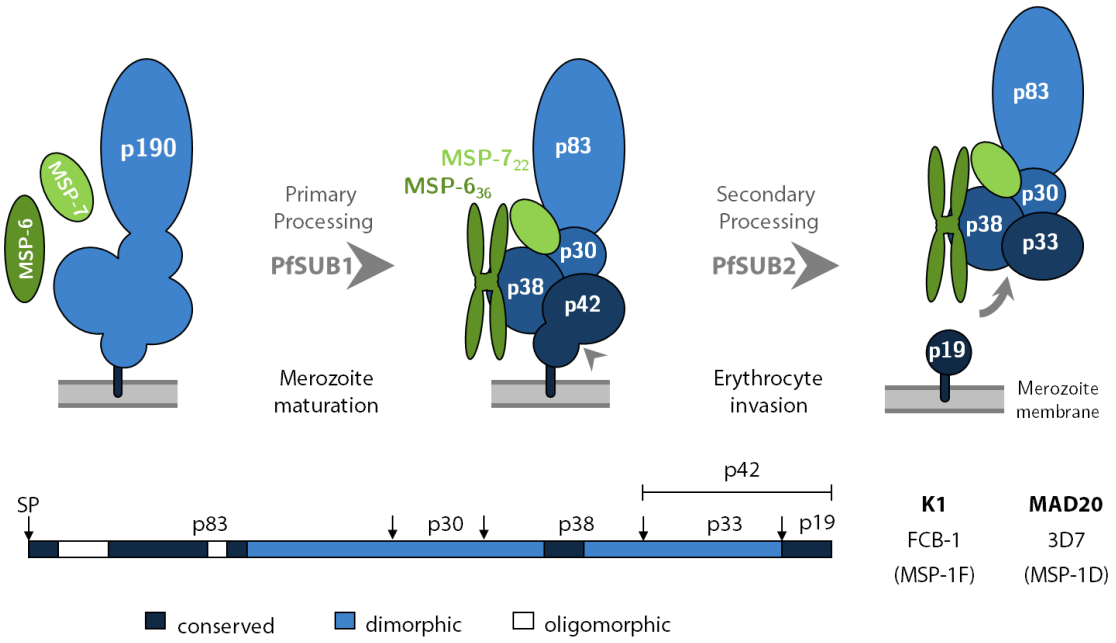

Figure 5 | Maturation of MSP-1 and allelic dimorphism.

During merozoite maturation MSP-1/6/7 precursor proteins are converted by primary processing of PfSUB1 into their mature forms: MSP-1_{36} (dark green), MSP-7_{22} (light green), MSP-1_{83}, MSP-1_{30}, MSP-1_{38} and MSP-1_{42} (different blue colours). They stay non-covalently attached to each other on the merozoite surface. Secondary processing by PfSUB2, which occurs following egress, involves further cleavage within MSP-1_{42} to produce MSP-1_{33} and MSP-1_{19}. The latter is carried into the newly invaded erythrocyte on the merozoite surface, whereas MSP-1_{33} is shed along with the remaining MSP-1/6/7 complex.
Primary sequence of MSP-1 with its conserved (dark blue), oligomorphic (white) and dimorphic (light blue) blocks according to Tanabe et al. (1987).

Several lines of evidence demonstrate that MSP-1 plays an essential role in the parasite's life cycle. All attempts to knockout the *msp-1* gene in *P. falciparum* failed, whereas the highly conserved C-terminal MSP-1_{19} fragment can be complemented with its homologue from the rodent parasite *P. chabaudi* (O'Donnell et al., 2000). In addition, MSP-1 is a target of the human immune response and antibodies blocking invasion as well as intracellular development of the parasite were identified (Bergmann-Leitner et al., 2009; Blackman et al., 1990; Woehlbier et al., 2010; Woehlbier et al., 2006)

Nonetheless, little is known about the structure and function of MSP-1. Due to the massive size of the protein, no crystal structure is available. Only the structure of the epidermal growth factor-like domain (EGF) containing MSP-1_{19} has been solved by NMR spectroscopy and X-ray analysis (Chitarra et al., 1999; Morgan et al., 1999).

In fact, the expression of recombinant MSP-1 proved to be challenging until the synthetic *msp-1* gene was cloned (Pan et al., 1999). This allowed for the expression of the entire protein in various different expression systems ranging from *E. coli*, CHO and HeLa cells, to adeno- and MVA- (modified vaccinia Ankara) viruses (Epp et al., 2003; Kauth et al., 2003; Pan et al., 1999; Westerfeld, 2002; Zong et al., 2011).

Functional, structural and conformational studies were performed using the codon-optimised *msp-1* sequences to produce MSP-1 in *E. coli* (Epp et al., 2003; Kauth et al., 2003). It was either synthesised as a full length protein or as individual subunits. These were pulse-renatured *in vitro* to form the MSP-1 complex bearing the same conformation as native MSP-1. This enabled to analyse the interaction of the various fragments with each other, showing that only the MSP-1_{30} fragment interacts with MSP-1_{83}, MSP-1_{38} and MSP-1_{42}. Whereas MSP-1_{38} and MSP-1_{42} interact with each other, MSP-1_{83} has no second interaction partner within the MSP-1 complex (see Figure 5) (Kauth et al., 2003).

Recombinant protein expression also allowed for the identification of interaction sites with other MSPs. Like MSP-1, MSP-6 and MSP-7 undergo processing by

PfSUB1 before binding to the MSP-1 complex. While MSP-7_{22} binds to the MSP-1_{38}, MSP-1_{30} and MSP-1_{83} subunits of MSP-1, MSP-6_{36} tetramerises and only contacts MSP-1_{38} (Kauth et al., 2006).

The aforementioned studies generated a unique set of MSP-1 subunits for both allelic isoforms, MAD20 and K1. Based on these MSP-1 was produced as a heterodimer expressing the 83/30 and the 38/42 fragment separately and co-renaturing them to form the MSP-1 complex. This production procedure was further employed for the production of MSP-1 under GMP conditions in order to develop a MSP-1 based vaccine.

1.7.2 Erythrocyte binding of MSP-1

Several studies report the interaction of MSP-1 with erythrocytes (Boyle et al., 2010; Goel et al., 2003; Nikodem and Davidson, 2000). However, the receptor identity is still highly debated.

Band 3 is an anion transporter in the erythrocyte membrane that moreover plays a role in maintaining the RBC integrity by anchoring the membrane to the underlying cytoskeleton (Cortes et al., 2004; Goel et al., 2003). Rather early, the protein was suggested to be involved in *Plasmodium* invasion as monoclonal antibodies to band 3 from rhesus erythrocytes blocked *P. knowlesi* invasion and immunoprecipitated band 3 from erythrocyte ghosts (Miller et al., 1983). In addition, monoclonal antibodies to band 3 inhibited *P. falciparum* invasion of human RBCs (Clough et al., 1995) and peptides of the band 3 ectodomain efficiently blocked merozoite invasion (Goel et al., 2003). The MSP-1 interaction site binding to band 3 by a chymotrypsin-sensitive, trypsin-insensitive and neuraminidase-insensitive mechanism (sialic acid-independent) was mapped to the fragments MSP-1_{42} and MSP-1_{19} (Goel et al., 2003).

In contrast, a different study found MSP-1_{38} to bind to erythrocytes, independent of glycophorin A (Nikodem and Davidson, 2000). The interaction was mapped to a 115 amino acid region of MSP-1_{38} fragment. Antibodies to MSP-1_{38} efficiently

inhibited parasite invasion *in vitro* and human sera from individuals in malaria-endemic countries recognised the domain within MSP-1_{38}.

Recently, additional interaction partners of MSP-1 were identified which are supposed to bind to erythrocytes. The MSPDBL 1 and 2 proteins (PF10_0348 and PF10_0355) are members of the *MSP-3* family (Singh et al., 2009; Wickramarachchi et al., 2009). They harbour a Duffy-binding like (DBL) domain as well as a secreted polymorphic antigen associated with merozoites (SPAM) domain. Immune sera from malaria-endemic individuals reacted to the MSPDBLs (Sakamoto et al., 2012; Wickramarachchi et al., 2009). Both MSPBDL1 and MSPDBL2 interact with MSP-1 *in vitro* and *in vivo* and are suggested to mediate the interaction with erythrocytes via their DBL domain in *in vitro* binding assays (Lin et al., 2014). Thus, MSP-1 is hypothesised to be the anchoring platform for associated proteins that in turn mediate the initial interaction of the merozoite with the erythrocyte (Lin et al., 2014).

Another potential receptor molecule identified is heparin (Boyle et al., 2010). Heparin and heparan sulphate proteoglycans are very abundant on the erythrocyte surface. They show different levels of N- and O-sulfation as well as epimerization of D-glucuronic acid (GlcA) to iduronic acid. Using real-time live microscopy, it was shown that merozoites in cultures containing 100 µg/ml heparin were unable to invade new erythrocytes (Boyle et al., 2010). These merozoites could attach but this initial interaction was not sustained and merozoites could not reorientate, thus detached again. Six different parasite lines were tested for their ability to invade in the presence of heparin and all showed a dose-depend growth phenotype. Interaction of heparin with MSP-1 was mapped to the MSP-1_{42} and MSP-1_{19} fragment by using heparin-coupled agarose beads and incubating them with recombinant fragments. The heparin binding motif xBBxBX (B, basic residue; x, hydrophobic residue) was found in both allelic isoforms of MSP-1. The level and pattern of sulfation and chain length of heparin-like molecules plays an important role for the binding to MSP-1 and, thus, for their inhibitory activity.

However, heparin is a very charged molecule that is well-known for its unspecific binding properties. This was demonstrated by a different study which revealed that the interaction of MSP-1_{42} with heparin is due to unspecific electrostatic interactions rather than a specific receptor-ligand interaction (Kobayashi et al., 2013). Indeed, proper washing procedures after incubation of erythrocytes with heparin did not block merozoite invasion like as stated. Using immunofluorescence analysis, heparin was found to interact with the merozoite surface. However, this interaction was mainly found at the tip and not throughout the whole merozoite. Thus, only partial co-localisation with MSP-1 was observed. Instead, other merozoite surface proteins were shown to interact very strongly with heparin such as PfRh1 and EBA-140. The authors concluded that "almost all erythrocyte-binding proteins of *P. falciparum* have the capacity to bind to heparin" (Kobayashi et al., 2013). According to these data, heparin would be able to inhibit invasion through its interaction with a number of parasite proteins, but not specifically with MSP-1.

1.7.3 The subtilisin-like protease PfSUB1

During merozoite maturation, MSP-1 is proteolytically processed by PfSUB1. This subtilisin-like protease is phylogenetically closely related to the bacterial subtilisin family A and was initially identified in a PCR-based approach to screen for subtilisin-like proteases within the *Plasmodium* genome (Blackman et al., 1998). Further studies localised PfSUB1 to previously unknown organelles within the parasite which were termed exonemes and are secreted into the PV prior to egress (Blackman et al., 1998; Yeoh et al., 2007). Like many proteases, PfSUB1 is synthesised as a zymogen and matures during its trafficking through the secretory pathway. Using a synthetic *pfsub1* gene, the maturation pathway has been reconstituted in an insect cell expression system as well as the production of recombinant PfSUB1 (Withers-Martinez et al., 1999; Withers-Martinez et al., 2002). PfSUB1 not only targets MSP-1 but has several targets which were identified via a bioinformatic screen. Among other PfSUB1 substrates are the

serine-rich antigens SERA 4, 5, 6, MSP-6, MSP-7, and RAP-1 (Silmon de Monerri et al., 2011; Yeoh et al., 2007). The protease is indispensable in blood stages and a key regulator of parasite egress (Child et al., 2010; Yeoh et al., 2007). As PfSUB1 is absent from the host, it appears a good drug target. A screen of over 170,000 compounds identified a selective inhibitor of PfSUB1, MRT12113 (IC_{50} of 0.3 µM) (Yeoh et al., 2007). Addition of MRT12113 to synchronous *P. falciparum* cultures did not affect intracellular growth. Yet, it specifically inhibited parasite egress with an effective dose (ED_{50}) against schizont rupture of 180 µM. Analysis of parasite cultures revealed immature SERA5 in the supernatant, resulting from the inactivation of PfSUB1 by MRT12113 (Yeoh et al., 2007). However, SERA5 in its mature form is an important protease involved in egress. Besides, lower concentrations of the inhibitor allowed for parasite egress, but prevented the merozoites from invading new erythrocytes (ED_{50} 25µM). This observation was explained by the fact that processing of merozoite surface proteins by PfSUB1 does not or only partially occur indicating an important role of PfSUB1 for preparing the merozoites for invasion (Koussis et al., 2009). In fact, MSP-1, 6 and 7 undergo proteolytic processing PfSUB1 that induces changes in their structural conformation and thus their binding properties (Boyle et al., 2010; Kauth et al., 2006). Of note, MSP-1 maturation occurs in a distinct order (Child et al., 2010). Using synthetic peptides, recombinant proteins and protein extracts from parasite cultures the processing order of MSP-1 by PfSUB1 was described (Child et al., 2010; Koussis et al., 2009). While the K1 variant of MSP-1 is cleaved starting from its N- up to its C-terminus, the cleavage order of the MAD20 isoform is different, with the 30/38 site being processed first, followed by the 83/30, 83 internal sites, and finally the 38/42 cleavage site (Child et al., 2010). These data indicate that PfSUB1-regulated maturation of MSP-1 is crucial for its function as well as parasite viability.

1.8 Molecular genetic tools in *Plasmodium falciparum*

Although the genome of *P. falciparum* was entirely sequenced more than a decade ago (Gardner et al., 2002), the function of approximately half of its ~ 5700 genes remains unknown (Kolevzon et al., 2014). While the transfection of *Plasmodium* parasites led to the establishment of a broad range of molecular genetic tools, these are effort- and time-intensive. Especially the genome composition of *Plasmodium* with ~ 80 % AT basepairs (Gardner et al., 2002) makes the functional analysis of genes challenging. In addition, transfection of plasmid DNA remains very inefficient at between 10^{-5} and 10^{-6} (O'Donnell et al., 2002b) and stable integration of transfected DNA relies on cycling periods of episomal plasmid replication and recombination before integrants are obtained (Meissner et al., 2007). As *Plasmodium* parasites are haploid during the blood stage development, disruption is only applicable to non-essential genes. Therefore, if the gene of interest is essential, tools that make use of gene expression engineering or mutagenesis are employed. Some of the latest methods will be described here or are summarised in Table 2.

One technique is the destabilisation domain (DD) system. Initially established in *Toxoplasma gondii* (Herm-Gotz et al., 2007), it was lately adapted to *P. falciparum* (Armstrong and Goldberg, 2007). The protein of interest is fused to the DD and stabilised by a small ligand. If this ligand is removed, the protein is dispatched to the proteasome. However, it is very important that the tag does not interfere with protein function. Furthermore, residual protein remains and the system has limited utility for proteins that are trafficked via the parasite secretory pathway (Collins et al., 2013).

The Tet repressor (TetR)-based regulation system of transcription has proven to be difficult in *Plasmodium*, as sufficient repression of transcription by TetR has not been achieved (Collins et al., 2013). Nevertheless, transactivation domains based on apicomplexan ApiAP2 transcription factors have recently been employed to obtain stage-dependent tetracycline-dependent gene knockdown in *T. gondii* and *Plasmodium* (Pino et al., 2012). Although of great potential, all of these

conditional approaches require transactivator-responsive minimal promoters that very accurately mimic the transcriptional profile of the gene of interest (Collins et al., 2013).

Despite promising reports, most other widely used gene silencing approaches that affect transcript stability, translation or splicing such as the self-cleaving glmS ribozyme (Prommana et al., 2013) or morpholino oligonucleotides (Augagneur et al., 2012) have been proven ineffective in *Plasmodium*. In contrast, site-specific recombination techniques for gene modification or deletion are well established e.g. recombinases Cre/lox and Flp/FRT. Nonetheless, robust regulation of these systems has yet not been achieved. Thus, the DiCre system was developed in which Cre recombinase is expressed as two separate, enzymatically inactive polypeptides, each fused to a different rapamycin-binding protein (FKBP12 or FRB). Addition of rapamycin induces heterodimerisation and, thus, activation of the Cre recombinase (Andenmatten et al., 2012). As much as this system works in principle, the vector design is challenging and genetically manipulated parasites harbouring the loxP sites for recombination are difficult to generate. As the *msp-1* gene was shown to be essential, functional analysis relies on conditional genetic tools regulating the expression. However, the above mentioned systems are not suitable for the expression of such a large protein that is furthermore post-translationally modified by proteases.

Table 2 | Molecular genetic tools in *P. falciparum*.

Genetic tool	reference
DiCre system	Andenmatten et al. (2012)
Flp/FRT system	Carvalho et al. (2004)
TetR system	Meissner et al. (2005)
glmS ribozymes	Prommana et al. (2013)
Destabilisation domain	Armstrong and Goldberg (2007)
CRISPR-Cas9	Ghorbal et al. (2014)
Auxin-based degron system	Kreidenweiss et al. (2013)
Zinc-finger nucleases	Straimer et al. (2012)
peptide-morpholino oligomer	Augagneur et al. (2012)

1.8.1 Blasticidin co-selection system

Upon transfection of *P. falciparum*, DNA is taken up as episomal plasmids that are usually present as concatamers at up to 15 copies (O'Donnell et al., 2002a; Williamson et al., 2002). Variation of the copy number influences the amount of gene expression from the episome. This can be exploited to regulate transgene expression levels as by the blasticidin co-seelction system (Epp et al., 2008). The method is based on the use of a bidirectional promoter that drives the expression of both, the selectable marker and the gene of interest (Figure 6). In contrast to conventional strategies, only one expression cassette is required, minimising the size of the construct and improving its stability in the parasite and in *E. coli* during cloning. Transgene expression is regulated by the addition of varying concentrations of blasticidin S to the culture medium. The selection marker blasticidin S deaminase (bsd) is required for detoxification and maintenance of parasite viability. Thus, only transfectants with a sufficiently high expression of *bsd* survive the treatment. Since *bsd* expression is in turn driven by the same promoter as the gene of interest, increasing the blasticidin concentration also enhances the transgene expression.

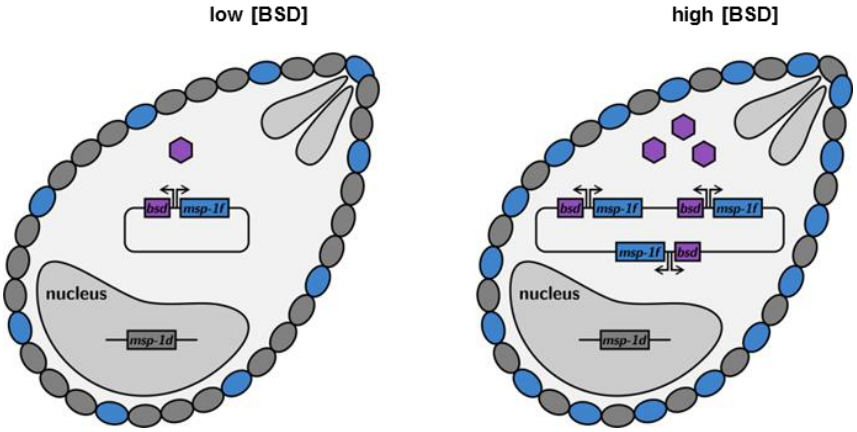

Figure 6 | Blasticidin co-selection system.
The blasticidin co-selection system comprises a plasmid containing a bi-directional promoter (*var* intron) driving the expression of the blasticidin S deaminase (*bsd*; purple) and *msp-1f* (blue). Upon transfection of *P. falciparum* parasites the plasmid is maintained episomally. Increasing blasticidin concentrations (purple hexagons) select for parasites harbouring concatamers of this plasmid, thus conferring resistance to high blasticidin concentrations and leading to the expression of more *msp-1f*. MSP-1F and MSP-1D protein on the merozoite surface are displayed as blue and grey ellipses, respectively.

1.8.2 Blasticidin resistance

Blasticidin S is a fungal toxin with a molecular weight of 422.2 Da which inhibits mRNA translation on ribosomes, thus killing most prokaryotic and eukaryotic cells (Yamaguchi et al., 1965). It is widely used in molecular transfections of various cell types as it selects for the expression of detoxifying enzymes. One of these is the blasticidin S deaminase from *Aspergillus terreus* used in this study which converts blasticidin S to a nontoxic deaminohydroxy derivative (Hill et al., 2007).

Recent findings showed that natural blasticidin resistance in *P. falciparum* parasites can occur via the altered expression of *clag 3* genes that are important for the formation of the plasmodial surface anion channel (PSAC) (Hill et al., 2007).

Upon infection, malaria parasites increase erythrocyte permeability to numerous solutes including nutrients required for intracellular parasite growth. Among them are sugars, amino acids, purines, vitamins, and organic cations. Besides, anti-malarial toxins have an increased uptake and parasites are able to alter permeability to acquire resistance to anti-malarials. The origin and nature of the uptake mechanism are still controversial, although the primary candidate for parasite-encoded ion channel involved in nutrient uptake is PSAC (Hill et al., 2007; Nguitragool et al.).

Using parasite mutants as well as specific inhibitors the genetic basis of PSAC activity has been addressed (Cortes et al., 2004; Cortes et al., 2007; Desai, 2014; Hill et al., 2007; Mira-Martinez et al., 2013; Nguitragool et al.). Thereby the *clag 3* genes, PFC0110w and PFC0120w, from the subtelomeric regions of chromosome 3 were identified as mediators for resistance (Desai, 2014). These two genes named *clag 3.1* and *clag 3.2* are separated by only 10 kb and share 95 % nucleotide sequence identity. They show a mutually exclusive expression (Mira-Martinez et al., 2013) that is controlled by the chromatic state of the bistable chromatin domain (Crowley et al., 2011). Using immunofluorescence analysis, Western blotting and ultracentrifugation, *clag 3* gene products were shown to be

synthesised hours before PSAC activity is detected, packaged in rhoptries, secreted, and trafficked to erythrocyte membrane (Nguitragool et al.). Resistance to blasticidin S is conferred by switching or even silencing of *clag 3* gene expression. *Clag 3.2* mediates more efficient uptake of blasticidin than *clag 3.1* and silencing of both genes completely blocks blasticidin uptake as well as transport of other solutes (Mira-Martinez et al., 2013). Likewise, blasticidin-resistant yeast was identified after UV-mediated mutation and appeared to use reduced permeability as the primary mechanism of resistance (Ishiguro and Miyazaki, 1985).

In summary, two models for *clag 3* contribution to PSAC activity were proposed. In the first, the *clag 3* gene product alone builds up the PSAC. The second proposes that the *clag 3* products interact with proteins to form functional PSAC (Nguitragool et al.). The mutually exclusive expression of the *clag 3* genes as well as gene switching is determined by epigenetic mechanisms. Therefore, they influence the parasites' susceptibility to inhibitors or toxins like blasticidin S.

Potential selection of blasticidin S-resistant mutants without plasmids carrying the resistance gene reveals the limitation to its use in transfections (Hill et al., 2007). This needs to be kept in mind when positively selecting parasites with blasticidin S using the blasticidin co-selection system.

1.9 Aim of thesis

The aim of this work was to gain insights into the biological significance of primary processing of MSP-1 and in turn MSP-1 function itself. Several approaches were pursued. Initially, processing sites of PfSUB1 within MSP-1 were identified *in silico*. Accordingly, recombinant forms of MSP-1 with mutations in the respective sites were generated for *in vitro* processing analysis and elucidation of actual usage by PfSUB1. Moreover, effects of non-cleavable MSP-1 variants were examined *in vivo* with respect to localisation, processing and effect on parasite growth. As these mutants are potentially lethal, blasticidin co-selection was employed to adjust the expression of mutant *msp-1*. Thus, the *in vitro* results and the feasibility of episomal *msp-1* expression were reviewed, while the biological effect of impaired primary processing were addressed. Finally, the effect of processing on the structure of MSP-1 as well as its binding properties to other proteins such as MSP-6 and MSP-7 or to erythrocytes were investigated.

2 Materials and Methods

2.1 Material

2.1.1 Laboratory Equipment

Table 3 | Laboratory equipment overview.

equipment	source
Autoclaves:	
- 2540 EL	Systec GmbH, Wettemberg
- 5075 ELV	Systec GmbH, Wettemberg
Blot developing machine, Hyperprocessor	GE Life Sciences, Freiburg
Camera, Kodak DC120 Digital Zoom	Kodak, Rochester, NY, USA
Centrifuge J2-MC	Beckman Instruments, Inc., Palo Alto, CA, USA
Centrifuge, Megafuge 1.0R	Heraeus Instruments, Hanau
Centrifuge, Pico 17	Heraeus Instruments, Hanau
Confocal laser scanning microscope LSM 510	Zeiss, Jena
Chromatography system, ÄKTA Purifier 100	GE Life Sciences, Freiburg
DNA electrophoresis apparatus	Biozyme, Hessisch Oldendorf
Electroporation device, Gene Pulser® II	Bio-Rad, Munich
Film developer, Hyperprocessor	Amersham Biosciences, Freiburg
Film exposition cassette	Roth, Karlsruhe
Freezer:	
- 20°C comfort	Liebherr International Deutschland GmbH, Biberach an der Riss
- 80°C	Thermo Fisher Scientific GmbH, Karlsruhe
Fridge	Bosch, Stuttgart
Gas burner, gasprofi 1 micro	WLD-TEC GmbH, Göttingen
Heating block	VWR International GmbH, Darmstadt
Ice machine, AF30	Scotsman, Vernon Hills, IL, USA
Incubators:	
- Cell Star cytoperm 2	Heraeus Instruments, Hanau
- CO_2-Incubator BBD6620	Heraeus Instruments, Hanau
- Hera Cell	Heraeus Instruments, Hanau
Incubator shaker, Innova 4000/4300	New Brunswick Scientific Co. Inc., Enfield, CT, USA
Inverted microscope, Axiolab	Zeiss, Jena
Laminar Flow Cell culture hood	Heraeus Instruments, Hanau

equipment	source
Magnetic stirrer	VWR International GmbH, Darmstadt
Microwave	Zanussi, Nuremberg
PAA gel system, MiniVE	GE Life Sciences, Freiburg
PCR machine, 2720 Thermal Cycler	Applied Biosystems, Darmstadt
pH meter InoLab® pH7110	WTW, Weilheim
PipetmanGilson P2, P10, P20, P200, P1000	Gilson International, Bad Camberg
Pipettus® akku	Hirschmann Labortechnik, Eberstadt
Power supply EV 245	Consort, Turnhout, Belgium
Printer hp LaserJet 1300	Hewlett Packard, Heidelberg
Protein electrophoresis system, Mighty Small II	Hoefer, Inc., Holliston, MA, USA
Quartz cuvettes	Hellma, Mühlheim
Real time PCR machine, ABI 7500	Applied Biosystems, Darmstadt
Rotors:	
SS-34, GS-3	DuPont Instruments, Bad Homburg
Scales:	
Laboratory MC1-LC-2200 P	Sartorius, Göttingen
Scaltec SBC 32	Scaltec, Heiligenstadt
Shaking incubator, Innova 4300	New Brunswick Scientific, Nürtigen
Sonifier, B-12 Branson	Sonic Power Company, Danbury, CT, USA
UV-lamp Typ N-6 L	M&S Laborgeräte GmbH, Wiesloch
UV-Transilluminator, TFX-35M,	Life Technologies, Gibco BRL, Darmstadt
Vortex	VWR International GmbH, Darmstadt
Waterbath precitherm PFV	Labora Mannheim GmbH, Mannheim
Western Blot aperture, XCell SureLock®Mini Cell	Invitrogen, Karlsruhe

2.1.2 Software

Table 4 | Software overview

software	source
CellQuest Pro	Becton Dickinson, Franklin Lakes, NJ, USA
ClustalW2	EMBL-EBI, Hinxton, UK
EndNote X7.1	Thomson Reuters, Philadelphia, PA, USA
EnzymeX	Nucleobytes, Aalsmeer, The Netherlands
Expasy Proteomics server	SIB Swiss Institute of Bioinformatics, Switzerland
FIJI image analysis	National Institutes of Health, Bethesda, MD, USA
GraphPad Prism 6	GraphPad Software, Inc., La Jolla, CA, USA

software	source
Kodak Digital Science 1D	Kodak, Rochester, New York, USA
Microsoft Excel 2010	Microsoft Corporation, Redmond, WA, USA
Microsoft PowerPoint 2010	Microsoft Corporation, Redmond, WA, USA
Microsoft Word 2010	Microsoft Corporation, Redmond, WA, USA
PlasmoDB	The EuPathDB Project Team, USA
Prediction of Protease Specificity PoPS	Monash University, Stanford, CA, USA
Primer3	(Rozen and Skaletsky, 2000)
SDS 1.3.1 software	Applied Biosystems, Damrstadt
Serial Cloner 2.6	Serial Basics
Zeiss Image Examiner	Zeiss, Jena

2.1.3 Disposables/Consumables

Table 5 | Overview of disposables and consumables.

disposable/consumable	source
1.5 ml tubes	Sarstedt AG & Co., Nümbrecht
15 ml tubes	Greiner Bio-One, Frickenhausen
50 ml tubes	Greiner Bio-One, Frickenhausen
96-well plates	Thermo Fisher Scientific Ltd., Loughborough, UK
Centrifugal filter units, Amicon	Millipore, Molsheim
Chelating Sepharose™ Fast Flow	GE Life Sciences, Freiburg
Cover glasses	Roth, Karlsruhe
Cryo vials	Greiner Bio-One, Frickenhausen
Cuvettes	Sarstedt AG & Co., Nümbrecht
Dialysis tubing, Spectra/Por	Roth, Karlsruhe
Electroporation cuvettes	Biorad, Munich
Glass slides	Paul Marienfeld GmbH, Lauda
Gloves	Hartmann, Heidenheim
Immobilon-P PVDF Membrane (0,45 µm)	Millipore Corp., Billerica, MA, USA
Kimwipes lite 200	Kimberly-Clark, Irving, TX, USA
Parafilm	Pechiney Plastic Packaging, Chicago, IL, USA
PCR tubes	Sarstedt AG & Co., Nümbrecht
Petri dishes	Greiner Bio-One, Frickenhausen
Pipette tips, Diamond (10 µl, 200 µl, 1000 µl)	Gilson International, Bad Camberg

disposable/consumable	source
Plastic pipettes (1 ml; 2 ml; 5 ml; 10 ml; 25 ml)	Corning Inc., Bodenheim
SP Sepharose HP	GE Life Sciences, Freiburg
Sterile filters, Rotilabo® (0.2µm; 0.45µm)	Roth, Karlsruhe
WhatmanTM 3MM paper	GE Healthcare, Freiburg

2.1.4 Chromatography media

Table 6 | Overview of chromatography media.

media	source
Chealting Sepharose Fast Flow	GE Healtcare, Freiburg
GSTrap™ HP	GE Healtcare, Freiburg
Q Sepharose HP	GE Healtcare, Freiburg

2.1.5 Chemicals

Table 7 | Overview of chemicals.

chemical	source
Acetic acid	Sigma Aldrich, Taufkirchen
Acyrlamide, 30%	Roth, Karlsruhe
Agar	AppliChem, Darmstadt
Agarose Ultra Pure®	Invitrogen, Karlsruhe
Albumax II	Invitrogen, Karlsruhe
Albumin Fraction V	Roth, Karlsruhe
Ammoniumdihydrogenphosphat	Roth, Karlsruhe
Ammoiniumpersulfat	Grüssing, Filsum
Amplicillin	Roth, Karlsruhe
BM Chemiluminescence Blotting Substrate (POD)	Roche Diagnostics, Mannheim
Biuret reagent	Merck, Darmstadt
Bradford reagent	Bio-Rad, Munich
Calcium chloride-2-hydrate	AppliChem, Darmstadt
Coomassie Brilliant Blue R250	Merck KGaA, Darmstadt
Dibutyl phthalate	Sigma Aldrich, Taufkirchen
Diethanolamin	Roth, Karlsruhe
Di-potassium hydrogen phosphate/ potassium hosphate	Grüssing, Filsum

chemical	source
Dimethylsulfoxid (DMSO)	Merck KGaA, Darmstadt
Disodiumhydrogenphosphate-2-hydrate	AppliChem, Darmstadt
DL-1,4-Dithiothreitol (DTT)	Roth, Karlsruhe
dNTPs	New England Biolabs, Schwalbach
D-Sorbit	Chemsolute®bio, Th. Geyer GmbH & Co. KG, Renningen
EDTA	AppliChem, Darmstadt
EGTA	Roth, Karlsruhe
Epoxysuccinyl-leucylamido(4-guanidino)butane (E-64)	Roche Diagnostics, Mannheim
Ethanolamine	Roth, Karlsruhe
Ethanol	VWR International GmbH, Darmstadt
Ethidium bromide	Sigma Aldrich, Taufkirchen
Giemsa (0.4 % (w/v))	Roth, Karlsruhe
Glutaraldehyde solution in water 25%	Sigma Aldrich, Taufkirchen
Glycerol	Chemsolute®bio, Th. Geyer GmbH & Co. KG, Renningen
Glycin	AppliChem, Darmstadt
Guanidinium hydrochloride	AppliChem, Darmstadt
Hoechst 33342	Invitrogen, Karlsruhe
Hydrochloric acid	Sigma Aldrich, Taufkirchen
Imidazol	Merck KGaA, Darmstadt
Immersion oil 518 C	Waldeck GmbH & Co KG, Münster
IPTG	Roth, Karlsruhe
Isopropanol	Sigma Aldrich, Taufkirchen
Kalium chloride	AppliChem, Darmstadt
Kanamycin	Roth, Karlsruhe
L-Arginin	Roth, Karlsruhe
LB-Broth	Sigma Aldrich, Taufkirchen
Leupeptin	Roche Diagnostics, Mannheim
L-Glutathion, oxidised	Roth, Karlsruhe
L-Glutathion, reduced	Roth, Karlsruhe
Heparin sodium salt	Sigma Aldrich, Taufkirchen
L-Histidin	Roth, Karlsruhe
2-Mercaptoethanol	Invitrogen, Karlsruhe
Magnesium chloride	Merck KGaA, Darmstadt
Magnesium sulfate	Sigma, Taufkirchen

chemical	source
Methanol	AppliChem, Darmstadt
Milk powder	Roth, Karlsruhe
Nickel $^{2+}$ions	Sigma Aldrich, Taufkirchen
Phosphate buffered saline tablets (PBS)	Sigma Aldrich, Taufkirchen
Pefabloc SC PLUS	Roche Diagnostics, Mannheim
Pepstatin	Roche Diagnostics, Mannheim
Percoll	GE Healthcare, Freiburg
Phenylmethanesulfonylfluoride (PMSF)	Roche Diagnostics, Mannheim
Potassium hydroxide	Sigma Aldrich, Taufkirchen
Potassium phosphate	Roth, Karlsruhe
Propidium iodide	Life Technologies, Darmstadt
RPMI 1640-Medium	Invitrogen, Karlsruhe
Saponin	Sigma Aldrich, Taufkirchen
Sodium acetate	Merck KGaA, Darmstadt
Sodium azide	Sigma Aldrich, Taufkirchen
Sodium chloride	Merck KGaA, Darmstadt
Sodium deoxycholate	Serva, Heidelberg
Sodium dihydrogen phosphate	Applichem, Darmstadt
Sodium dodecyl sulfate (SDS)	Roth, Karlsruhe
Sodium hydrogen carbonate	Applichem, Darmstadt
Tetramethylethylendiamine (TEMED)	Roth, Karlsruhe
Trichloric acid	Sigma Aldrich, Taufkirchen
TRI reagent solution	Ambion, Life Technologies, Darmstadt
Tris	Roth, Karlsruhe
Tween20	Merck KGaA, Darmstadt

2.1.6 Enzymes

Table 8 | Enzyme overview.
All restriction enzymes were ordered from New England BioLabs, Schwalbach.

enzyme	source
Antarctic Phosphatase	New England Biolabs, Schwalbach
Taq DNA Polymerase	Invitrogen, Karlsruhe
Phusion DNA Polymerase	New England Biolabs, Schwalbach
Platinum Pfx DNA Polymerase®	Invitrogen, Karlsruhe

enzyme	source
DNase I	Roche Diagnostics, Mannheim
rPfSUB1 (expressed in insect cells; 1.5 units/µl)	Dr. Michael Blackman, NIMR London, UK
T4 DNA Ligase	Invitrogen, Karlsruhe
Chymotrypsin	Sigma Aldrich, Taufkirchen
Trypsin	Sigma Aldrich, Taufkirchen
Neuraminidase	Sigma Aldrich, Taufkirchen

2.1.7 Markers

Table 9 | Macromolecular marker overview.

marker	source
2-log DNA ladder	New England Biolabs, Schwalbach
Color Plus Protein marker (prestained)	New England Biolabs, Schwalbach
Protein ladder 10-250kDa (unstained)	New England Biolabs, Schwalbach

2.1.8 Molecular Biology Kits

Table 10 | Molecular biology kit overview.

kit	source
BM Chemiluminescence Blotting Substrate (POD)	Roche, Mannheim
NucleoBond® PC2000	Macherey-Nagel GmbH & Co. KG, Düren
NucleoSpin® Extract II	Macherey-Nagel GmbH & Co. KG, Düren
NucleoSpin® Plasmid	Macherey-Nagel GmbH & Co. KG, Düren
SensiFAST SYBR® Lo-ROX Kit	Bioline, Luckenwalde
DNeasy Blood & Tissue Kit	Qiagen, Hilden
pGEM®-T Vector System	Promega, Madison, WI, USA
Pure Link RNA Mini Kit	Invitrogen, Karlsruhe
SuperScript® II Reverse Transcriptase	Invitrogen, Karlsruhe
TOPO® blunt-end cloning	Life Technologies, Darmstadt

2.1.9 Antibodies

Table 11 | Antibody overview.
Applications for different dilutions are indicated in brackets.

antibody	dilution	origin
α-MSP-1F33 rabbit serum	1:200 (IFA) 1:1000 (Western Blot)	Prof. M. Blackman, NIMR London, UK
mAb 111.4 (mouse)	1:200 (IFA)	Prof..M. Blackman, NIMR London, UK
α-MSP-1$D_{42\Delta EGF}$ rabbit serum	1:10,000	Prof. H. Bujard, ZMBH
Anti-AMA1/DiCo rabbit serum)	1:5,000	Dr. E. Remarque, BPRC, Leiden, NL
α-Beide Hälften MSP-1D (rabbit)	1:10,000	Prof. H. Bujard, ZMBH,
α-Beide Hälften MSP-1F (rabbit, Montanide)	1:1000	Prof. H. Bujard, ZMBH
α-MSP-1F K1 S(rabbit)	1:1000	Prof. H. Bujard, ZMBH
α-MSP-1F (Aotus monkeys)	1:10,000	Prof. H. Bujard, ZMBH
α-rabbit IgG Peroxidase conjugate	1:20,000 – 1:30,000	Sigma-Aldrich, St. Louis, MO, USA
α-rabbit IgG Alkaline Phosphatase conjugate	1:30,000	Sigma-Aldrich, St. Louis, MO, USA
α-mouse IgG Peroxidase conjugate	1:30,000	Sigma-Aldrich, St. Louis, MO, USA
α-rabbit IgG Alkaline Phosphatase conjugate	1:30,000	Sigma-Aldrich, St. Louis, MO, USA
α-human IgG Alkaline Phosphatase	1:30,000	Sigma-Aldrich, St. Louis, MO, USA

2.1.10 Plasmids

Table 12 | Bacterial expression vector overview.

vector	source
pZE12-d-190H	Prof. H. Bujard, ZMBH
pZE23-f-GX190H	Prof. H. Bujard, ZMBH
pZE23-f-GX190H-mut30/38	this study
pZE13-f-83/30	Prof. H. Bujard, ZMBH
pZE13-f83/30-mutDG	this study
pZE23-f-38/42	Prof. H. Bujard, ZMBH
pZE23-f-38/42-mutG/E	Prof. M. Blackman, NIMR London, UK
pZE23-f-38/42-mutG/V	Prof. M. Blackman, NIMR London, UK

vector	source
pZE23-f-38/42-mutG/T	Prof. M. Blackman, NIMR London, UK
pZE23-f38/42-mutKKcan	this study
pZE23-f38/42-mutKKcanKKalt	this study
pZE23-f38/42-mutKKcanKKaltLLC&B	this study
pZE23-f38/42-mutKKcanKKaltLLC&B	this study
pZE23-f38/42-mutKKcanKKaltLLC&BKK2ndalt	this study
pZE23-f38/42-mutKKcanLLC&B	this study

Table 13 | *Plasmodium* vectors overview.

vector	source
pHBIMFwt	Thilo Fobes, AG Epp, Dept. of Infectious Diseases, Heidelberg
pHBIMF38/42mutG/E	Anna Sierakowski, AG Epp, Dept. of Infectious Diseases, Heidelberg
pHBIMF38/42mutG/V	Anna Sierakowski, AG Epp, Dept. of Infectious Diseases, Heidelberg
pHBIMF38/42mutG/T	Anna Sierakowski, AG Epp, Dept. of Infectious Diseases, Heidelberg
pHBIMF38/42mutKKcan	this study
pHBIMF38/42mutKKcanKKalt	this study
pHBIMF38/42mutKKcanKKaltKK2ndalt	this study
pHBIMF38/42mutKKcanKKaltLLC&BKK2ndalt	this study
pHBIMFmutall	this study
pHBIRH	Dr. C. Epp, Dept. of Infectious Diseases, Heidelberg
pCC1	Dr. A. Maier, The Walter and Eliza Hall Institute of Medical Research, Melbourne, Australia
pCC1-PfMSP1D-KO	this study
pHTK	Dr. M. Deponte, Dept. of Infectious Diseases, Heidelberg
pHTK-PfMSP1D-KO	this study
PF_0350_3'HA-DD29	Sophia Deil, AG Lanzer, Dept. of Infectious Diseases, Heidelberg
msp1d-HA-DD29	this study
msp1d-HA-DD29-p19-GPI	this study
msp1d-HA-DD29-GPI	this study

2.1.11 Oligonucleotides

Table 14 | Oligonucleotide overview.

oligonucleotide	Sequences 5' to 3'	T_m [C]
General primers		
f8330 seq up	CCTCATCGTACTCAAGAAAGAG	53
f3038 seq up	CAGCTCCATGCAACCACTGTC	56.3
Seq up f38-42 \ Anna Sierakowski	GCCTATCTTCGGCGAGAGCG	57.9
Seq down f38-42 \ Anna Sierakowski	GGCCTCCAGGTGAATTACGAAG	56.7
hsp86 3'UTR seq for	TTGGGGTGATGATAAAATGAAA	47.4
Site-directed mutagenesis		
f8330 mutGT For	GAACATTAAAGGTGAAACACAGTCAGATAACTCCG	62.1
f8330 mutGT RC	CGGAGTTATCTGACTGTGTTTCACCTTTAATGTTC	62.1
f8330 mut DG For	CATTAAAACTGAAGACCAGTCAGGTAACTCCGAGCC	65.6
f8330 mut DG RC	GGCTCGGAGTTACCTGACTGGTCTTCAGTTTTAATG	65.6
f3038 mut VA For	CAAGCCCGAAGCGAGCGTTAACGACGACACC	68.3
f3083 mut VA RC	GGTGTCGTCGTTAACGCTCGCTTCGGGCTTG	68.3
f3038 mut AD For	CCGAAGTGAGCGATAACGACGCCACCTCTCACTCG	70.3
f3038 mut AD RC	CGAGTGAGAGGTGGCGTCGTTATCGCTGCTCACTTCGG	72
f3038 DD For	GACAAGCCCGAAGATAGCGATAACGACGACACC	66.9
f3038 DD RC	GGTGTCGTCGTTATCGCTATCTTCGGGCTTGTC	66.9
f3038 KK For	GACAAGCCCGAAAAGAGCAAGAACGACGACACC	66.9
f3038 KK RC	GGTGTCGTCGTTCTTGCTCTTTTCGGGCTTGTC	66.9
f3842can mutKK For	CTCGGCCAGGTGAAGACCAAGGAGGCTGTCACTCC	71.5
f3842can mutKK Rev	GGAGTGACAGCCTCCTTGGTCTTCACCTGGCCGAG	71.5
f3842can mutDD For	CTCGGCCAGGTGGACACCGATGAGGCTGTCACTCC	72.6
f3842can mutDD Rev	GGAGTGACAGCCTCATCGGTGTCCACCTGGCCGAG	72.6
f3842 mutEG For	GTGCCTATCTTCGAAGGGAGCGAGGAGGACTAC	68.1
f3842 mutEG Rev	GTAGTCCTCCTCGCTCCCTTCGAAGATAGGCAC	68.1
f3842 mutGI For	CATCATTGTGCCTGGCTTCATCGAGAGCGAGGAG	68
f3842 mutGI Rev	CTCCTCGCTCTCGATGAAGCCAGGCACAGGCACAATGATG	71.7
f3842 mutSG For	GTGCCTATCTTCTCCGAGGGCGAGGAGGAC	68.5
f3842 mutSG Rev	GTCCTCCTCGCCCTCGGAGAAGATAGGCAC	68.5

oligonucleotide	Sequences 5' to 3'	T_m [C]
f3842 alt mutKK For	CATCATTGTGCCTAAGTTCAAGGAGAGCGAGGAG	65.6
f3842 alt mutKK Rev	CTCCTCGCTCTCCTTGAACTTAGGCACAATGATG	65.6
f3842 alt mutDD For	CATCATTGTGCCTGACTTCGACGAGAGCGAGGAG	68
f3842 alt mutDD Rev	CTCCTCGCTCTCGTCGAAGTCAGGCACAATGATG	68
f3842 2nd alt mutKK For	CCTGCATCTACTCATGTCAAAAAAGAGTCCAATAC	62.1
f3842 2nd alt mutKK Rev	GTATTGGACTCTTTTTTGACATGAGTAGATGCAGG	62.1
f3842 2nd alt mutDD For	CCTGCATCTACTCATGATGAGGACGAGTCCAATAC	65.6
f3842 2nd alt mutDD Rev	GTATTGGACTCGTCCTCATCATGAGTAGATGCAGG	65.6
new primer mut VV 2nd alt	CCTGCATCTACTCATGTCGTTGTCGAGTCCAATACAATTACC	67.4
new primer mut VV 2nd alt Rev	GGTAATTGTATTGGACTCGACAACGACATGAGTAGATGCAGG	67.4
new primer mut DED 2nd alt	GCCTGCATCTACTCATGATGAGGACGAGTCCAATACAATTACC	68.3
new primer mut DED 2nd alt Rev	GGTAATTGTATTGGACTCGTCCTCATCATGAGTAGATGCAGGC	68.3
mut KK rev Cooper Bujard	ATCGTCGACGTTCTGCTTTGTTTTAATTGTATTGGACTC	63.4
mut KK for Cooper Bujard	GAGTCCAATACAATTAAAACAAAGCAGAACGTCGACGAT	63.4
CB mut LL P1P2 for	GTCCAATACAATTACCACATTGTCGAACGTCGACGATG	65.5
CB mut LL P1P2 rev	CATCGTCGACGTTCAGCAATGTGGTAATTGTATTGGAC	65.5
CB mut LL P2P4 for	GTCCAATACAATTCTCACATTGCAGAACGTCGACGATG	65.5
CB mut LL P2P4 rev	CATCGTCGACGTTCTGCAATGTGAGAATTGTATTGGAC	65.5
Knockout via pCC1 / pHTK system		
pHTK 5 KO for	ACTAGTTGTGTGTAAAAGTGTTTTTGTTTTG	55.1
pHTK 5 KO rev	AGATCTTTAGGACCACTTGGACCACTTGT	60.1
pHTK 3 KO for (14-16)	CCATGGCCATTTTTGGAGAATCCGAAG	59.7
pHTK 3 KO rev (14-16)	CCTAGGCGCATTGGTGTTGTGAAATG	59.5
pHTK 3 KO for (16)	CCATGGCCAGCAAAAACAGACGAACA	59.5
pHTK 3 KO rev (16)	CCTAGGGCTTCGAAGTCGTAAGGGTTT	61.3
pHTK mut for	GCTTTAATTCAATATAGAAGATCATATTC	51.6
pHTK mut rev	GAATATGATCTTCTATATTGAATTAAAGC	51.6
pCC1 5 KO for	CCGCGGTGTGTGTAAAAGTGTTTTTGTTTTG	60.4
pCC1 5 KO rev	ACTAGTTTAGGACCACTTGGACCACTTGT	60.1
hdhfr for	GCATGGTTCGCTAAACTGCATC	54.8
hdhfr rev	GCCTTTCTCCTCCTGGACATC	56.3
pHTK seq for	GCTATTTACATGCATGTGCATGC	53.3
pHTK seq rev	TACCCGAGCCGATGACTTAC	53.8
pCC1 CD seq for	GCTATTTACATGCATGTGCATGC	53.5

oligonucleotide	Sequences 5' to 3'	T_m [C]
pCC1 CD seq rev	GGTCGTGGTCACAACATGAG	53.8
msp-1 ingene for	CAGCAAGCGAAACAACTGAA	49.7
msp-1 ingene rev	TTGTGTTTCGGTCAAACCTG	49.7
Cam 5 rev	ACCAATAGATAAAATTTGTAGAG	46.4
hrp 2 3 for	TAAACATATGTTAAATATTTATTTCTC	46.1
msp-1 prom for	AAATGACCATTGGAAACAAAA	44.6
msp-1 end rev	TCTGCATCACATCCACCATT	49.7
Knockout via pARL		
pARL KO 5 for NotI	GCGGCCGCTGGTCCAAGTGGTCCAAG	67.4
pARL KO 5 rev AvrII	CCTAGGTTCTTCGTGTTCCTCGATTTTT	58.5
pARL KO 5 rev XhoI	CTCGAGTTCTTCGTGTTCCTCGATTTTT	58.5
pARL KO 3 for NotI	GCGGCCGCTTGTAACTCCACCTCAACCAGA	67.1
pARL KO 3 rev AvrII	CCTAGGGCTTCGAAGTCGTAAGGGTTT	61.3
pARl KO 3 rev XhoI	CTCGAGGCTTCGAAGTCGTAAGGGTTT	61.3
GFP_272AS	CCTTCGGGCATGGCACTC	54.9
Knockout via DD system		
DD 1 for	GGATGCGGCCGCTTGTAACTCCACCTCAACCAGA	69.2
DD 1 rev	CCGCTCGAGAATGAAACTGTATAATATTAACATGAG	61
DD 2 rev	CCGCTCGAGTGTTGGTGGTGATGATGGG	65.8
DD 3 for	CCGCTCGAGCAGAGCTATACAAATAATATCTTGGAT	63.3
DD 3 rev	AAGGTACCGCACTAGTTTCCAGTTTTAGAAGCTCCACACGGAAG	69.2
DD 4 for	GCACTAGT ACGCCGCCCTCTCCAGCC	67.4
DD 4 rev	GCGGTACCTTAGATAAATGAGTACAGAATTAG	59.3
DD 5 rev	CCGCTCGAGGGAACTGCAGAAAATACCATC	64.4
DD 6 for	GCACTAGTAGCAATTTCCTCGGGATTTCTTTTC	61.9
Real-time PCR Primers		
clag 3.1 clag 3.2 for	TAGTAATGAGAATTAGTTGGACA	48.1
clag 3.1 rev	ATAAATATTTGGATGCTTCAGCA	48.1
clag 3.2 rev	ACAAATATGTTTCTGAACTAGGA	48.1
bsd 3 up	TGGCAACCTGACTTGTATCG	51.8
bsd 3 down	AGCAATTCACGAATCCCAAC	49.7
f83 up	AACCAATCCATCTGACAAC	46.8

oligonucleotide	Sequences 5' to 3'	T_m [C]
f83 down	ATTTGAAGCCATGAATGTT	42.5
msp-1d up	TACAAGTCCATCATCTCGTT	47.7
msp-1d down	TGGTTAAATCAAAGAGTTCG	45.6
p61 FBA up	TGTACCACCAGCCTTACCAG	53.8
p61 FBA down	TTCCTTGCCATGTGTTCAAT	47.7
p100 actin up	AGCAGCAGGAATCCACACA	51.1
p100 actin down	TGATGGTGCAAGGGTTGTAA	49.7
renilla RT up	TTCGAAAGTTTATGATCCAG	45:6
renilla RT down	AACATGTCGCCATAAATAAG	45:6
sbp1 RTup	AATCCACAACTGATTTGGTA	45:6
sbp1 RTdown	GAATAGGGGACATAGATTCG	49:7

2.1.12 Bacteria strains

Table 15 | Bacteria strain overview.

strain	genotype	source
E. coli DH5α-Z1	Δ(lac)U169, end A1, gyrA46, hsdR17(rK-mK+), phi80,Δ(lacZ)M15, recA1,relA1, supE44, thi-1, laciq, tetR, SPr	Dr. Rolf Lutz, ZMBH
E. coli W3110Z1	ATCC Nr. 27325, laciq, tetR, SPr	Dr. Rolf Lutz, ZMBH

2.1.13 Parasite strains

Table 16 | Parasite strain overview.

strain	source
Plasmodium falciparum 3D7	Prof. M. Lanzer, Dept. of Infectious Diseases, Heidelberg
Plasmodium falciparum FCB-1	Prof. M. Lanzer, Dept. of Infectious Diseases, Heidelberg
P. falciparum 3D7 pHBIMFwt	this study
P. falciparum 3D7 pHBIMFmut38/42	this study
P. falciparum 3D7 pHBIMFmutall	this study
P. falciparum 3D7 pHBIRH	Tilo Fobes, AG Epp, Dept. Of Infectious Diseases, Heidelberg
P. falciparum 3D7 pHBIMFwt pHTK KO	this study
P. falciparum 3D7 pHBIMFwt pCC1 KO	this study

2.1.14 Antibiotics & Drugs

Table 17 | Overview of antibiotics used for *E. coli* cultivation.

All antibiotics were prepared as 1000x stock solutions, sterile filtered and stored at -20°C.

antibiotic	concentration [mg/ml]	preparation
Ampicillin	50 mg/ml	500 mg Ampicillin ad 10 ml ddH_2O
Kanamycin	25 mg/ml	250 mg Kanamycin ad 10 ml ddH_2O
Spectinomycin	100 mg/ml	1 g spectinomycin ad 10 ml ddH_2O

Table 18 | Overview of antibiotics and drugs used for *P. falciparum* cultivation.

antibiotic	concentration	source
5-fluorocytosine (Ancotil)	10 mg/ml	Sigma Aldrich, Taufkirchen
Blasticidin S	10 mg/ml	Invivogen, San Diego, CA, USA
Ganciclovir (Cymeven)	20 mM in H_2O	Roche, Mannheim
WR99210	10 mM in 20% DMSO (v/v)	Invitrogen, Karlsruhe

2.1.15 Common solutions

Table 19 | Composition of common solutions.

solution	composition
10x PBS	1.37 M NaCl 27 mM KCl 100 mM Na_2HPO_4 18 mM KH_2PO_4 pH 7.4
1xPBS	100 ml 10x PBS ad 1L ddH_2O
1x HTPBS	16 mM Na2HPO4 4 mM NaH2PO4 120 mM NaCl pH 7.4
6x DNA sample buffer	3 ml glycerol (3 %) 25 mg bromphenol blue (0.25 %) 25 mM EDTA ad 10 ml ddH_2O

solution	composition
Transformation buffer	70 mM $CaCl_2$ 35 mM $MgCl_2$
TE buffer	10 mM Tris-HCl (pH 7.5) 1 mM EDTA -
dNTP mix	10 mM each dATP, dCTP, dGTP, dTTP pH 7.5

2.1.16 Recombinant protein expression and renaturation

Table 20 | Composition of solutions for recombinant protein expression and renaturation.

solution	composition
Lysis buffer for *E. coli*	3 mM β-mercaptoethanol 20 U/ml DNAse I 10 µg/ml Lysozym in PBS
Renaturation buffer for MSP1-F	500 mM L-Arginine 50 mM NaH_2PO_4 1 mM EDTA 10 mM Glutathione 1 mM Glutathione disulfide pH 8.0
Solubilisation buffer	6 M Guanidinium chloride 2 mM EDTA 50 mM DTT 50 mM Tris, pH 8.0

2.1.17 Chromatographic purification of recombinant proteins

Table 21 | Composition of solutions for chromatographic purification of MSP-1 heterodimers using Q Sepharose column.
All buffers were sterile filtered and degased.

solution	composition
D1 buffer (equilibration buffer)	10 mM Na-P, pH 8.0 50 mM NaCl
D2 buffer (elution buffer 1)	10 mM Na-P, pH 8.0 100 mM NaCl
D3 buffer (elution buffer 2)	10 mM Na-P, pH 8.0 500 mM NaCl

solution	composition
Washing buffer 1	ddH_2O
Washing buffer 2 (activation buffer)	1 M NaCl
storage buffer	20 % Ethanol

Table 22 | Composition of solutions for chromatographic purification of full length MSP-1F using GST column.
The buffer system was adapted from Dr. Christian Kauth, ZMBH. All buffers were sterile filtered and degased.

solution	composition
Buffer E (equilibration buffer)	1x PBS 3 mM β-mercaptoethanol 10 % glycerol pH 7.3
Buffer J (washing buffer 1)	1x PBS 1 M NaCl 3 mM β-mercaptoethanol 10 % glycerol pH 7.3
Buffer K (washing buffer 2)	1x PBS 1 mM β-mercaptoethanol 10 % glycerol pH 7.3
Buffer L (elution buffer)	1x PBS 1 mM β-mercaptoethanol 10 % glycerol 10 mM GSH pH 7.3

Table 23 | Composition of solutions for chromatographic purification of full length MSP-1F using NTA column.
The buffer system was adapted from Dr. Christian Kauth, ZMBH. All buffers were sterile filtered and degased.

solution	composition
Ni^{2+} solution	0.2 M Ni^{2+} ions in ddH_2O pH 4.3.
acidic washing buffer	0.02 M sodium acetate 0.5 M NaCl pH 4.0

solution	composition
Buffer C (protein dilution buffer)	1x PBS 3 mM β-mercaptoethanol 10 % glycerol 20 mM Imidazole pH 8.0
Buffer D (equilibration buffer 1)	1x PBS 3 mM β-mercaptoethanol 10 % glycerol 10 mM Imidazole pH 8.0
Buffer E (equilibration buffer 2)	1x PBS 3 mM β-mercaptoethanol 10 % glycerol pH 7.3
Buffer F (washing buffer 1)	1x PBS 1 M NaCl 3 mM β-mercaptoethanol 10 % glycerol pH 6.3
Buffer G (washing buffer 2)	1x PBS 3 mM β-mercaptoethanol 10 % glycerol 25 mM imidazole pH 7.3
Buffer H (elution buffer)	1x PBS 3 mM β-mercaptoethanol 10 % glycerol 250 mM imidazole pH 7.3

2.1.18 Analysis of proteins

Table 24 | Composition of solutions for biochemical protein analysis.

solution	composition
4x 'Upper' Tris	500 mM Tris/HCl, pH 6.8
4x 'Lower' Tris	1 M Tris/HCl, pH 8.8
SDS-PAGE running buffer	250 mM Glycine 0.1 % SDS 25 mM Tris/HCl, pH 8.3

solution	composition
4x SDS-PAGE sample buffer	8 % SDS 50 % Upper Tris 40 % Glycerol 0.08 % Bromphenol blue
Western Blot transfer buffer	0.01 % SDS 25 mM Tris/HCl 192 mM Glycine 10 % methanol
TBS buffer	150 mM NaCl 10 mM Tris/HCl, pH 8.0
TBST buffer	0.2 % Tween 20 in TBS
Blocking buffer	2 % Skim milk powder in TBS
Stripping buffer	62.5 mM Tris/HCl, pH 6.8 2 % SDS 100 mM β-mercaptoethanol

2.1.19 *In vitro* processing assay

Table 25 | Composition of solutions for *in vitro* protein processing.

solution	composition
Pf-SUB1 buffer	50 mM Tris/HCl, pH 7.6 15 mM $CaCl_2$

2.1.20 Cell culture of *Plasmodium falciparum*

Table 26 | Composition of solutions for cultivating *Plasmodium falciparum*.

solution	composition
Freezing solution	56 % (v/v) Glycerol 3 % (w/v) Sorbitol 0.65 % (w/v) NaCl
Incomplete cytomix	120 mM KCl 0.15 mM $CaCl_2$ 2 mM EGTA 5 mM $MgCl_2$ 10 mM K_2HPO_4 10 mM KH_2PO_4 25 mM HEPES pH 7.6

solution	composition
RIPA buffer	50 mM Tris/HCl pH 7.8 150 mM NaCl 5 mM EDTA 50 mM NaF 0.5 % sodium desoxycholate 0,1 % SDS 1 % Triton X-100
1 x SSC buffer	7.5 mM NaCl 0.25 mM sodium citrate pH 7.0
Albumax, 5% (w/v)	25 g Albumax Ad 500 ml RPMI 1640 medium Sterile filtrate, aliquot in 25 ml store at –20° C
Parasite culture medium RPMI 1640	0.1 mM hypoxanthin 20 µg/ml gentamycin 10 % (v/v) human serum
Transfection medium RPMI 1640	0.1 mM hypoxanthin 20 µg/ml gentamycin 5 % (v/v) human serum 5 % (v/v) albumax II
90 % Percoll/6%Sorbitol solution	20 ml 10x RPMI-HEPES 180 ml Percoll 12 g D-Sorbitol sterilise by filtration through 0.22 µm filter
70 % Percoll/Sorbitol solution	37.5 ml 90 % Percoll / 6 %Sorbitol solution 10.5 ml 1x RPMI
40 % Percoll/Sobritol solution	21 ml 90 % Percoll / 6 % Sorbitol solution 27 ml 1x RPMI
1 % Saponin solution (10x)	0.1 g saponin in 1 ml ddH_2O

2.2 Molecular Biological Methods

2.2.1 Isolation of plasmid DNA from *E. coli*

For small-scale isolation of plasmid DNA from transformed bacteria, the NucleoSpin Plasmid Kit (Macherey Nagel) was used. Fresh LB-medium with respective antibiotic was inoculated with bacterial colonies previously picked from agar plates. Bacteria were grown overnight at 37°C with gentle shaking at 200 rpm. The following day, bacterial cultures were centrifuged for 2 min at 6,000 g and plasmid DNA was isolated according to the manufacturer's instructions.

2.2.2 Determination of concentration and purity of DNA and RNA

Nucleic acids absorb light at different wavelengths. This feature can be used to determine the concentration and purity of a DNA and RNA sample by measuring the absorption at a wavelength of 260 nm. Using the Lambert-Beer law $A = \varepsilon * c * d$ with ε extinction coefficient, c concentration and d distance, the A absorbance can be related to the concentration of the sample. At a wavelength of 260 nm, the average extinction coefficient ε for double-stranded DNA is 0.020 $(\mu g/ml)^{-1}$ cm^{-1}, for single-stranded DNA and RNA is 0.027 $(\mu g/ml)^{-1}$ cm^{-1}. Thus, an optical density (OD) of 1 corresponds to a concentration of 50 µg/ml for dsDNA, and 40 µg/ml for RNA. In contrast, proteins display a maximum light absorption at 280 nm. Hence, the ratio of absorbance at 260 and 280 nm ($A_{260/280}$) is used to assess the purity of nucleic acids. Protein-free DNA solutions have a ratio of about 1.8 and RNA solutions of about 2.0. Lower ratios indicate less pure nucleic acids.

2.2.3 Precipitation of DNA

For concentration and purification, DNA was precipitated. 0.1 volume sodium acetate (3 M, pH 5.2) and 2.5 volumes of isopropanol (100 %) were added to the DNA solution, mixed and incubated either for 30 min at -80°C or overnight at -20°C. The DNA was then pelleted by centrifugation at 13,000 rpm, 4°C for 30 min and washed twice with 500 µl 70 % ethanol (13,000 rpm, 4°C, 5 min) to remove residual salt and other contaminants. Subsequently, the DNA pellet was air-dried and resuspended in an adequate volume of DNase-free water.

2.2.4 Agarose gel electrophoresis of DNA

Agarose gel electrophoresis is a widely used method to separate molecules based on charge, size and shape (Sambrook *et al.*, 1989). Gel electrophoresis of DNA was carried out in 50 ml horizontal gels containing 1 % agarose in 1x TAE buffer supplemented with 10 µl intercalating ethidium bromide (500 µg/ml) to label and visualize the DNA in ultraviolet (UV) light. Prior to loading onto the gel, DNA samples were mixed with 0.2 volumes of 6x DNA loading dye. The 2-log DNA ladder (NEB) was used as reference for the size of the DNA strands. Gel electrophoresis was run at 100 V for 30 to 60 minutes. Afterwards, gels were illuminated on an ultraviolet transilluminator (UVP) and photographed using the Electrophoresis Documentation and Analysis System 120 (Kodak).

2.2.5 Primer design

Gene-specific primers for PCR and real-time PCR were designed using Primer3 software (Rozen and Skaletsky, 2000). All primers were ordered from Invitrogen.

2.2.6 Polymerase Chain Reaction (PCR)

The polymerase chain reaction is a technique that amplifies sequences from a DNA template (Saiki et *al.*, 1985; Mullis et *al.*, 1986). Via thermal cycling, DNA is denatured and can afterwards hybridize with short DNA fragments (primers) while cooling the reaction to a certain temperature. Afterwards, the polymerase elongates the primers according to the single stranded template DNA. These three steps, denaturation, annealing and elongation, are constantly repeated doubling the amount of template DNA in each round. For amplification of specific target sequences from genomic *P. falciparum* DNA, cDNA or vectors, primers were designed (Table 14). Three different DNA polymerases were used throughout this study. Taq DNA polymerase (Invitrogen) was sufficient for amplification of short DNA fragments. It produces 3´A-overhangs enabling the cloning of DNA fragments into the pGEM-T vector (Promega). Phusion High Fidelity DNA Polymerase (New England Biolabs) was used for amplification of large DNA fragments, because it harbours a proofreading domain (3´→5´ exonuclease) and is therefore not error-prone. In addition, this polymerase leaves blunt ends facilitating the insertion into TOPO vectors (Life Technologies). For site-directed mutagenesis, Platinum Pfx DNA polymerase (Invitrogen) was used as it likewise exerts proofreading (3´→5´ exonuclease) which is critical for mutagenesis experiments. PCRs were performed using the following reagents and conditions:

Table 27 | PCR composition and conditions for Taq DNA Polymerase.

compound	volume
Template DNA (cDNA, gDNA)	0.5 – 1 µl
Forward primer (50 µM)	2.5 µl
Reverse primer (50 µM)	2.5 µl
10x PCR reaction buffer (-$MgCl_2$) (Invitrogen)	10 µl
$MgCl_2$ (25 mM) (Invitrogen)	3 µl
dNTP mix (10 mM) (Invitrogen)	2 µl
Taq (*Thermus aquaticus*) DNA polymerase (5 U/µl) (Invitrogen)	0.5 µl
ddH_2O	ad 100 µl

Cycle step	Temperature	Time	number of cycles
Initial denaturation	94°C	2 min	
Denaturation	94°C	30 sec	30-35
Annealing	54°C	20 sec	
Elongation	72°C	1 min/kb	
Final elongation	72°C	10 min	
Final hold	4°C	∞	

Table 28 | PCR composition and conditions for Phusion High-Fidelity DNA Polymerase.

compound	volume
Template DNA (cDNA, gDNA)	0.5 – 1 µl
Forward primer (50 µM)	2.5 µl
Reverse primer (50 µM)	2.5 µl
5x Phusion HF buffer (NEB)	10 µl
dNTPs (10 mM) (Invitrogen)	1 µl
Phusion DNA polymerase (5 U/µl) (NEB)	0.5 µl
ddH_2O	ad 50 µl

Additionally 0.2 µl $MgCl_2$ can be added to the reaction mix.

Cycle step	Temperature	Time	number of cycles
Initial denaturation	98°C	30 sec	
Denaturation	98°C	10 sec	30-35
Annealing	54°C	35 sec	
Elongation	72°C	30 sec/kb	
Final elongation	72°C	10 min	
Final hold	4°C	∞	

Table 29 | PCR composition and conditions for Platinum Pfx DNA Polymerase.

compound	volume
Template DNA (cDNA, gDNA)	0.5 – 1 µl
Forward primer (50 µM)	1.5 µl
Reverse primer (50 µM)	1.5 µl
10x Pfx Amplification buffer	5 µl
10x PCR Enhancer Solution	5 µl
$MgSO_4$ (50 mM) (Invitrogen)	1 µl
dNTP mix (10 mM) (Invitrogen)	1.5 µl
Platinum Pfx DNA polymerase (2.5 U/µl) (Invitrogen)	0.45 µl
ddH_2O	ad 50 µl

Cycle step	Temperature	Time	number of cycles
Initial denaturation	94°C	2 min	
Denaturation	94°C	15 sec	30-35 or 18 for site-directed mutagenesis
Annealing	54°C	30 sec	
Elongation	68°C	1 min/kb	
Final elongation	68°C	10 min	
Final hold	4°C	∞	

The reaction samples were analysed by agarose gel electrophoresis. DNA fragments used for cloning were purified with the NucleoSpin® Gel and PCR Clean-Up Kit (Macherey-Nagel) according to the manufacturer's instructions.

2.2.6.1 Colony PCR

In order to examine the successful transformation of prepared competent *E. coli* cells, a PCR reaction mix was prepared as described above. 10 µl of the mix per PCR tube were inoculated with one *E. coli* colony and PCR was carried out with the standard PCR programme.

2.2.7 TOPO and pGEM-T cloning

Amplified and purified DNA fragments with either blunt ends or 3' A-overhangs were ligated into TOPO (Life Technologies) or pGEM-T (Promega) vectors, respectively, according to the manufacturer's instructions.

2.2.8 DNA restriction

Restriction endonucleases catalyse the hydrolysis of the phosphodiester bonds in the backbone of double-stranded DNA. They recognize specific nucleotide sequences with lengths between four and eight nucleotides. Depending on the enzyme, "blunt" ends or "sticky" end overhangs are produced. DNA restriction was carried out using the buffers and conditions according to the manufacturers' instructions. Typically, one international unit (U) of a given enzyme digests 1 µg DNA within one hour. For the preparation of plasmid DNA for cloning (preparative digest), a total volume of 50-100 µl was prepared and incubated overnight at 37°C. Analytical restriction of plasmid DNA from small-scale isolations in a total volume of 20 µl was carried out for 2 h at 37°C. Simultaneous digests were carried out with two different restriction endonucleases when the conditions for the optimal activity of the enzymes matched. Otherwise, restrictions were carried out sequentially, including purification between the digestions. Following restriction, the samples were analysed by agarose gel electrophoresis. For further use, specific DNA strands were purified using the NucleoSpin® Gel and PCR Clean-Up Kit (Macherey-Nagel) according to the manufacturer's instructions.

2.2.9 DNA dephosphorylation

Dephosphorylation of linearized plasmids is employed to prevent re-circularization of the majority of plasmids during DNA ligation (see below). After restriction, blunt and sticky 5'-DNA ends were dephosphorylated using the alkaline

phosphatase (AP). 1 µl AP (1 U/µl) and 5 µl 10x reaction buffer were added to 50 µl linearised vector. The reaction mix was incubated at 37°C for 1 h before the DNA was purified by spin-column purification (NucleoSpin® Gel and PCR Clean-Up Kit, Macherey-Nagel).

2.2.10 Ligation

The DNA ligase of the bacteriophage T4 catalyses the formation of a phosphodiester bond between the 3' hydroxyl group of one DNA nucleotide and the 5' phosphate group of another one in the presence of ATP (Sambrook et *al.*, 1983). In this work, linearized vector and insert DNA were mixed in different molar ratios of 1:7, 2:6 or 3:5. A total reaction volume of 10 µl contained 1 µl T4 DNA Ligase (Invitrogen) and 1 µl 10x T4 DNA Ligase buffer. The reaction was carried out either at RT for 2 h or at 16°C overnight. Additionally, a control containing water instead of insert DNA was set up in the same way to assess the risk of vector religation.

2.2.11 Isolation of total parasitic RNA

For isolation of RNA from different *P. falciparum* strains, all reagents and materials must not contain RNase to prevent RNA degradation. Therefore, pipettes and centrifuges had been treated with RNase away (Merck). A 20 ml culture of synchronized schizonts (40 h) with 5 % parasitemia was spun down at 1,900 rpm for 5 min. The pellet was lysed in 0.15 % saponin/PBS for 5 min on ice, centrifuged at 2,200 g for 5 min and washed twice with ice-cold PBS. The parasite pellet was then resuspended in 750 µl TRI Reagent® solution (Ambion) and frozen at -80°C. After thawing, the sample was homogenized by alternatingly pipetting up and down using a grey syringe needle for several times. The sample was incubated for 5 min at RT before adding 150 µl chloroform and shaking for 15 sec. Subsequently, the sample was allowed to rest again for 3 min at RT, then shaken vigorously for 15 sec and spun down at 12,000 g for 10 min at 4°C. The

aqueous supernatant was transferred into a new RNase-free tube and 500 µl isopropanol per ml TRIzol were added to the RNA. After 10 min incubation at RT, 1 h or overnight at -20°C, the RNA was precipitated for 20 min at 12,000 g, 4°C. The supernatant was discarded and the pellet was washed with 1 ml ice-cold 75 % ethanol, briefly vortexed and centrifuged again at 7,500 g and 4°C for 5 min. Once more, the supernatant was discarded and the RNA pellet was air-dried before resuspending in 21 µl DEPC-treated H_2O. RNA samples were stored at -80°C.

2.2.12 DNase digestion

Prior to reverse transcription of isolated RNA, remaining DNA was removed by DNase digestion. Therefor, 1 µg RNA was incubated with 1 U of Amplification Grade DNase I (Invitrogen) and 1 µl of 10x DNaseI buffer in a total volume of 10 µl for 15 min at RT. To terminate the reaction, 1 µl of 25 mM EDTA was added and the sample was heated for 10 min at 65°C.

2.2.13 Reverse Transcription PCR (RT-PCR)

Retroviral reverse transcriptase was used to transcribe RNA into its complement DNA (cDNA) which was then amplified by PCR.

First strand synthesis of cDNA was performed using the *SuperScript® II First-Strand Synthesis Kit* (Invitrogen). Therefor, 2 µl of random hexamer primers and 1 µl of dNTP mix (10 mM each) were added to 0.5 µg of RNA and diluted in DEPC-treated water to a total volume of 10 µl per PCR tube. The mixture was then incubated at 65°C for 5 min to disrupt secondary structures. After incubation on ice for at least 1 min, the following components were added to the RNA in the indicated order:

Table 30 | RT-PCR composition.

compound	volume
10x RT Buffer	2 µl
25 mM $MgCl_2$	4µl
0.1 M DTT	2 µl
RNase OUT	1 µl
Total volume	19 µl

Following incubation at RT for 2 min, either 1µl of SuperScript® II Reverse Transcriptase or DEPC-H_2O was added to the reaction mix. Reverse transcription of the RNA was carried out in a thermal cycler by incubating the reaction for 10 min at 22°C followed by 50 min at 42°C and terminating the reaction by heating to 70°C for 15 min. The reverse transcription product can directly be used in PCR applications or stored at -20°C.

2.2.14 Quantitative Real time PCR (qRT-PCR)

Quantitative Real time PCR is a technique used to amplify and simultaneously quantify a targeted DNA sequence using fluorescent reporter molecules. For this purpose, the dsDNA-binding dye SYBR Green was used. With progressing amplification of the dsDNA products, SYBR Green's fluorescence increases. The detection baseline or threshold cycle (Ct) above which the signal is clearly distinguishable from the background noise depends on the initial concentration of the target DNA. The higher the initial DNA concentration, the lower its Ct. In this work, qRT-PCR was performed with genomic DNA (gDNA) and cDNA preparations using the ABI 7500 sequence detection system and SensiFAST™SYBR® Lo-ROX Kit (Bioline) according to the manufacturer's instructions.

Table 31 | qRT-PCR composition.

compound	volume
SensiFAST™SYBR® Lo-ROX	10 µl
Primer forward 5 µM	2 µl
Primer reverse 5 µM	2 µl
DNA template	2 µl
H_2O	4 µl
Final volume	20 µl

The concentration of gDNA templates was adjusted to 30 ng/µl while cDNA was diluted 1:5 prior to usage as template. qRT-PCR was performed in triplicates using the PCR programme shown below.

Table 32 | Programme for Real-time PCR in ABI 7500.

cycle step		time	temperature
Preheating		2 min	50°C
Denature template and activate enzyme		3 min	95°C
40 cycles	Denture	15 sec	95°C
	Anneal	15 sec	54°C
	Extend	1 min	60°C
Dissociation step: Denature		30 sec	95°C
Dissociation step: Staring		30 sec	60°C
90 cycles	melting	10 sec	60°C + 0.5°C/cycle

Data were analysed with SDS 1.3.1 software (Applied Biosystems).

In order to determine the absolute copy number of genes or transcripts number, standard curves were generated. The relative gene copy or transcript number was determined by normalisation with the respective data for actin (p100). Mean values with corresponding standard error of the mean were plotted.

2.2.15 Standard curve and absolute quantification

Each gene used for absolute quantification was amplified using serial dilutions from either genomic DNA (*msp-1d*, *actin, clag 3.1, clag 3.2*) or from plasmid DNA (*msp-1d*, *msp-1f*, *bsd, renilla luciferase*). The DNA concentration was determined by spectrophotometry and prepared to 10^8 copies per 20 µl solution ($5x10^7$ copies $µl^{-1}$ solutions). Serial 10-fold dilutions ranging from 10^7 to 10^{-1} copies per real-time PCR were made in ddH_2O. Triplicate measurements were made for each dilution. Calculations and data are shown in the appendix (Table 40). The obtained Ct values were plotted against the copy number and a best-fit standard curve was generated. The standard curves were linear across a range of seven logs of DNA concentrations. The detection limit varied between the analysed genes but usually was 10 copies. Standard curve equations were used to calculate the copy numbers obtained by analysing the transgenic parasite lines.

2.3 Biochemical Methods

2.3.1 Enzymatic treatment of RBCs

Enzymatic treatment of erythrocytes may identify moieties that are important for MSP-1 binding and thus for initial attachment of merozoites *in vivo*. Commonly, three enzymes are used to discriminate between different invasion pathways of *P. falciparum* parasites. Neuraminidase is used to remove negatively charged sialic acid residues on the red blood cell surface by cleaving terminal N-acetyl neuraminic acid from a variety of glycoproteins. Trypsin cleaves proteins on the C-terminal side of lysine and arginine residues while chymotrypsin selectively hydrolyses peptide bonds on the C-terminal side of tyrosine, phenylalanine, tryptophan, and leucine allowing the discrimination between different protein receptors for merozoite or MSP-1 attachment.

Fresh erythrocytes were treated with neuraminidase (0.067 U/ml in RPMI-HEPES, pH 7.4), TPCK(*N*-alpha-tosyl-L-phenylalanine chloromethyl ketone)–

treated trypsin (1.2 mg/ml in RPMI-HEPES, pH 7.4) or TLCK(*N*-tosyl-L-lysine chloromethyl ketone)–treated chymotrypsin (1.2 mg/ml in RPMI-HEPES, pH 7.4) for 1 hour at 37°C with rocking. Treatment with trypsin or chymotrypsin was followed by one wash in RPMI-HEPES and 10 min treatment at RT with cOmplete mini EDTA-free protease inhibitor (10x in ddH_2O). All cells were washed twice with RPMI-HEPES and then with HTPBS before resuspension in HTPBS for usage in erythrocyte binding assays.

2.3.2 Erythrocyte Binding Assay

Recombinant MSP-1 protein (60 µg) was incubated with human erythrocytes (50 µl packed volume) in HTPBS for 2 hr at 4°C in 300 µl. The mixture was passed through 400 µl dibutyl pthalate (Sigma) by centrifugation at 12,000 g for 30 sec. Supernatant was taken off and the pellet was washed thrice with cold HTPBS before eluting in 1.5 M NaCl/PBS for 45 min and centrifugation. Protein standard as well as all supernatants were subjected to SDS-PAGE followed by immunoblotting.

2.3.3 *In vitro* processing assay

Recombinant MSP-1 and modified versions of MSP-1F are digested *in vitro* by recombinant PfSUB1 protease (obtained from Prof. M. Blackman, NIMR London, UK) according to a previously published protocol (Koussis et al., 2009) with sight modifications. In this work the incubation temperature is lowered to 16°C to reduce the precipitation of protein after longer incubation times. Additionally, protease inhibitors inhibit unspecific cleavage by other proteases, potentially contaminating the protein or PfSUB1 preparations. Furthermore, controls without PfSUB1 ensure that the processing events rely on specific protease activity.

For *in vitro* processing assays the protein concentration was adjusted to 0.5 mg/ml with PfSUB1 buffer. 10 µM E64, 10 µg/ml leupeptin and 100 µg/ml Pefabloc were added as well as 1.5 units PfSUB1 per 100 µl of volume. The reaction was incubated at 16°C. For time-course digest seven reactions were set up and the reaction was stopped after 0 hours, 30 minutes, 1 hour, 3 hours and 6 hours and overnight by boiling in SDS sample buffer for 10 min at 80°C.

2.3.4 SDS polyacrylamide gel electrophoresis (SDS-PAGE)

SDS-PAGE (Laemmli, Nature, 1970) is a technique used to separate proteins according to their electrophoretic mobility which is dependent on the size and net charge of the protein. The detergent sodium dodecyl sulphate denatures secondary and tertiary structures of proteins and applies a negative charge to each protein in proportion to its mass. Samples to be analysed were supplemented with 4x SDS loading buffer and denatured for 10 min at 80°C. Additionally, 50 mM DTT were added to the 4x SDS loading buffer in specific cases to reduce disulphide bonds of proteins. Denatured protein samples were centrifuged briefly to pellet insoluble components and a defined amount of sample was loaded onto the SDS gel. To achieve a good separation, proteins first pass through a stacking gel (4 %, pH 6.8) and then afterwards through a separating gel (10 %, pH 8.8). The pH difference at the interface of both gels leads to a focussing effect enabling a sharp separation of the proteins. Electrophoresis was carried out for ~1.5 hours applying 125-200 V and 25 mA per gel which was continuously immersed in 1x Tris-glycine electrophoresis buffer.

Table 33 | Chemical volumes for preparation of SDS polyacrylamide gels.

Chemicals	Stacking gel (4%)	Separating gel (10%)
30 % acrylamide / 0.8 % bisacrylamide	330 µl	1.65 ml
lower Tris	-	1.25 ml
upper Tris	625 µl	-
ddH_2O	1.55 ml	2.1 ml
10 % APS	25 µl	50 µl
TEMED	5 µl	10 µl
Final volume	**2.5 ml**	**5 ml**

2.3.5 Western Blot analysis

In order to make proteins accessible to chemiluminescence (Thorpe and Kricka, 1986) or colorimetric antibody detection (Knecht and Dimond, 1984), they were transferred from the polyacrylamide gel onto a PVDF membrane by an electrical current.

After separation of the proteins, the gel was shortly incubated in 1x transfer buffer and filter paper as well as sponges were. Sponges soaked in 1x transfer buffer and drained, Whatman-3MM-filter-papers, the gel and the membrane were assembled and placed in the transfer chamber according to the schematic shown in Figure 7. Air bubbles were carefully removed before electroblotting. As the chamber was filled with 1x transfer buffer, the method is commonly referred to as wet blot.

Protein transfer was performed for 2 h at 20 V and 125 mA. Afterwards, the membrane was incubated for either 1 h in 2 % MTBST at RT (1× TBS, 0.05 % Tween, 2 % milk powder) or overnight at 4°C. Subsequently, it was washed three times with TBST buffer for 10 minutes and incubated with the primary antibody diluted in 2 % MTBST for at least 1 h at RT or overnight at 4°C while gently shaking. Following another three wishes with TBST for 10 minutes, the secondary antibody diluted in 2 % MTBST was applied and gently shaken for 1 h at RT.

Finally, the membrane was washed three times with TBST before chemiluminescent or colorimetric detection.

For the first detection method, 2 ml of the mixed chemiluminescence solution (BM Chemiluminescence Western Blotting Substrate (POD), Roche) were added to the membrane. 2 ml of agent 1 and 20 µl of agent 2 were mixed (ratio of 10:1) prior to use. The membrane was sprinkled with the mixed chemiluminescence solution for 1 min, and subsequently transferred to a film cassette. The horseradish peroxidase-linked secondary antibody cleaves the chemiluminescent agent, whereby the reaction product exerts luminescence in proportion to the amount of available protein. Light emitted by this reaction was then detected on photographic films (Kodak Biomax XAR film, Sigma-Aldrich) that were placed upon the membrane for 10 sec to 1 h. The photographic films were then developed (Hyperprocessor Amersham Biosciences).

For colorimetric detection, the membrane was incubated with 1 tablet BCIP/NBT solved in 10 ml ddH_2O. AP dephosphorylates BCIP, yielding a bromochloro indoxyl intermediate. The indoxyl is then oxidised by NBT to produce a purple precipitate, while NBT is thereby converted into a blue precipitate. The combination of both forms purple-blue marks visualising the proteins on the western blot.

Protein size was determined by transcribing the bands of the protein ladder from the blotted membrane to the photographic film. For detection of another protein, e.g. the loading control, the antibodies were removed by stripping of the membrane. Therefor, the membrane was washed 4-5 times 10 min each with TBST and then incubated with stripping buffer for 30 min at 55°C. Afterwards, the membrane was washed another 5 times and blocked again with MTBST for 1 h at RT or 4°C overnight before incubation with the primary and secondary antibodies.

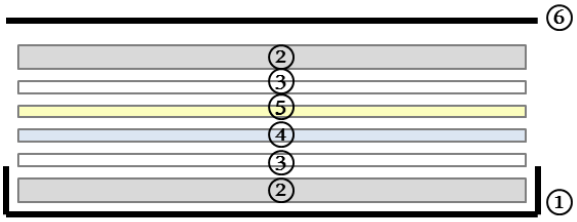

Figure 7 | Schematic representation of the assembly of the Western Blot.
1: cathode; 2: sponge; 3: layers of 3MM filter; 4: gel; 5: PVDF membrane; 6: anode.

2.3.6 Mass Spectrometry

Mass spectrometry analysis was carried out at the Mass Spectrometry Core Facility of the ZMBH (Zentrum für Molekulare Biologie der Universität Heidelberg). Recombinant proteins after PfSUB1 cleavage were separated by SDS-PAGE, and stained by Coomassie blue. Protein bands of interest were either directly labelled within the gel and then digested with trypsin or labelling was carried out after cutting and trypsin digestion according to the protocol from (Boersema et al., 2009). Samples were analysed by LTQ Orbitrap, Thermo Scientific followed by ProteomeDiscoverer (Thermo Scientific).

2.3.7 Indirect Immunofluorescence analysis (IFA)

Immunofluorescence analysis is a technique to specifically visualise proteins within fixed cells and tissues using antibodies.

For IFA, blood smears from parasite cultures were prepared and air-dried. These smears were fixed with ice-cold 100 % methanol for 5 min. They may be stored at 4°C for up to 3 days. Afterwards, the smears were washed once with 1x PBS and wells were painted onto the glass slide using a hydrophobic pen. Cells were then blocked with 3 % BSA/PBS for at least 1 h at RT or overnight at 4°C. After two consecutive washes with PBS for 5 min, the primary antibody solved in 3 % BSA/PBS was added to the wells and incubated for 1 h at RT. Following another wash with PBS for 5 min, the secondary antibody in 3 % BSA/PBS was added

and incubated for 1 h at RT in the dark. Afterwards, smears were washed three times with PBS.

In case of double-staining of IFA samples, the smears were again blocked and incubated with primary and secondary antibody. Then, the nuclei were stained by incubating the smears with Hoechst diluted 1:10,000 in PBS for 5 min at RT in the dark. Following another wash with PBS, the smears were mounted in 50 % glycerol/PBS and sealed with nail varnish. IFA samples were stored at 4°C in the dark.

2.4 Microbiological Methods

2.4.1 Liquid culture of *E. coli*

Fresh LB culture medium (LB, Luria broth) was inoculated with bacteria from prior liquid culture, colonies picked from agar plates or a glycerol-bacteria stock solution (cryostock). For small-scale plasmid isolation using the NucleoSpin® Plasmid Kit (Macherey-Nagel), 3 ml LB medium were inoculated with bacteria and incubated at 37°C shaking at 200 rpm overnight. Supplemental antibiotics in the appropriate concentration were used to select genetically modified bacteria containing selection markers conferring resistance to the respective antibiotics.

2.4.2 Recombinant protein expression and renaturation

2.4.2.1 Synthesis of recombinant proteins in *E. coli*

For expression of recombinant proteins, the *E. coli* strain W3110Z1 was used. To this end, pZ expression vectors (Kauth et al., 2003) harbouring different MSP1-F constructs were transformed into *E. coli* and an overnight culture was prepared.

On the next day, 500 ml antibiotic-containing LB medium were inoculated with 1:50 of the overnight culture and incubated at 37°C while shaking at 200 rpm until early log-phase (OD_{600} = 0.2–0.4). An aliquot of 1 ml was taken for

electrophoretic analysis, centrifuged and resuspended in 200 µl SDS-PAGE sample buffer with 50 mM DTT.

Protein expression was induced by addition of 1 mM IPTG to the culture and incubating for 4 h at 37°C 200 rpm. An aliquot was taken as described above and the remaining culture was sedimented by centrifugation at 6,000 g for 30 min at 4°C. The bacterial pellet was weighed in and either stored at -20°C or directly used for purification of recombinant proteins.

Analysis of the taken aliquots by SDS-PAGE indicated the outcome of the induction and yield of protein expression. Using the above described conditions, 500 ml culture yield approximately 5 g bacterial wet mass.

2.4.2.2 Disruption of *E. coli* cells

Recombinant MSP-1 protein synthesised in *E. coli* aggregated due to misfolding and accumulated in so-called inclusion bodies. In order to recover the protein, *E. coli* cells were disrupted, the inclusion bodies were solubilised and the protein was refolded. All steps were carried out on ice to avoid degradation of the protein.

For disruption of *E. coli*, the bacterial pellet was resuspended in 2 ml lysis buffer per 1 g wet mass and homogenised by a magnetic stirrer for 20 min at 4°C. Afterwards, the cells were lysed by several one minute sonifications with one minute breaks each. The cells were sedimented by centrifugation at 27,800 g for 40 min at 4°C (SS34 rotor of Sorvall centrifuge). A 200 µl aliquot from the supernatant was taken and prepared for SDS-PAGE. The lysis by sonification was repeated once more and likewise an aliquot of the supernatant was taken. In the end, the remaining pellet mainly consisted of inclusion bodies ready to be solubilised.

2.4.2.3 Solubilisation of inclusion bodies (IBs)

For solubilisation, the IB pellet was resuspended in 2 ml solubilisation buffer per 1 g pellet and sonificated until the suspension turned homogenous. After incubation at RT either for 2 hours or overnight with constant stirring, the sample was centrifuged at 27,800 g for 40 minutes at 4°C (SS34 rotor of Sorvall centrifuge). Finally, the protein-containing supernatant was stored at -80°C. An aliquot of the supernatant was prepared for SDS-PAGE analysis.

The protein concentration in the supernatant was determined by Biuret Assay. Usually, the concentration ranged from 20 to 40 mg/ml. To assess successful protein extraction from IBs, aliquoted samples were diluted 1:10-1:100 in 1x PBS and examined by SDS-PAGE.

2.4.2.4 *In vitro* refolding of solubilised inclusion bodies by pulse renaturation

Recombinant protein that aggregated in inclusion bodies was refolded by pulse renaturation according to Rudolph and Lilie (1996). This method is based on step-wise refolding of the recombinant protein. Prior to refolding, inclusion bodies were diluted to a concentration of 0.1 mg/ml in renaturation buffer, containing solubility enhancing substances such as a high concentration of L-arginin. Then, the protein was allowed to fold at 8-10°C with mild stirring. Every hour, the protein concentration was increased by 0.1 mg/ml by adding solubilised inclusion bodies. This procedure was repeated eight to ten times yielding a final protein concentration of 0.8-1.0 mg/ml. The protein was incubated at 8-10°C overnight for completion of the renaturation. Afterwards, the protein was dialysed into a buffer appropriate for subsequent affinity chromatography purification. In case of MSP-1F, the two separately produced halves of the protein, called f-83/30 and f-38/42, were associated during refolding. Both fragments were added in equal amounts (0.1 mg/ml) at each step.

2.4.3 Chromatographic purification of recombinant proteins

2.4.3.1 Chromatographic purification of MSP-1F heterodimers

Renatured MSP1-F heterodimers were purified via anion-exchange chromatography. This method is based on an insoluble matrix, the stationary phase, that carries covalently bound, positively charged groups to which anions in the mobile phase associate. For this work, the matrix was Q-Sepharose, a strong anion exchanger with a quaternary amine group as functional unit. In order to facilitate binding of MSP-1F to the stationary phase, the protein was negatively charged by setting the buffer's pH above the protein's pI of 6. Elution occurred by raising the ionic strength of the mobile phase as the respective ions compete with the protein for binding spots on the stationary phase. As protein separation exclusively relies on physicochemical properties, tags are not needed to purify proteins.

The Q-Sepharose column (GE Healthcare) used in this work had a capacity of 10 mg/ml and 47 cm/h were used as flow rate. Prior to purification, MSP-1F constructs were dialysed in D1 buffer o/n at 4°C. The column was first washed with at least 5 column volumes (CV) of ddH_2O and then equilibrated with min 1 CV of D1 buffer. After activation with 5 CV of 1 M NaCl, the column was again equilibrated with D1 buffer until the conductivity reached 0. By activation of the column, exchangeable counter ions were associated to the exchanger groups. These were displaced by the counter ions from the protein that was loaded onto the column subsequently. Weakly bound substances were washed out with 5 CV of D2 buffer. The protein was eluted in a gradient from buffer D2 to D3 ranging from 100 to 280 mM NaCl over 12 CV. The protein was retrieved from one of the collected 1 ml fractions.

After purification, the matrix was regenerated by removal of substances remaining on the stationary phase with 1M NaCl. Ultimately, the column was washed with H_2O and stored in 20 % ethanol. All purification steps were analysed by SDS-PAGE. To this end, 30 µl sample were mixed with 10 µl 4x SDS-sample

buffer and 2 µl 1 M DTT and boiled at 80 °C for 10 min before loading on a polyacrylamide gel.

2.4.3.2 Chromatographic purification of full length MSP-1F

For expression of full length MSP-1F, the expression plasmid pZE23/f-GX190H, as well as mutated versions of this plasmid were used. In order to get a high purity of the protein without degradation products, MSP-1F was N-terminally fused to a GST-tag and C-terminally to a His_6-tag as well as purified using affinity chromatography at 6°C. The purification process had been established by Dr. Christian Kauth and was slightly modified in this study.

2.4.3.3 Chromatographic purification via GST-column

Refolded MSP-1F constructs were purified via a GSTrap™ HP (GE Healthcare) affinity column. The column capacity was 10 mg/ml and 47 cm/h were used as flow rate. Prior to purification, MSP-1F constructs were dialysed in buffer E (equilibration buffer 1) overnight at 4°C. The column was equilibrated with at least 6 CV of buffer E. Then, the protein was loaded onto the column, leading to the immobilised GST binding to the GST-tag of the protein. Afterwards, the column was washed with at least 6 CV of buffer E, followed by washing with 6 CV of buffer J and K (washing buffer 1 and 2). Elution was carried out by an excess of GSH contained in the buffer L (elution buffer) that displaced the GST-tag. The protein was retrieved from one of the collected 1 ml fractions.

After purification, the column was consecutively washed with at least 6 CV of buffer E, H_2O and 20 % ethanol. All purification steps were analysed by SDS-PAGE. To this end, 30 µl sample were mixed with 10 µl 4x SDS-sample buffer and 2 µl 1 M DTT and boiled at 80 °C for 10 min before loading on a polyacrylamide gel.

2.4.3.4 Chromatographic purification via NTA-Superflow

Following purification by GST-column, MSP-1F constructs were purified via Chelating Sepharose Fast Flow affinity chromatography (GE Healthcare). The column capacity was 10 mg/ml and a flow rate of 47 cm/h was used.

First, the column was washed with 2 CV of ddH_2O. Then 0.2 CV of the Ni^{2+} solution was applied and washed again with 5 CV of ddH_2O and subsequently with 5 CV of acidic washing buffer to remove an excess of ions. After charging the column with Ni^{2+} ions, the column was equilibrated with 5 CV buffer D (equilibration buffer 1). The protein constructs purified by the GST-column (in buffer L) were diluted 1:1 in buffer C (protein dilution buffer) and applied to the column. pH 8.0 maintained high affinity of the His_6-tag to the matrix while the imidazole concentration largely prevented unspecific binding of proteins. The column was washed with at least 5 CV of buffer E (equilibration buffer 2) and contaminations were removed by washing with 5 CV of the high salt washing buffer F. Then, the column was again equilibrated with buffer E and finally washed with 5 CV of buffer G (wash buffer 2). The intermediate step with buffer E was necessary, as the imidazole in buffer D and G in combination with substances from buffer F would have led to a premature elution. Ultimately, the protein was eluted by an excess of imidazole in buffer H and collected in 1 ml fractions. Fractions containing the protein were dialysed into PBS pH 7.3 overnight at 4°C and then into PfSUB1 buffer for cleavage assays.

After purification, the ÄKTA system was consecutively washed with at least 6 CV of buffer D, H_2O and 20 % ethanol. All purification steps were analysed by SDS-PAGE. To this end, 30 µl of the sample were mixed with 10 µl 4x SDS-sample buffer and 2 µl 1 M DTT and boiled at 80 °C for 10 min before loading on a polyacrylamide gel.

2.4.4 Preparation of competent *E. coli* cells

For transformation, the uptake of extracellular non-native DNA by prokaryotes, *E. coli* bacteria were treated with $CaCl_2$. Using this method, the permeability of the cell wall for linearized or plasmid DNA was highly increased.

Initially, a 5 ml overnight culture was prepared from a single colony picked from a purity plate. On the next day, 500 ml fresh LB medium were inoculated with 2 ml of the overnight culture and incubated at 37°C 200 rpm until an OD_{600} of 0.3–0.4 was reached. The culture was cooled down on ice for 15 min and then sedimented by centrifugation for 5 min at 500 rpm and 4°C. The supernatant was discarded and cells were resuspended in 250 ml ice-cold solution A. After incubation on ice for 30 min, cells were spun down for 5 min at 500 rpm and 4°C. Again, the supernatant was discarded and the cells were carefully resuspended in 25 ml ice-cold solution B. Aliquots of 200 µl were prepared and immediately frozen in liquid nitrogen to finally be stored at -80°C.

2.4.5 Transformation of self-made competent cells

During the process of transformation, competent bacteria take up extracellular non-native DNA, thus allowing the amplification and further studies of the transformed DNA. Therefore, *E. coli* cells used for this work were treated with $CaCl_2$ to enhance their competence for plasmid uptake. For the purpose of plasmid amplification the strain DH5α-Z1 was used, whereas recombinant protein expression was performed in W3110Z1 cells

In order to transform self-made competent cells, either 200 µl bacteria solution were thawed on ice or 1 ml of freshly prepared competent cells were used. 5-10 µl of a ligation sample or 3–10 µl of purified plasmid DNA were added to the competent cells and incubated on ice for 10-15 min. A heat shock at 42°C was performed for 70 sec, immediately followed by cooling on ice for 1 min. Subsequently, 1 ml LB medium at 37°C were added and the cells were incubated for 1 h at 37°C shaking at 200 rpm. Afterwards the competent cells were spun

down and the pellet was resuspended in approximately 250 µl LB and plated on agar plates using autoclaved glass beads. Agar plates contained appropriate antibiotics for the selection of genetically modified bacteria. Plates were incubated overnight at 37°C.

On the next day, single colonies were picked for the inoculation of liquid cultures in order to isolate the plasmids or for analysing the clones directly by colony PCR. Plates were stored at 4°C.

2.4.6 Preparation of Cryopreservation stocks

In order to store transformed bacteria, glycerol stocks were prepared. Therefor, 625 µl of *E. coli* liquid culture were mixed with 375 ml of 80% glycerol. This stock was stored at -80°C.

2.5 *Plasmodium falciparum* experimental methods

2.5.1 Microscopic demonstration of *P. falciparum* using Giemsa staining

Blood smears are a diagnostic tool that allows differentiation between the various blood stages of *Plasmodium* and determination of the parasitemia, i.e. quantification of parasites in the blood.

A drop of blood from the culture plate was withdrawn and smeared on a microscope slide. The air-dried blood was fixed with methanol for 30 seconds and subsequently stained with fresh Giemsa staining solution (1:10 diluted in deionised water) for 15 min. After staining, the microscope slide was rinsed with tap water and air-dried before examination of the blood smear by light microscopy at 100-fold magnification with oil immersion.

2.5.2 Determination of parasitemia by blood smear

The quantitative determination of parasitemia was carried out by counting the uninfected and infected erythrocytes in a blood smear. The percentage of parasitemia was calculated by dividing the number of parasite-infected erythrocytes by the number of uninfected erythrocytes and multiplying by 100 %.

2.5.3 Determination of parasitemia by flow cytometry

Flow cytometry allowed for simultaneous multiparametric analysis of physical and chemical properties of cells. They were passed through a laser beam and scattered the light which was detected as forward scatter (FSC) and side scatter (SSC). These measures directly correlated to the size and the granularity of the cells. In addition, fluorescent light was detected from cells containing fluorochromes. In this study, propidium iodide was used to stain the DNA of the parasites. It was excited with light of a wavelength of 531 nm and emitted light at 604 nm that was detected in the flow cytometer with the channel FL3. As erythrocytes do not contain any DNA, infected and uninfected red blood cells were accordingly differentiated by flow cytometry.

2.5.3.1 Staining of infected erythrocytes

50 µl of parasite culture were resuspended in 50 µl fixing solution (0.05 % glutaraldehyde/PBS) and incubated at 4°C for at least 24 h. The supernatant was discarded and erythrocytes were stained with staining solution (10 µg/ml propidium iodide/PBS) for 1 h at RT in the dark. Then, the supernatant was removed and cells were resuspended in 100 µl PBS to be analysed by flow cytometry.

2.5.3.2 Determination of parasitemia

Measurements were carried out using FACSCalibur (Becton-Dickinson). As negative controls, stained uninfected erythrocytes as well as unstained infected erythrocytes were used. Settings were modified from the PhD thesis of Dr. C. Epp (Epp, 2003).

Table 34 | FACSCalibur settings for parasitemia determination.

parameter	detector	voltage	AmpGain	modus
P1	FSC	E00	1,81	Lin
P2	SSC	382	1,25	Lin
P3	FL1	736	(1,0)	Log
P4	FL2	715	(1,0)	Log
P5	FL3	580	(1,0)	Log
P6	FL2-A		9,99	Lin
P7	FL2-W		8,19	Lin

For determination of parasitemia, 100,000 erythrocytes per sample were counted. Results were displayed in a histogram plotting the fluorescence FL3 (x-axis) and the total cell count (y-axis). This representation allowed the discrimination of different parasite stages by their DNA content and thus their different fluorescence intensities. While ring and trophozoite stages harbour only one genome copy, schizonts contain several genome copies and accordingly emit fluorescence at higher intensity. For the determination of the parasite growth factors, one life cycle was measured. Late schizonts were set to 0.5 % parasitemia and measured by flow cytometry. After one cycle, approximately 42 h, the parasitemia was measured again. The growth factor was calculated by dividing the parasitemia at 42 h by the starting parasitemia at 0 h. Significance was determined using Kruskal-Wallis test.

2.5.4 *Plasmodium falciparum* transfection

For analysis of gene functions *in vivo,* gene targeting is the method of choice. Thereby, genes were specifically altered or completely disrupted to gain insights into gene functions. In the case of *P. falciparum*, a transfection vector was introduced into blood stages. It was supposed to be either inserted into the genome by homologous recombination or kept episomally. In order to select transfected parasites, selection markers were used. To date, seven selectable markers exist for the transfection of *P. falciparum* (Limenitakis, Soldati-Favre 2011): human dihydrofolate reductase (hDHFR), *Toxoplasma gondii* dihydrofolate reductase-thymidylate synthase (DHFR-TS), fungal blasticidin S deaminase (BSD), bacterial neomycin phosphotransferase II (NEO), yeast dihydroorotate dehydrogenase (DHOD) are used as positive selection markers while thymidine kinase (TK) of the *herpes simplex virus* and yeast cytosine deaminase/uracil phosphoribosyl transferase (CD) are used as negative selection markers.

In this study, BSD and hDHFR were used. While BSD confers resistance to the antibiotic blasticdin S, hDHFR enables resistance to pyrimethamine and the anti-malarial drug WR99120.

Stable transfection of *Plasmodium falciparum* was achieved by DNA loading of red blood cells, utilizing the natural ability of malaria parasites to actively take up DNA upon erythrocyte infection. The advantage of this transfection method compared to other protocols is the improved viability of *Plasmodium* parasites as they are not exposed to the trauma of electroporation. Thus, more rapid selection of stably transformed parasites was enabled.

2.5.5 DNA loading of erythrocytes

For DNA loading of red blood cells, 2 ml of RBC-stock (50 % haematocrit) were mixed with 6 ml incomplete cytomix and centrifuged for 2 min at 800 g. The supernatant was removed and washing was repeated once. Then, 400 ml of the RBC pellet were mixed with 400 µl incomplete cytomix and 100 µg of plasmid

DNA. The mixture was transferred to two pre-chilled cuvettes and incubated on ice. Electroporation was performed at 0.31 KV and 960 µFD capacitance. The time constant was in the range of 10 to 13 ms. Immediately after electroporation, the cuvette was returned on ice for 5 min. The cells were transferred completely to a 15 ml tube by rinsing the cuvette twice with 2 ml culture medium each. Cells were spun down at 800 g for 2 min and supernatant containing lysed red blood cells was discarded. The 400 µl transfected erythrocytes were then mixed with 100 µl schizont-infected red blood cells (1 % parasitemia) to achieve a final parasitemia of 0.2–0.3 %. Lastly, 10 ml culture medium was added and the plate was returned to the incubator. On the next day, the medium was exchanged. The parasitemia was 1–2 % rings. The transfection procedure was repeated once 48 h afterwards to increase transfection efficiency, meaning increase the chance of the parasites to invade a loaded RBC. When parasitemia was 2–4 %, 4 µg/ml blasticidin was added to the culture. In case of selection with WR99120, 2.5 µl of 20 mM stock of the drug (final concentration 5 µM) was added 24 h after the second transfection. The medium was exchanged every day. When blasticidin resistant parasites appeared and reached a parasitemia of at least 1 % rings, the culture was split and grown in presence of different blasticidin concentrations.

2.5.6 Purification of mature schizont-stage parasites

Schizont-stage parasites can be purified from rings and trophozoite-stage parasites by means of Percoll gradient. Percoll consists of colloidal silica particles and is a tool for efficient density separation. In this study 70 % and 40 % Percoll gradient was used to separate schizont-stage parasites. Therefore, the 70 % and 40 % Percoll solutions were pre-warmed at 37°C and laid carefully above each other in a 15 ml tube, with 70 % Percoll at the bottom and 40 % Percoll on top of it. The parasite culture (10 ml or 20 ml) was spun down at 1,900 rpm for 2 min and the supernatant was discarded except for 0.5-1 ml. Infected erythrocytes were resuspended in the remaining culture medium to 50 % haematocrit and carefully placed onto the top of the prepared gradient. The total volume of cells can be up

to 2 ml. Centrifugation was carried out at 2,000 rpm for 5 min at RT w/o brake at 300 rpm. The schizonts were recovered from the 40/70 interface and transferred into a 50 ml tube. 10 volumes of either culture media or pure RPMI were added drop by drop, shaking after each addition. Cells were spun down at 1,900 rpm for 5 min and washed once more. The supernatant was removed and cells were either put back into culture or used for RNA or protein extraction.

2.5.7 Protein extraction

Protein expression of transgenic as well as endogenous MSP-1 was analysed by extraction of total proteins from a highly synchronous culture of late schizonts with a parasitemia above 3 %. Protein concentrations from all extracts were adjusted by photometric protein quantification prior to analysis by SDS-PAGE and subsequent Western blotting.

A 30 ml culture of highly synchronous late schizonts was pelleted by centrifugation at 800 g for 2 min. The pellet was resuspended in 36 ml SSC buffer containing 0.2 % saponin for red blood cell lysis. Following incubation on ice for 15 min and inverting from time to time the parasites were collected by centrifugation at 2,200 g for 8 min at 4°C. The supernatant was removed and the pellet was washed three times with 12 ml ice-cold PBS. The parasite pellet was resuspended in 90 µl RIPA buffer supplemented with 1 mM DTT and 1x cOmplete protease inhibitor (Roche) and incubated on ice for 20 min to allow for complete lysis. After final centrifugation step of 10 min at 2,200 g at 4°C the protein extract-containing supernatant was transferred into a fresh tube and stored at -80°C.

2.5.8 Cryopreservation of *P. falciparum*

Long-term storage of blood-stage parasites can be accomplished by the preparation of frozen parasite stocks. For this purpose, one culture plate of

P. falciparum was spun down at 1,900 rpm for 5 min. The supernatant was discarded and slowly 0.33x V of freezing solution was added through gentle mixing. The tube was let stand for 5 min before adding dropwise 1.33x V of freezing solution and mixing gently. The mixture was distributed to labelled cryovials (1 mL per cryovial and frozen at -80°C. Cryovials can either be stored at -80°C or transferred to liquid nitrogen after at least 18 h at -80°C.

3 Results

3.1 *In silico* identification of novel putative PfSUB1 cleavage sites

The first aim of this PhD thesis was to generate MSP-1 mutants that are refractory to cleavage by the PfSUB1 protease.

Previously, a consensus PfSUB1 recognition motif has been described (Koussis et al., 2009), namely Ile/Leu/Val/Thr-Xaa-Gly/Ala-Paa(not Leu) ↓ Xaa, whereby Xaa is any amino acid residue and Paa tends to be a polar residue with a tendency for acidic residues at the proximal five positions on the prime side of the scissile bond (Schechter and Berger nomenclature P1'-P5' (Schechter and Berger, 1967)).

For prediction of PfSUB1 cleavage sites within MSP-1, the computational application Prediction of Protease Specificity (PoPS) was used (Boyd et al., 2004; Boyd et al., 2005). This software enables the *in silico* prediction of potential protease substrates and its specificity. A PfSUB1 specificity model, based on the known consensus sequence, was already established and used to scan the whole *P. falciparum* proteome for further PfSUB1 substrates (Silmon de Monerri et al., 2011). For this thesis, the existing PfSUB1 specificity model was applied to identify putative cleavage sites within both allelic isoforms of MSP-1. An alignment of both MSP-1 variants as well as a schematic representation of the predicated processing site is displayed in Figure 8.

While seven putative processing sites were found for the MAD20 allelic isoform (MSP-1D), nine PfSUB1 cleavage sites were predicted by PoPS for the K1 isoform of MSP-1 (MSP-1F). An internal PfSUB1 cleavage site within the MSP-1_{83} fragment of MSP-1D has already been described (Stafford et al., 1994). Furthermore, another putative internal cleavage site closer to the N-terminus was predicted. Both internal MSP-1_{83} cleavage sites were also found for the K1 isoform. For the 83/30 cleavage junction, PoPS found three putative PfSUB1 sites for MSP-1F but only one for MSP-1D. Further to the C-terminus, only one cleavage site was predicted for the 30/38 junction of both allelic variants.

Strikingly, two and three putative processing sites were found between the MSP-1_{38} and MSP-1_{42} fragments of the MAD20 and K1 allele, respectively. Besides, an additional cleavage site was identified previously by Edman sequencing (Cooper and Bujard, 1992). The latter site, however, is an atypical PfSUB1 site as it does not completely reflect the consensus recognition sequence. Instead of a glycine or alanine, the position P2 featured either a leucine or serine for the MAD20 and K1 variants, respectively. For the sake of clarity, the different cleavage sites at the 38/42 junction were numbered 1-4 starting from the C-terminus of MSP-1.

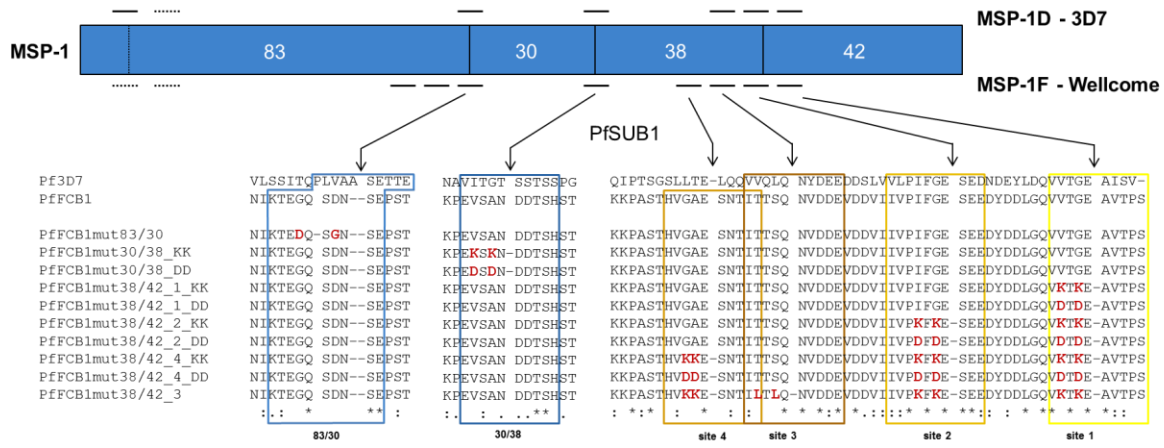

Figure 8 | Predicted PfSUB1 cleavage sites within MSP-1 and mutations introduced.
Schematic representation of MSP-1 primary structure and its predicted PfSUB1 cleavage sites (black horizontal lines). Processing sites were predicted with the PoPS algorithm (Boyd et al., 2004; Boyd et al., 2005) using the protease model according to Silmon de Monerri et al. (2011).
Alignment of MSP-1 sequences from *Plasmodium falciparum* 3D7 and FCB1 and the mutated FCB1 versions using ClustalW2. While only one cleavage site is found for MSP-1D at the 83/30 junction, three sites are predicted for MSP-1F. The 38/42 cleavage junction contains three predicted cleavage sites (site 1, 2, 4) as well as a previously identified site (site 3) (Cooper and Bujard, 1992). Mutations were introduced at positions P2 and P4 which were described to be the most conserved amino acids (Silmon de Monerri et al., 2011), with the exception of site 4 (positions P1 and P2).

3.2 Mutagenic analysis of predicted PfSUB1 processing sites

To address the actual usage of the identified PfSUB1 processing sites within MSP-1, this study included a mutagenic analysis. For this purpose, the K1 isoform of MSP-1 was chosen. Defined mutations were introduced at the most of the aforementioned cleavage sites (Figure 8) and recombinant proteins of these mutants were generated (Kauth et al., 2003). These were subsequently tested for their susceptibility to cleavage by recombinant PfSUB1.

So far, mutagenic studies on the PfSUB1 recognition motif were mainly restricted to fluorogenic peptides with exchanges of the conserved amino acids at positions P1 and P2 and an alanine scan of the non-prime amino acids (Koussis et al., 2009). These studies provided valuable information on the importance of the amino acids at these positions. Based on this evidence, amino acids at position P1, P2 and P4 were mutated to charged amino acids, either lysine or aspartic acid, using site-directed mutagenesis (Appendix Table 35). However, in case of the cleavage site 3, this was not possible (Cooper and Bujard, 1992). Thus, leucines were introduced instead. An alignment of all mutated MSP-1F versions generated in this study is displayed in Figure 8.

Due to the large size of MSP-1, the protein was split into two parts, the 83/30 half including the fragments MSP-1_{83} and MSP-1_{30}, as well as the 38/42 half with MSP-1_{38} and MSP-1_{42}, which were separately produced in *E. coli* DH5α-Z1 as recombinant proteins. MSP-1 fragments were found in inclusion bodies from which they were purified and renatured *in vitro* such that an MSP-1 heterodimer corresponding to the native protein was formed (Kauth et al., 2003). Therefore, two bands representing both protein halves can be seen in a denaturing SDS PAGE (Figure 9B). Addition of recombinant PfSUB1 in a time-course digest of MSP-1 led to the appearance of MSP-1_{83}, MSP-1_{30}, MSP-1_{38} and MSP-1_{42} fragments upon cleavage of 83/30 and 38/42. Following overnight incubation of MSP-1 with PfSUB1, the protein was completely processed into its fragments. As a control, MSP-1 was incubated without the protease overnight to ensure that the samples were clean from other contaminating proteases.

For mutation of the 83/30 junction, amino acids at positions P2 and P2' were interchanged which introduced a non-favoured aspartic acid at position P2 on the prime side of the scissile bond. Incubation of the recombinant MSP-1 heterodimer with PfSUB1 produced the MSP-1_{42} fragment, while the 83/30 half was not susceptible to PfSUB1 cleavage showing that the introduced mutations completely ablated processing at this site (Figure 9 C). Although two additional cleavage sites were predicted at the 83/30 junction, these were not processed by PfSUB1 *in vitro*.

At the 30/38 cleavage junction, only one processing site was predicted by the PoPS algorithm. For mutagenesis and recombinant protein production, a hexahistidine (His_6)-tag and a Glutathione-S-transferase (GST)-tag were fused to full length MSP-1. This enabled the purification of the wildtype (wt) and mutated MSP-1 protein via Ni^{2+}-chelate and GSH affinity chromatography (Kauth et al., 2003). Due to a low yield of pure protein, the analysis of the cleavage assay was performed applying Western blotting with an antibody against the conserved MSP-1_{38} fragment (Figure 9 D). While overnight incubation of the wildtype protein with PfSUB1 produced the MSP-1_{38} fragment, the mutated MSP-1F protein was processed into a fragment of approximately 60 kDa in size. This fragment corresponded to the uncleaved 30/38 fragment confirming that the mutations made the 30/38 cleavage junction refractory to PfSUB1 processing.

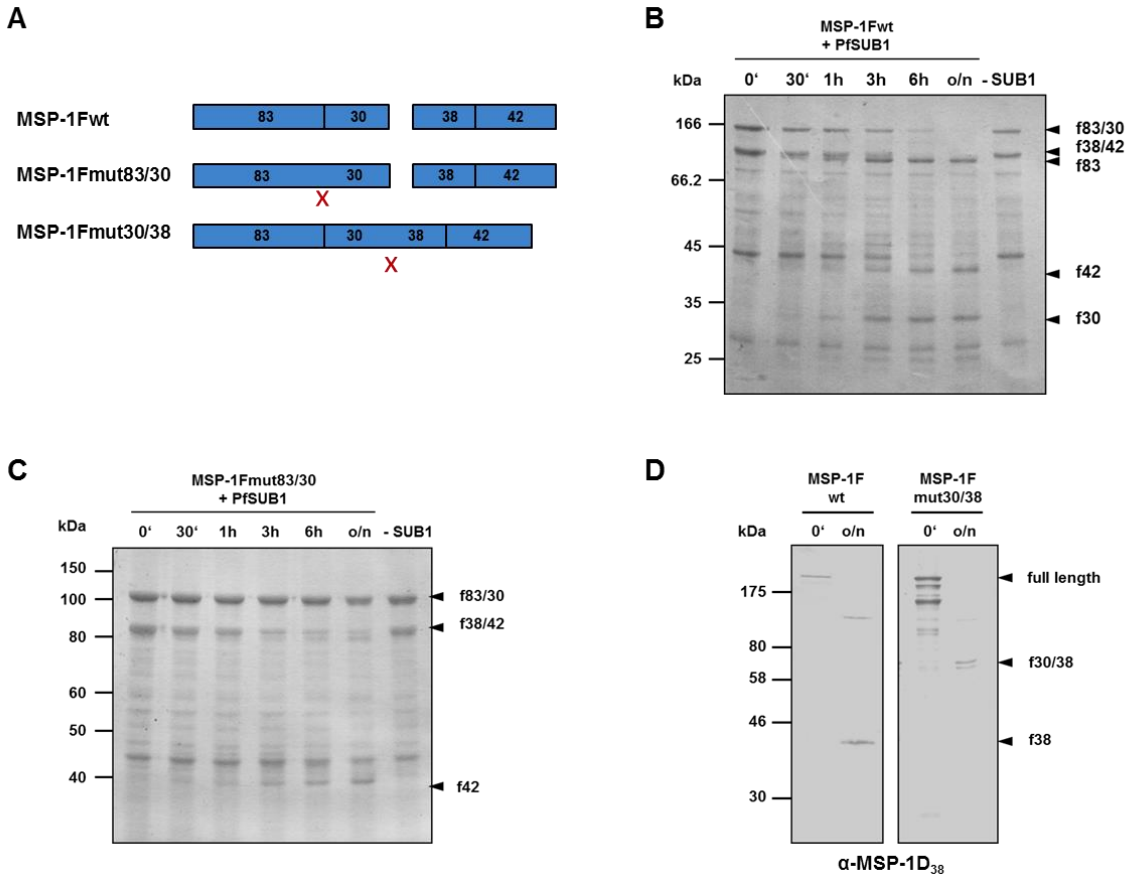

Figure 9 | PfSUB1-mediated proteolytic processing of MSP-1F.
(A) Schematic representation of wildtype MSP-1F and its mutants mut83/30 and mut30/38.
(B-D) Typical time-course of digestion of recombinant MSP-1F. 50 µg MSP-1F were incubated at 16°C in the presence of recombinant PfSUB1 (rPfSUB1). Samples taken at intervals were analysed by SDS-PAGE and subsequent Coomassie staining or Western Blot. Heterodimer fragments and processing products are marked with arrows.
(B) Cleavage of MSP-1Fwt heterodimer. Processing products f83, f42 and f30 appear after 3 h of incubation with rPfSUB1. Coomassie-stained SDS gel.
(C) Processing of MSP-1Fmut83/30. Coomassie-stained SDS gel.
(D) Proteolytic processing of recombinant wildtype and mutated full length MSP1-F. Western Blot analysis using anti-MSP-1D_{38} antibody.
Left: Processing of MSP-1Fwt.
Right: Processing of MSP-1mut30/38.

At the 38/42 junction, three cleavage sites were expected. In addition to the canonical site 1, two sites were predicted by PoPS and one had been described previously (Cooper and Bujard, 1992). Therefore, mutations were consecutively introduced into all cleavage sites located at this junction, starting with site 1, followed by sites 2 and 4 to site 3. A schematic representation of these mutations is displayed in Figure 10 A. All mutations introduced were analysed by Western Blot probed with an anti-MSP-1F$_{33}$ antibody specifically recognising the MSP-1$_{42}$ fragment (Figure 10 C). Upon mutation of site 1, the MSP-1F$_{42*}$ fragment generated by PfSUB1 after overnight incubation was slightly larger than the wildtype MSP-1F$_{42}$ fragment. Accordingly, the 38/42 part of MSP-1 was processed further N-terminally, namely at site 2 which corresponds to the calculated molecular weight of a MSP-1F$_{42*}$ fragment Figure 10 B).

In order to make the 38/42 junction refractory to PfSUB1 cleavage, aspartic acids and lysines were introduced into positions P2 and P4 at site 2 in addition to the mutated site 1. Analysis of the respective cleavage assays resulted in the production of even higher molecular weight MSP-1F$_{42}$ fragments indicated by two asterisks in Figure 10 C. Therefore, additional mutations were introduced into site 4. However, these were still not sufficient to render the protein refractory to PfSUB1 processing, as demonstrated by a MSP-1F$_{42**}$ fragment produced after overnight incubation. Finally, mutation of all 4 cleavage sites led to ablation of processing at the 38/42 junction.

In summary, several PfSUB1 cleavage sites within MSP-1F were predicted by the PoPS algorithm. However, only the junction between MSP-1$_{38}$ and MSP-1$_{42}$ featured apparent redundant PfSUB1 recognition sequences that were actually processed by PfSUB1 *in vitro*. All other putative PfSUB1 processing sites at the 83/30 and 30/38 junction were not cleaved in this assay.

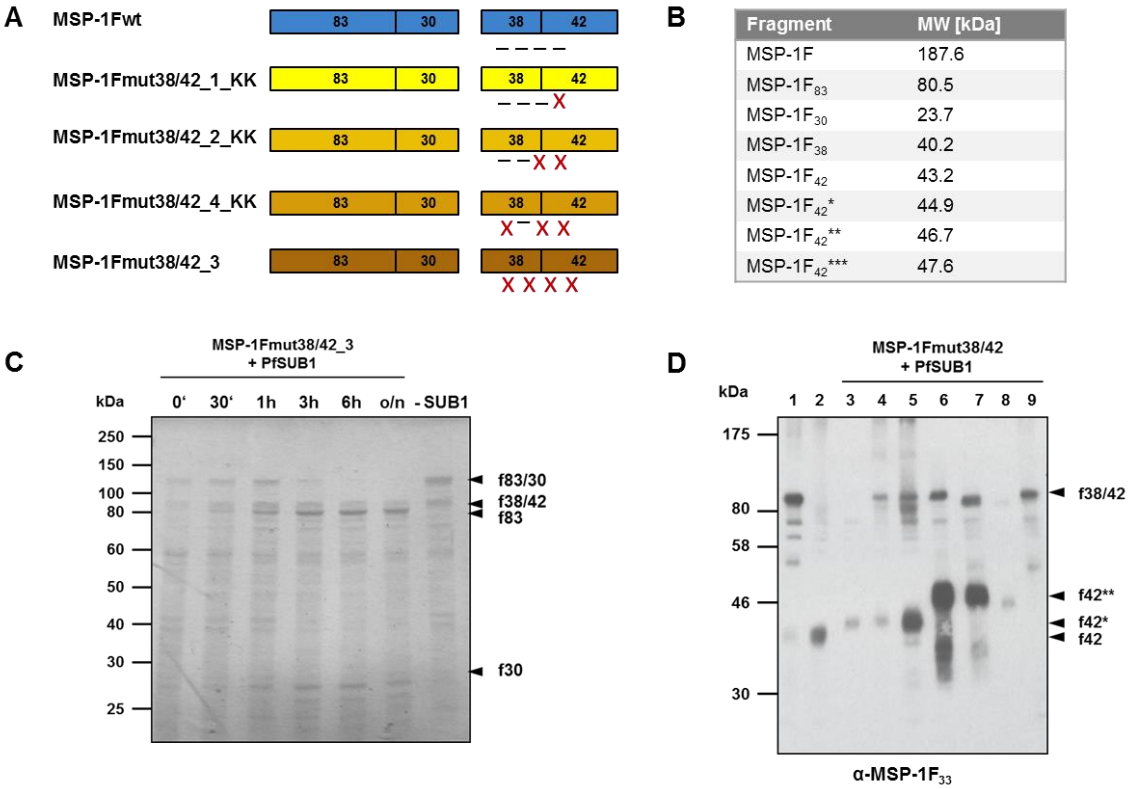

Figure 10 | PfSUB1-mediated proteolytic processing of MSP-1F.
(A) Schematic representation of mutations introduced at the 38/42 cleavage junction of MSP-1F.
(B) Processing fragment of MSP-1F after PfSUB1 cleavage and their calculated molecular weights.
(C) Processing of MSP-1Fmut38/42_3. MSP-1F was mutated at all four cleavage sites found at the 38/42 junction and incubated with rPfSUB1 in time-course digest. Coomassie-stained SDS gel.
(D) Summary of all cleavage mutants of MSP-1Fmut38/42. Recombinant wildtype and mutated MSP-1F heterodimer were incubated o/n at 16°C in the presence of rPfSUB1. Samples taken were analysed by Western Blot probed with anti-MSP-1F$_{33}$ antibody. MSP-1 processing fragments f38/42 and f42 are indicated. Asterisks indicate cleavage at alternative cleavage site.
Lane 1 & 2: MSP-1Fwt heterodimer was incubated for 0‘and overnight with rPfSUB1.
Lane 3: MSP-1Fmut38/42_1_DD. Introduction of two aspartic acids into P2 & P4 at the site 1.
Lane 4: MSP-1Fmut38/42_1_KK. Introduction of two lysines into P2 & P4 at the site 1.
Lane 5: MSP-1Fmut38/42_2_DD. Introduction of two aspartic acids into P2 & P4 at the sites 1&2.
Lane 6: MSP-1Fmut38/42_2_KK. Introduction of two lysines into P2 & P4 at the sites 1 & 2.
Lane 7: MSP-1Fmut38/42_4_DD. Introduction of two aspartic acids into P2 & P4 at sites 1, 2 & 4.
Lane 8: MSP-1Fmut38/42_4_KK. Introduction of two lysines into P2 & P4 at the sites 1, 2 and 4.
Lane 9: MSP-1Fmut38/42_3. Introduction of two lysines into P2 & P4 at the sites 1, 2, 3 and 4.

3.3 Identification of PfSUB1 cleavage sites by LC-MS

Mass spectrometry is a powerful tool to analyse the amino acid sequence of peptides. We employed this technique to identify the exact PfSUB1 cleavage sites within mutant MSP-1F proteins. Therefore, recombinant MSP-1F proteins with mutations of site 1, or sites 1 and 2 at the 38/42 junction were subjected to primary processing by PfSUB1 (see also Figure 8 and Figure 10 C). Emerging fragments were separated by SDS-PAGE, stained with Coomassie and bands corresponding to the molecular weight of the MSP-1F_{42*} and MSP-1F_{p42**} fragments were analysed by liquid chromatography-mass spectrometry (LC-MS) (Boersema et al., 2009).

Therefore, the N-terminus and the side chain of lysine residues of the peptides, all primary amines, were converted to dimethylamines. Samples were labelled with isotopomeric dimethyl labels using either formaldehyde (light) or its deuterated version (medium) that lead to a minimum mass difference of 4 Da between the samples. These can be mixed and analysed simultaneously.

Two strategies were pursued, first the N-terminus of the MSP-1F_{42} fragment was attempted to be identified directly. This was achieved by direct labelling of protein fragments within the SDS gel prior to trypsin digest and LC-MS analysis. Second, the PfSUB1 cleavage site was narrowed down to an amino acid stretch by trypsin digest of the peptides followed by labelling and LC-MS analysis. The complete data set obtained from LC-MS analysis can be found in the appendix (Table 35 and Table 36).

Direct identification of the N-terminus of the MSP-1F_{42*} fragment of MSP-1Fmut38/42_1_KK which contained mutation in cleavage site 1 unfortunately did not work. Thus, the second method was applied in which the undigested precursor protein was labelled with the medium mass formaldehyde and the PfSUB1-digested MSP-1F_{42*} fragment was labelled with normal formaldehyde (light). The ratio of medium/light obtained by LC-MS reflects the specific enrichment of protein fragments in the MSP-1 38/42 precursor (medium) over the MSP-1F_{42} fragment (light). Figure 11 summarises the identified peptides,

highlighting in blue peptides that were found with a high medium/light ratio. Thus, these peptides are predominantly found in the unprocessed MSP-1F precursor protein. The yellow shade indicates peptides with a ratio around 1, which were present in both preparations. Of special interest are the peptides SEEDYDDLGQV and EAVTPSVIDNILSK flanking the mutated site 1. Tryptic digest leads to cleavage at lysine residues (K). Hence, all the tryptic peptides start directly 3' of K. The only identified peptide not starting directly 3' of K is the SEEDY peptide. Furthermore, the very low medium/light ratio of 0.153 strongly indicates that this peptide only occurs upon PfSUB1 cleavage at this position which represents cleavage site 2. In addition, the peptide EAVTPS with a ratio of 119.358 could be present in both unprocessed and PfSUB1 digested samples. However, the presence of the lysine residue as a target for trypsin digest directly 3' of the peptide strongly suggests that this peptide occurs upon tryptic digest and is not a processing product of PfSUB1. Besides, PfSUB1 would cleave the peptide directly after the glutamic acid (E) and not after the lysine residue as found here. Nevertheless, the LC-MS analysis of this mutant MSP-1F should be repeated as the amount of data is not 100 % conclusive.

In contrast, the data obtained for the mutant MSP-1Fmut38/42_2_KK with mutated PfSUB1 cleavage sites 1 and 2 are clear (Figure 11). Using the medium/light ratio the cleavage site can be narrowed down to origin between amino acids 270 and 353. Blue shaded peptides were predominantly found in the MSP-1F precursors, while yellow shaded peptides were only found in the MSP-1F$_{42^{**}}$ fragment. In addition, in-gel labelling directly identified the N-terminus of the MSP-1F $_{42^{**}}$ fragment as NDDEVDDVIVFK (Figure 11, bold), which corresponds to the PfSUB1 cleavage site 3 identified by Cooper and Bujard (1992).

In summary, the analysis of mutant MSP-1F proteins by dimethyl-labelling and mass spectrometry proved the usage of alternative cleavage sites at the 38/42 junction by PfSUB1.

MSP-1Fmut38/42_1_KK

MNDDTSHSTNLNNSLKLFENILSLGKNKNIYQELIGQKSSENFYEKILKDSDTFYNESFTNFVKSKADDINSLNDESKRKKLEEDIN
KLKKTLQLSFDLYNKYKLKLERLFDKKKTVGKYKMQIKKLTLLKEQLESKLNSLNNPKHVLQNFSVFFNKKKEAEIAETENTLENTKI
LLKHYKGLVKYYNGESSPLKTLSEESIQTEDNYASLENFKVLSKLEGKLKDNLNLEKKKLSYLSSGLHHLIAELKEVIKNKNYTGNSPS
ENNTDVNNALESYKKFLPEGTDVATVVSESGSDTLEQSQPKKPASTHVGAESNTITTSQNVDDEVDDVIIVPIFGESEEDYDDLG
QVKTKEAVTPSVIDNILSKIENEYEVLYLKPLAGVYRSLKKQLENNVMTFNVNVKDILNSRFNKRENFKNVLESDLIPYKDLTSSNY
VVKDPYKFLNKEKRDKFLSSYNYIKDSIDTDINFANDVLGYYKILSEKYKSDLDSIKKYINDKQGENEKYLPFLNNIETLYKTVNDKID
LFVIHLEAKVLNYTYEKSNVEVKIKELNYLKTIQDKLADFKKNNNFVGIADLSTDYNHNNLLTKFLSTGMVFENLAKTVLSNLLDG
NLQGMLNISQHQCVKKQCPQNSGCFRHLDEREECKCLLNYKQEGDKCVENPNPTCNENNGGCDADAKCTEEDSGSNGKKIT
CECTKPDSYPLFDGIFCSSSN*

MSP-1Fmut38/42_2_KK

MNDDTSHSTNLNNSLKLFENILSLGKNKNIYQELIGQKSSENFYEKILKDSDTFYNESFTNFVKSKADDINSLNDESKRKKLEEDIN
KLKKTLQLSFDLYNKYKLKLERLFDKKKTVGKYKMQIKKLTLLKEQLESKLNSLNNPKHVLQNFSVFFNKKKEAEIAETENTLENTKI
LLKHYKGLVKYYNGESSPLKTLSEESIQTEDNYASLENFKVLSKLEGKLKDNLNLEKKKLSYLSSGLHHLIAELKEVIKNKNYTGNSPS
ENNTDVNNALESYKKFLPEGTDVATVVSESGSDTLEQSQPKKPASTHVGAESNTITTSQ**NVDDEVDDVIIVPKFK**ESEEDYDDL
GQVKTKEAVTPSVIDNILSKIENEYEVLYLKPLAGVYRSLKKQLENNVMTFNVNVKDILNSRFNKRENFKNVLESDLIPYKDLTSSN
YVVKDPYKFLNKEKRDKFLSSYNYIKDSIDTDINFANDVLGYYKILSEKYKSDLDSIKKYINDKQGENEKYLPFLNNIETLYKTVNDKI
DLFVIHLEAKVLNYTYEKSNVEVKIKELNYLKTIQDKLADFKKNNNFVGIADLSTDYNHNNLLTKFLSTGMVFENLAKTNLQGML
NISQHQCVKKQCPQNSGCFRHLDEREECKCLLNYKQEGDKCVENPNPTCNENNGGCDADAKCTEEDSGSNGKKITCECTKPD
SYPLFDGIFCSSSN*

Figure 11 | LC-MS analysis of MSP-1Fmut38/42.
Recombinant mutated MSP-1F protein was digested with PfSUB1 overnight. Processing fragments were separated by SDS-PAGE and analysed by LC-MS (Boersema et al., 2009). Sequences of MSP-1Fmut38/42_1_KK (top) and MSP-1Fmut38/42_2_KK (bottom) are displayed. Colour code: red, lysine residues (K) that were introduced to render the site refractory to PfSUB1 processing; bold, N-terminus of PfSUB1-processed fragment MSP-1F$_{42}$** identified after in-gel labelling; yellow shade, peptides found by LC-MS with a medium/light ratio ≤1; blue shade, peptides found with a high medium/light ratio ≥100.

3.4 Expression of mutant MSP-1F variants in *P. falciparum*

Cleavage-deficient mutants of MSP-1F identified *in vitro* were to be confirmed *in vivo*. More importantly, the consequences of the cleavage deficiency on the growth of *P. falciparum* parasites should be investigated as well. Therefore, different MSP-1F mutants were co-expressed in *P. falciparum* 3D7 parasites using the blasticidin co-selection system allowing for the discrimination between endogenous *msp-1d* and transgenic *msp-1f*. Besides, this system provided the opportunity to regulate levels of transgene expression and thereby allowed to investigate phenotypes with respect to transgene levels. So far, co-expression of full-length *msp-1f* by other regulable systems has never been achieved. Thus, the study also tested whether the blasticidin co-selection system can be applied for the expression and functional analysis of large, essential transgenes.

3.4.1 Generation of *P. falciparum* expression vectors

To create suitable constructs for the adjustable expression of mutant *msp-1f* in *P. falciparum* 3D7 parasites, the mutations within the cleavage junctions had to be conveyed from the *E. coli* expression vectors to the *P. falciparum* transfection vector pHBIMF that already carried the synthetic gene *msp1f* (Figure 26). For the expression construct pHBIMFmut38/42 this was achieved by excising the sequence, flanking the modified 38/42 cleavage junction, with *PstI* from pZE23-f38/43-mutKKcanKKaltLLC&BKK2ndalt (Figure 25) and cloning it between identical sites in pHBIMF to create the vectors pHBIMFmut38/42.

For the generation of the expression vector pHBIMFmutall, the mutation of the 83/30 cleavage junction within the *E. coli* expression vector pZE13-f-GX190H-mut30/38 was introduced by site-directed mutagenesis (Figure 25). Following the successful mutation, the sequence containing both mutated cleavage junctions (83/30 and 30/38) were conveyed to the pHBIMFmut38/42 vector. Therefore, the mutation-containing sequence was excised with *StuI* and *BglII* and cloned between the identical sites in the pHBIMFmut38/42 vector. The

resulting vectors contain the modified *msp-1f* genes and a gene for blasticidin S deaminase, flanking a bi-directional promoter from a *var* intron.

3.4.2 Generation of transgenic parasite lines

In the course of this study, three different MSP-1F versions were expressed using the blasticidin co-selection system (Figure 12 A): wildtype *msp-1f* (pHBIMFwt), *msp-1f* with mutated 38/42 cleavage junction (pHBIMFmut38/42), and a completely non-cleavable *msp-1f* variant (pHBIMFmutall). The renilla luciferase already described by Epp et al. (2008) served as a positive control to ensure that the system is functional. Vectors for the expression of mutant *msp-1f* versions were transfected into *P. falciparum* 3D7 parasites by electroporation. Following transfection, parasites were first grown in medium containing a low blasticidin concentration for two weeks. Then they were selected applying four different blasticidin concentrations 2, 5, 10 and 15 µg/ml blasticidin. Afterwards, plasmid rescue experiments were performed (Figure 12 B). pHBIMF expression vectors could be recovered from all transgenic parasite lines by plasmid rescue, as shown by restriction digest with *BglII* and *XhoI* as well as PCR analysis using gene-specific primers (Figure 12 B). Hence, the synthetic *msp-1f* gene in combination with the *bsd* gene was successfully introduced into all transfectant parasite lines.

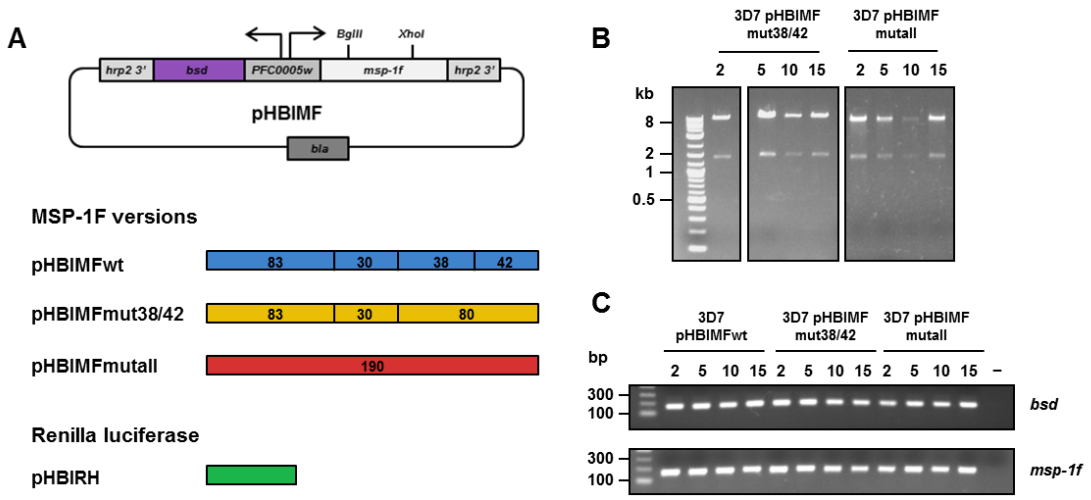

Figure 12 | Generation of *msp-1f* expressing parasite lines.
(A) Illustration of bidirectional expression construct pHBIMF containing the intron from the *var* gene PFC0005w with bidirectional promoter activity. *hrp2 3'*: 3'untranslated region from *Pfhrp2*; *bsd*: blasticidin S deaminase gene; *msp-1f* merozoite surface protein 1 FCB1 strain; *bla*: ampicillin resistance gene. The *msp-1fwt* was replaced either by different mutated versions of *msp-1f* or renilla luciferase. pHBIMFwt: *msp-1fwt*; pHIBMFmut38/42: *msp-1f* mutated at 38/42 junction; pHBIMFmutall: *msp-1f* mutated at all PfSUB1 cleavage sites; pHBIRH: renilla luciferase.
P. falciparum 3D7 parasites stably transformed with pHBIMFwt (blue), pHBIMFmut38/42 (yellow), pHBIMFmutall (red) or pHBIRH (green) were grown in presence of different blasticidin concentrations.
(B) Plasmid rescue and subsequent digest with *Bgl II* and *Xho I*, yielding two fragments of 8494 bp and 1874 bp.
(C) PCR analysis of recovered plasmids. Primers specifically amplified a 180 bp fragment for *msp-1d*, *msp-1f* and *bsd*. – water control.

3.4.3 Proteolytic processing of MSP-1in transgenic parasite lines

In order to detect co-expression of MSP-1F and MSP-1D in *Pf*3D7 parasites and analyse whether the mutated proteins are processed *in vivo*, protein extracts of the different parasite lines were subjected to Western blotting (Figure 13). Extracts were prepared from synchronous cultures of late schizonts. At this stage, MSP-1 levels are highest and primary processing of MSP-1 has already occurred. For evaluation and comparison of transgenic MSP-1F protein with endogenous MSP-1D protein, anti-MSP-1F_{33} and anti-MSP-1$D_{42\Delta EGF}$ antibodies were used, respectively. Both antibodies are directed against MSP-1 regions with low conservation between the two allelic subtypes MSP-1D and MSP-1F and, thus, should specifically detect only the respective allelic isoform. To compare the

MSP-1 expression levels of different transgenic parasite lines, equal amounts of total were analysed by Western blotting. To ensure equal protein amounts, the concentration was determined by Bradford and accordingly adjusted. In addition, one Western blot was also probed with an anti-AMA1 antibody as loading control (Appendix Figure 23). When probing with the anti-MSP-1D$_{42\Delta EGF}$ antibody, the same pattern was observed for all transgenic parasite lines and the *Pf*3D7 control (Figure 13 left panel). The top band corresponds to the unprocessed 196 kDa precursor of MSP-1D while the next band of approximately 120 kDa size probably represents the MSP-1D 30/38/42 fragment which resulted from the first step of primary processing at the 83/30 cleavage junction. Below this band, a fragment of 100 kDa was observed representing the MSP-1D 38/42 fragment. Finally, four bands of around 42 kDa size of the MSP-1$_{42}$ fragment were observed probably corresponding to fragments generated by processing at the alternative cleavage sites found at the 38/42 junction. These patterns showed that processing of the endogenous MSP-1D took place in the transgenic parasite lines as observed in the control parasites *Pf*3D7.

When the Western Blots were probed with an antibody against MSP-1F, the observed processing pattern was different between the transgenic parasite lines (Figure 13 right panel). Control *Pf*FCB1 parasite extracts showed protein bands of 190, 180, 84 and 42 kDa representing the full length MSP-1F, 38/42 and MSP-1F$_{42}$ fragments, respectively. The antibody also recognised an unspecific band of approximately 80 kDa. The same was true for protein extracts from *Pf*3D7 pHIMBFwt parasites although the protein amounts were lower. Here, MSP-1Fwt protein was co-expressed and normal processing was observed. In contrast, protein extracts from *Pf*3D7 pHBIMFmut38/42 and mutall parasites did not show the same pattern as *Pf*3D7 pHBIMFwt or *Pf*FCB1 and expressed much less MSP-1F protein. Protein extracts from *Pf*3D7 pHBIMFmut38/42 showed a 190 kDa protein band corresponding to the full length MSP-1F protein as in the *Pf*FCB1 control. In addition, a 120 and 100 kDa band were observed most likely corresponding to the processing products MSP-1F 30/38/42 and MSP-1F 38/42, respectively. The observed 80 kDa band is due to an unspecific binding of the

antibody as this band is also present in the *Pf*3D7 control. Last, a 50 kDa band can be observed. The identity of this protein fragment is not clear and should be sent for sequencing via mass spectrometry to identify its nature. However as this band is also found in the *Pf*FCB1 control it is very likely a fragment of MSP-1F. Nevertheless, no protein fragment corresponding to the MSP-$1F_{42}$ processing product was observed in the protein extracts from *Pf*3D7 pHBIMFmut38/42 parasites. Western Blot analysis of extracts from *Pf*3D7 pHBIMFmutall parasites only showed the 190 kDa full length MSP-1F protein and the unspecific 80 kDa band but no processing products as in the *Pf*FCB1 control.

In theory, the amount of transgenic protein should increase with increasing blasticidin concentrations. However, this could not be observed by Western blotting. This is most probably due to the adjustment of total protein amounts prior to analysis, the low overall MSP-1F protein level and the non-quantitative method used here.

In summary, both MSP-1 variants are indeed co-expressed in transgenic parasite lines. While the endogenous MSP-1D is processed normally by PfSUB1, the introduction of mutations into cleavage junctions within the *msp-1f* sequence made the protein refractory to PfSUB1 cleavage *in vivo*. These data complement and support the presented *in vitro* data where mutated recombinant MSP-1F was also refractory to PfSUB1 processing (Figure 10)

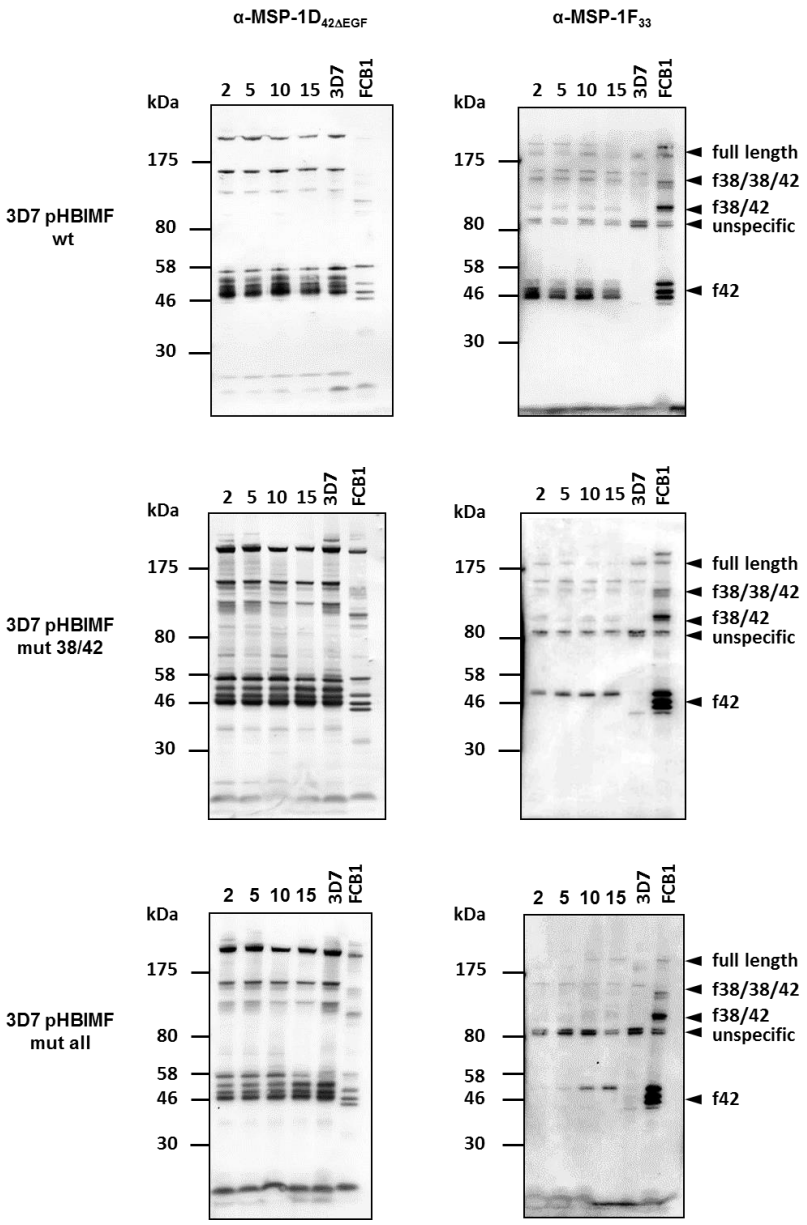

Figure 13 | Protein expression and cleavage by PfSUB1.
Protein extracts from control parasites *Pf*3D7 and *Pf*FCB1 as well as transgenic parasites *Pf*3D7 pHBIMFwt, *Pf*3D7 pHBIMFmut38/42 and *Pf*3D7 pHBIMFmutall grown in the presence of 2, 5, 10 and 15 µg/ml blasticidin were subjected to SDS-PAGE and subsequent Western blotting. Expression of endogenous MSP-1D was probed with anti-MSP-1D$_{42\Delta\ EGF}$ (rabbit, 1:10,000) and transgenic MSP-1F with anti-MSP-1F$_{33}$ (rabbit, 1:100) antibodies.

3.4.4 Co-localisation of MSP-1D and MSP-1F in transgenic parasites

MSP-1 is localised to the surface of *P. falciparum* 3D7 merozoites, to which the episomally expressed MSP-1F should also localise. To check for the localisation of both MSP-1 versions, immunofluorescence analysis of transgenic parasites in late schizont stages was performed using antibodies specifically detecting MSP-1D and MSP-1F, respectively (Figure 14 A). Specificity of both antibodies was validated by staining of *Pf*3D7 and *Pf*FCB1 wildtype parasites. DNA staining with Hoechst 33342 revealed multiple nuclei of daughter merozoites, thus proving that the parasites were in late schizont stages. All parasite lines generated in this study and grown at different blasticidin concentrations were analysed by IFA. Three representative images from the transgenic parasite lines are shown in Figure 14 A.

In all parasite lines, MSP-1F was expressed and localised to the merozoite surface like endogenous MSP-1D. Both MSP-1 variants moreover co-localised as shown in the merged images. The degree of co-localisation was quantified by determining the Pearson's R value (Figure 14 B). As control, *Pf*3D7 and *Pf*FCB1 parasites showed a Pearson's correlation coefficient of 0.4 and 0.2, respectively, corresponding to the background. In contrast, all transgenic parasite lines displayed a Pearson's R value of 0.8 to 0.9 showing that MSP-1D and MSP-1F indeed co-localise in these parasites independent of the blasticidin concentrations used. Hence, transgenic MSP-1F was demonstrated to be expressed and co-localised with MSP-1D to the merozoite surface.

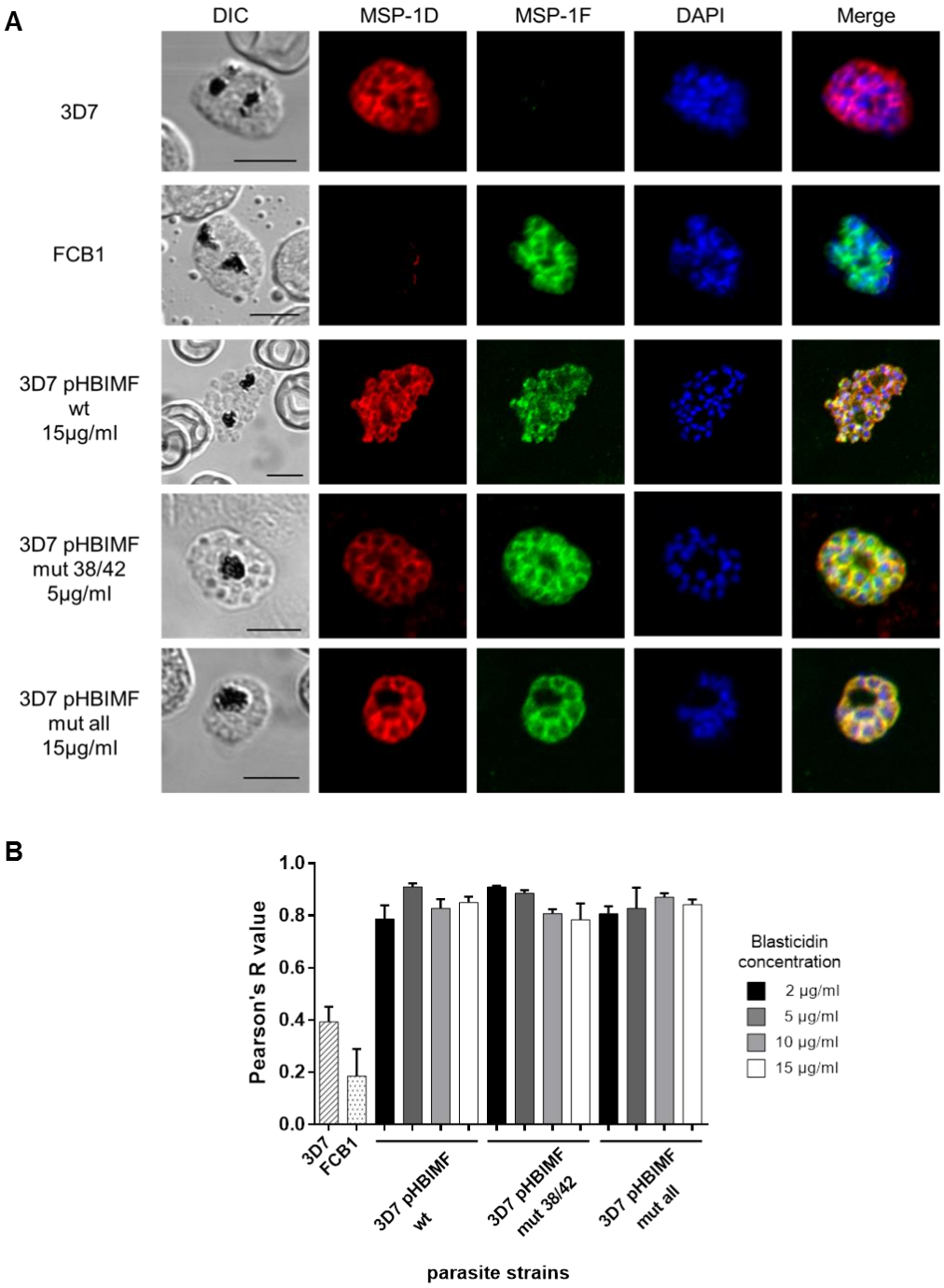

Figure 14 | Immunofluorescence analysis of parental and transgenic parasite lines.
(A) Confocal images of late segmented *P. falciparum* schizonts stained with anti-MSP-1F$_{33}$ (rabbit) and anti-MSP-1D (mAb 111.4) antibodies to detect both allelic MSP-1 isoforms and demonstrate co-localisation. Antibodies specifically recognise only one allelic isoform as demonstrated in the upper two panels *Pf*3D7 and *Pf*FCB1. The lower panels show representative images of the three transgenic parasite lines 3D7 pHBIMFwt, 3D7 pHBIMFmut38/42 and 3D7 pHBIMFmut all. Scale bar 5µm.
(B) Co-localisation of MSP-1D and MSP-1F in all parasite lines kept in different blasticidin concentrations was quantified by calculating the Pearson's R values using the plugin Coloc2 in Fiji. Columns correspond to mean values with standard error of mean.

3.4.5 Regulation of episome copy number by blasticidin concentrations

Theoretically, the stably transformed *P. falciparum* parasites should carry episomes that are present as concatamers (O'Donnell et al., 2002b; Williamson et al., 2002). It is expected to obtain direct correlation of drug concentration and the number of plasmid copies. Hence, increasing blasticidin concentrations should lead to higher copy numbers of both the blasticidin S deaminase (*bsd*) and *msp-1f* gene.

To address this, total DNA consisting of genomic and episomal material was extracted from all transgenic parasite lines and plasmid copy numbers were determined by real-time PCR using gene-specific primers for *msp-1f,* renilla luciferase and blasticidin S deaminase. The generation of standard curves allowed for the calculation of absolute copy numbers (Appendix Table 40, Figure 24). Values were normalised to actin and, as an internal control, the copy number of the endogenous *msp-1d* gene was determined (Figure 12 C).

While gene copy numbers of *msp-1fwt* and renilla luciferase could be up-regulated with increasing blasticidin concentrations to approximately ten copies per parasite, the copy numbers of mutated *msp-1f* genes behaved differently. For the plasmid pHBIMFmut38/42, the copy number was highest at 10 µg/ml blasticidin but decreased at 15 µg/ml blasticidin from seven to four copies per parasite. This was even more pronounced for the parasites transfected with pHBIMFmutall. Here, *msp-1f* copy numbers reached only three copies at 10 µg/ml blasticidin and decreased at 15 µg/ml blasticidin as well. This might be a consequence of the different mutations introduced into the *msp-1f* sequence.

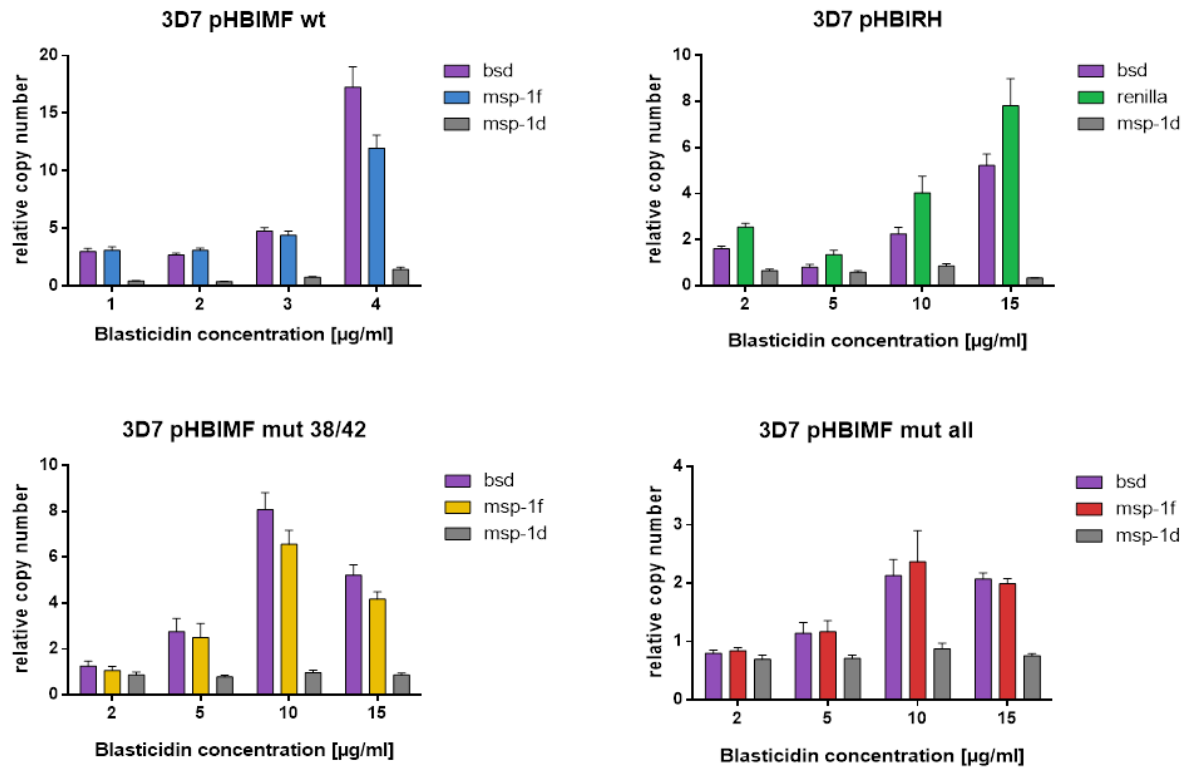

Figure 15 | DNA copy number of episomes using variable blasticidin concentrations.
P. falciparum 3D7 parasites stably transformed with pHBIMFwt (blue), pHBIMFmut38/42 (yellow), pHBIMFmutall (red) or pHBIRH (green) were grown in presence of different blasticidin concentrations. Total DNA was purified and DNA copy numbers of blasticidin S deaminase (*bsd*), merozoite surface protein 1 FCB1 strain (*msp-1f*), renilla luciferase (*renilla*), and the endogenous *msp-1* gene (*msp-1d, grey*) were determined by quantitative PCR. Values were normalised to the control gene *actin*. Samples were measured in triplicates and error bars indicate the standard error.

3.4.6 Regulation of *msp-1f* expression by altering blasticidin concentration

Although immunofluorescence analysis showed that MSP-1F is indeed expressed and localised correctly, this technique did not allow for quantification of transgene expression. Therefore, total RNA was extracted from synchronised parasite cultures of late trophozoite stage (~40 h.p.i). The transcript levels of blasticidin S deaminase (*bsd*), *msp-1f*, renilla luciferase and endogenous *msp-1d* were determined by synthesis of cDNA followed by quantitative real time PCR analysis. Values were normalised to the reference gene actin (Figure 16 A). As a control, the relative transcript number of *msp-1d* was determined and remained ~1 across all parasite lines analysed. *Pf*3D7 pHBIMFwt parasites showed an

increase in transcript number for both, *msp-1d* and *bsd* with increasing blasticidin concentrations. However, the relative transcript number compared to *msp-1d* did not reach 1 and thus the transgene expression in these parasites was always lower than the expression of the endogenous *msp-1d*. In contrast, the relative transcript number of the renilla luciferase was up-regulated to 1.2 in parasites kept at 15 µg/ml blasticidin. This already indicated that the expression of large genes such as *msp-1f* cannot be up-regulated to the extent of short reporter gene expression. The expression of mutant *msp-1f* transcripts always stayed below the endogenous *msp-1d* transcript numbers, not even reaching 0.1 relative transcript numbers. This effect was more pronounced in the *Pf*3D7 pHBIMFmutall parasites that were expressing completely cleavage-deficient *msp-1f*. To determine an effect of the cleavage site mutations, the values of *msp-1fwt* were used as a valid reference for *msp-1fmut38/42* and *msp-1fmutall*. The comparison of the expression levels of the *msp-1* variants indicates the extent to which MSP-1D was replaced by MSP-1F (Figure 16 B). While *msp-1fwt* expression reached 36 % of *msp-1d* expression, expression of mutant *msp-1f* was dramatically lower and reached only 15 % and 10 % for *msp-1fmut38/42* and *msp-1fmutall*, respectively. In contrast, renilla luciferase expression could be up-regulated to 150 % of *msp-1d*.

Together with the DNA copy number (Figure 15), these data demonstrate that MSP-1Fwt is tolerated by the parasites substantially better than the mutant versions, indicating a deleterious effect on parasite growth.

A

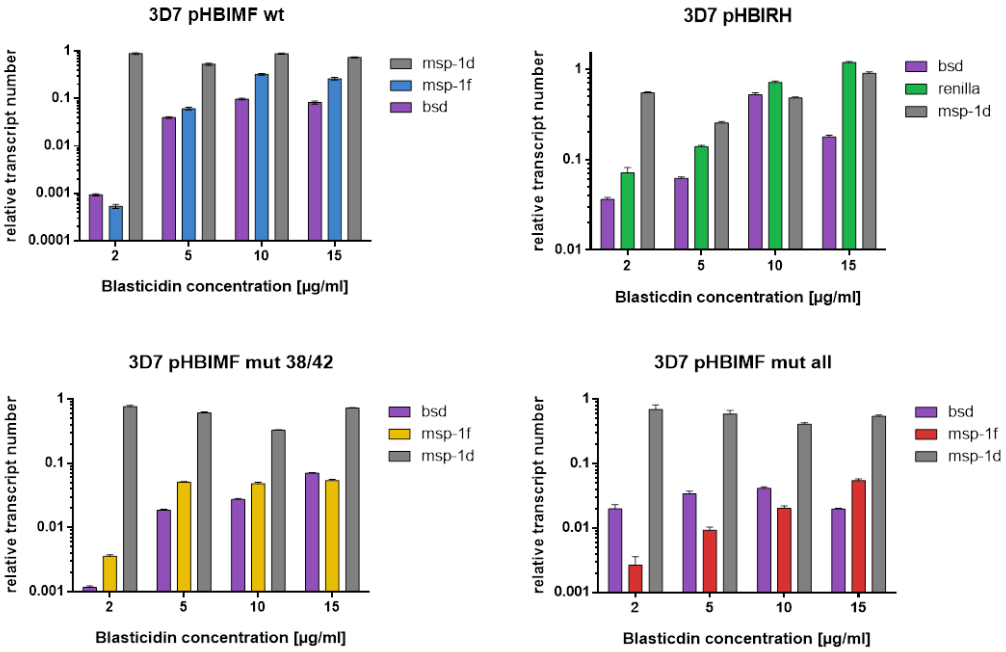

B

Blasticidin concentration	MSP-1F wt	MSP-1F mut 38/42	MSP-1F mut all	Renilla
2 µg/ml	**0.1** (± 0.001)†	**0.5** (± 0.001)	**0.4** ± (0.04)	**13.0** (± 0.02)
5 µg/ml	**11.6** (± 0.01)	**8.4** (± 0.004)	**1.6** ± (0.06)	**54.5** (± 0.03)
10 µg/ml	**36.7** (± 0.02)	**14.8** (± 0.008)	**5.0** ± (0.10)	**148.8** (± 0.07)
15 µg/ml	**35.4** (± 0.02)	**7.5** (± 0.004)	**10.1** ± (0.10)	**132.0** (± 0.06)

† standard error of mean in brackets

Figure 16 | Regulated transgene expression via variable blasticidin concentrations.
P. falciparum 3D7 parasites stably transformed with pHBIMFwt, pHBIRH, pHBIMFmut38/42 or pHBIMFmutall were grown in presence of different blasticidin concentrations.
(A) RNA was extracted from synchronized parasite cultures in the late trophozoite stage (~40 h.p.i) and mRNA levels were determined by synthesis of cDNA followed by quantitative real time PCR analysis. The transcript levels of blasticidin S deaminase (*bsd*), merozoite surface protein 1 of the FCB1 strain (*msp-1f*) and 3D7 strain (*msp-1d*), and Renilla luciferase (*renilla)* were determined. Values were standardised to the control gene *actin*. Samples were measured in triplicate. Columns represent mean values and the corresponding standard errors are indicated by bars.
(B) Transgene expression was displayed as percentile of *msp-1d* (100 %) with standard error of the mean in brackets.

3.4.7 Parasite growth is affected by expression of cleavage-deficient *msp-1f*

Although the expression of *msp-1f* was lower than anticipated, MSP-1F protein was found on the merozoite surface co-localising with MSP-1D. In order to analyse whether the co-expression of *msp-1f* does affect parasite growth, the parasitemia of all transgenic parasite lines was investigated by flow cytometry. Comparison between all *P. falciparum* lines was carried out by determining the parasitemia over one replication cycle. Therefore, the parasitemia of late schizonts was set to 0.5 % (0 h) and measured again after 42 h. Afterwards, the growth factor was calculated by dividing the parasitemia measured at 42 h by 0 h. For statistical analysis, the Kruskal-Wallis test was applied (Figure 17). Initially, mean growth factors of parental *Pf*3D7 line, *Pf*FCB1, *Pf*3D7 pHBIMFwt and *Pf*3D7 pHBIRH lines were determined (Figure 17 A and B). These control parasite lines displayed a growth factor of approximately 7 which was comparable to values from the literature (Woehlbier et al., 2010). Also, transgenic parasites *Pf*3D7 pHBIMFwt expressing *msp-1f* wt did not show a significant difference to the parental *Pf*3D7 line or *Pf*FCB1. Thus, these parasites were used as controls and compared to transgenic parasite lines expressing mutant *msp-1f* kept at the same blasticidin concentrations. *Pf*3D7 pHBIMFmutall parasites displayed a small but yet significant growth defect in all blasticidin concentrations. In contrast, a significant growth defect of *Pf*3D7 pHBIMFmut38/42 was only observed when parasites were kept at 2 µg/ml and 15 µg/ml blasticidin (Figure 17 C-F).

Taken together, transgenic parasite lines expressing mutant *msp-1f* displayed a growth defect, although the expression of the transgene was rather low compared to renilla luciferase or *msp-1fwt*. This already pointed towards a deleterious effect of non-cleavable MSP-1F.

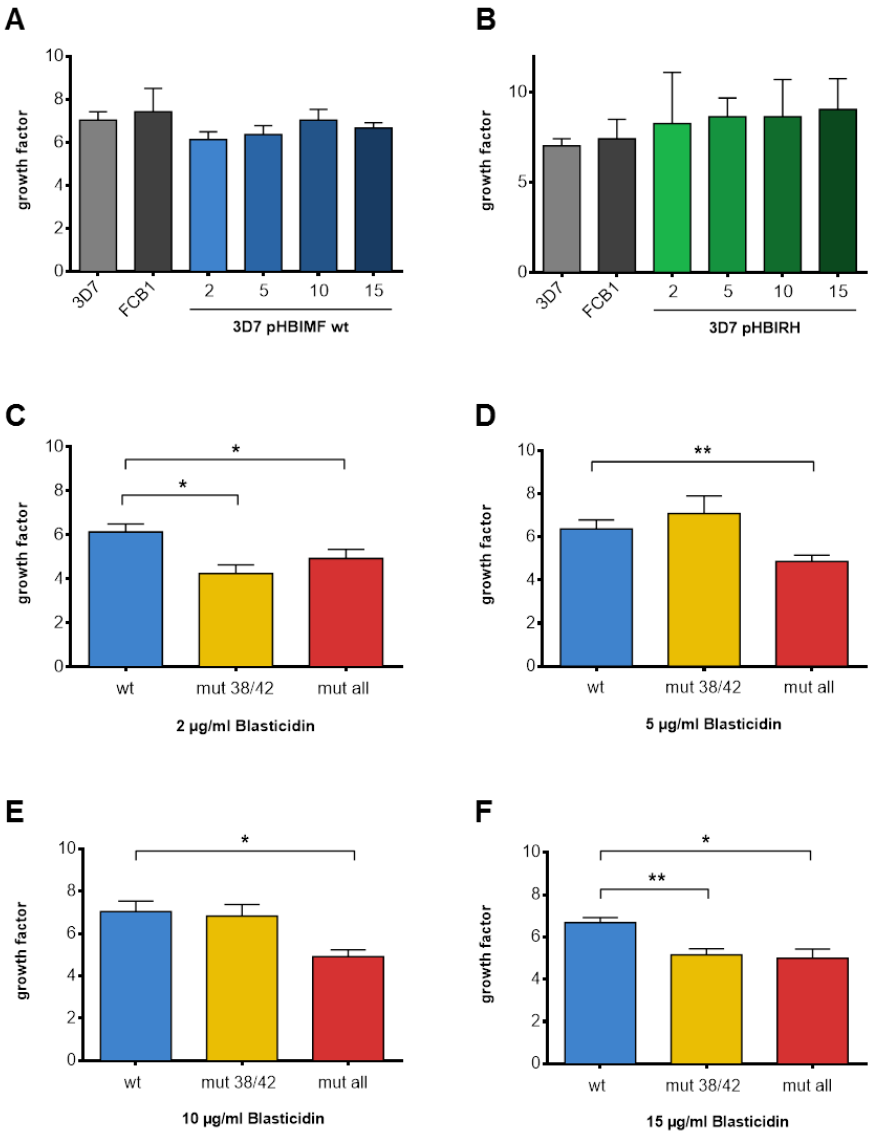

Figure 17 | Growth analysis of transgenic parasites.
Parasite growth was followed by flow cytometry over 42 h. Comparison between all *P. falciparum* lines was carried out by determining the growth factor; calculating the ratio of parasitemia at 42 h/0 h. Initially, growth factors of parental *Pf*3D7 line, *Pf*FCB1, *Pf*3D7 pHBIMFwt and *Pf*3D7 pHBIRH lines were determined (A&B). Growth of transgenic parasite lines expressing mutant MSP-1F (C-F) were compared to controls *Pf*3D7 pHBIMFwt kept at the same blasticidin concentration. Columns show mean values of multiple measurement, standard errors of the mean are indicated. Statistical significance was determined by Kruskal-Wallis test. *:$P<0.05$, **:$P<0.01$

3.4.8 Nutrient uptake of transgenic parasite lines is not impaired

The parasites expressing cleavage-deficient *msp-1f* carry only few copies of the blasticidin S deaminase gene and less blasticidin S deaminase is transcribed compared to control lines expressing renilla luciferase or *msp-1fwt*. Nevertheless, the parasites can grow under high concentrations of blasticidin. The lack of blasticidin S deaminase might be compensated by alternative mechanisms of resistance. The acquisition of resistance to blasticidin can occur via the differential expression of *clag 3* genes (Hill et al., 2007; Mira-Martinez et al., 2013). *Clag 3.1* and *clag 3.2* are involved in the formation of the plasmodial surface anion channel (PSAC) which is an important mediator of nutrient import (Nguitragool et al.). Down-regulation of both genes leads to blasticidin resistance as the PSAC is not properly formed and both nutrients as well as drugs are not taken up into the parasite (Mira-Martinez et al., 2013).

To investigate, if the transgenic parasite lines have acquired blasticidin resistance by switching of *clag 3* expression, the transcription of both *clag* genes was analysed by real time PCR (Figure 18). For that, total RNA was extracted from synchronous parasites at 40 hp.i and mRNA levels were investigated by cDNA synthesis and subsequent real time PCR using *clag 3.1* and *clag 3.2* gene-specific primers.

All transgenic parasite lines showed predominant expression of the *clag 3.1* gene while *clag 3.2* expression was almost shut down, independent from blasticidin concentration used for culture maintenance. *Clag 3.1*'s transcript number was the highest in *Pf*3D7 pHBIMFwt parasites and ten times lower in transgenic parasites expressing mutated *msp-1f*. However, this was also observed for the control parasites expressing renilla luciferase instead of *msp-1f*. Thus, this might be due to technical variations of different real time PCR measurements. Nevertheless, all transgenic parasite lines expressed clag genes and thus, did not develop blasticidin resistance by switching or down-regulation of *clag 3* gene expression. Therefore, parasites should exert normal nutrient uptake by PSAC. This further proved that

the observed growth defect is due to impaired MSP-1F processing and is not a consequence of impaired nutrient uptake by the parasite.

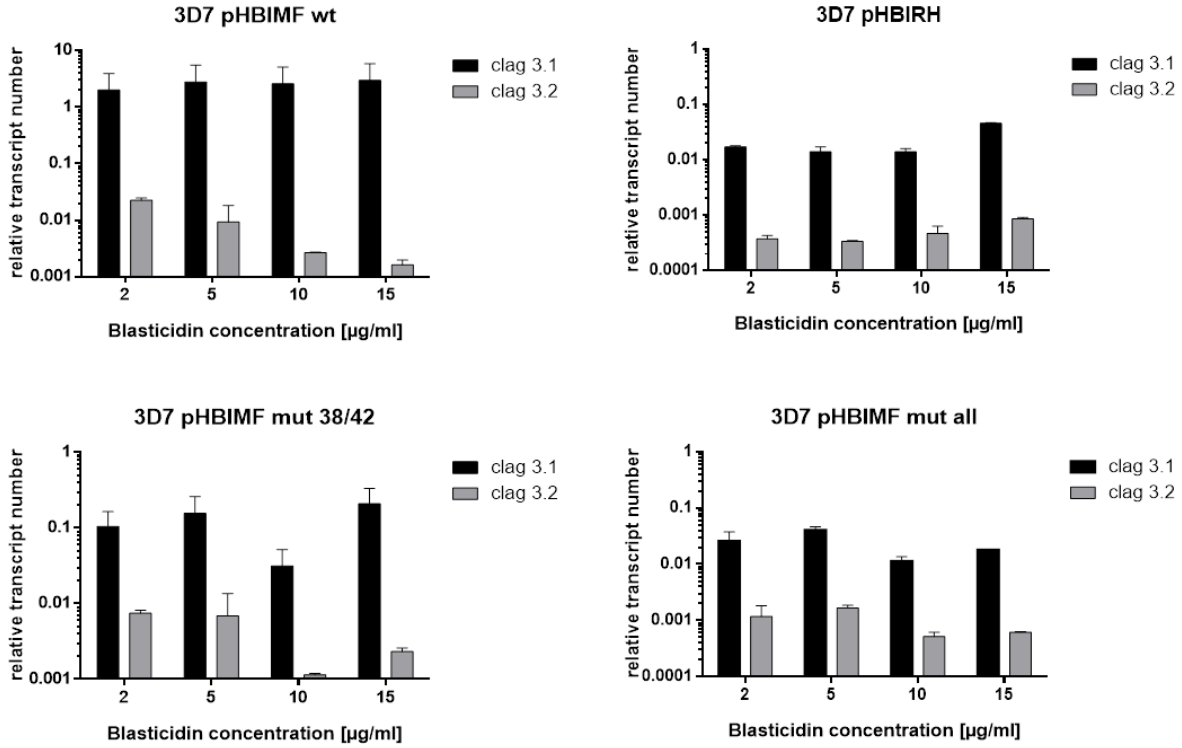

Figure 18 | Growth phenotypes of transgenic parasite lines are not associated with changes in *clag3* expression.
RNA was extracted from synchronized parasite cultures in the late trophozoite stage (~40 h.p.i) and mRNA levels were determined by synthesis of cDNA followed by quantitative real time PCR analysis. The transcript levels of *clag 3.1* and *clag 3.2* were determined. Values were normalised to the control gene *actin*. Samples were measured in triplicate. Columns represent mean values and the corresponding standard errors are indicated by bars.

3.4.9 Knockout attempts on *Pfmsp-1d* via double homologous crossover recombination

In the past, gene disruptions in *P. falciparum* were mainly achieved by single homologous crossover recombination using a positive selection marker such as hDHFR. As integration events are very rare, several drug on/off cycles were needed to obtain *P. falciparum* parasites containing stably integrated plasmids.

Transfection vectors with positive and negative selection markers were shown to increase the efficiency of gene targeting via double homologous crossover recombination (Duraisingh et al., 2002; Maier et al., 2006). The introduction of a negative selection marker such as the thymidine kinase (TK) of the *Herpes simplex* virus in the pHTK vector (Duraisingh et al., 2002), or the bifunctional cytosine deaminase/uracil phosphoribosyl transferase (CDUP) from *Saccharomyces cerevisiae* in the vector pCC1 (Maier et al., 2006), greatly enhanced the selection pressure for recombination events. Both enzymes allow for the conversion of the normally innocuous metabolites, ganciclovir (TK) and 5-fluorocytosine (5-FC; CDUP), respectively, into toxic derivatives. These toxic metabolites then inhibit the *de novo* pyrimidine biosynthesis pathway and nucleic acid synthesis directly (Duraisingh et al., 2002; Maier et al., 2006; Ménard, 2013). Only parasites that have successfully introduced the plasmid by double homologous crossover during excision of the plasmid backbone survive the treatment with these compounds.

Both vector systems were employed for the generation of *msp-1* knockout parasites. Two 1 kb homologous fragments of the 5' untranslated region (UTR) and 3' end of MSP-1 were cloned into the pCC1 and pHTK vectors flanking the positive selection marker hDHFR (Figure 19 A). *Pf*3D7 as well as *Pf*3D7 pHBIMFwt parasites were transfected with these constructs and positively selected on WR99210. As *msp-1* was already shown to be essential, viable parasites should only be obtained after transfection of *Pf*3D7 pHBIMFwt parasites as they episomally express *msp-1fwt* which may complement for the knockout of the endogenous *msp-1d*.

Upon re-appearance after positive selection, transfectants were either subjected to different concentrations of the negative selection drugs 5-FC (500 nM, 1 µM, 6 µM, 12 µM), or ganciclovir (20 µM) or cycled without WR99210. A complete cycling and selection pressure overview is provided in Table 41 in the appendix. The concentrations tested for 5-FC and ganciclovir were based on personal communication with Dr. Sophia Deil who performed IC_{50} measurements with her transfectants (Deil, 2014) and literature values from (Maier et al., 2006). According to (Maier et al., 2006), a dosage of 5-FC should be used that would kill most of the parasites (IC_{90}) but would prevent toxic 'bystander' effects on integrants. The concentrations used in this study were much higher than those recommended by (Maier et al., 2006) which might be due to differences in culture conditions. However, parasites did not die after treatment with 5-FC or ganciclovir, or even after several drug on/off cycles. Following positive and negative selection and parasite recovery, gDNA was extracted and subjected to PCR analysis. Primers were chosen to control for gDNA, episomal presence of the plasmid, as well as 5' and 3' recombination events into the *PfMSP-1D* locus. As *Pf*3D7 pHBIMFwt parasites were transfected with pCC1-MSP1D-KO or pHTK-MSP1D-KO vectors, the presence of the pHBIMF plasmid was also detected by PCR (*bsd, msp-1f*). One representative DNA gel is shown in Figure 19 B. Both plasmids, the pCC1-MSP1D-KO and the pHBIMFwt, were present in the parasites as PCR bands for *msp-1f*, *bsd*, *hDHFR*, *CDUP* and episome were detected. Besides, the endogenous *msp-1d* gene was detected. The primers amplifying the 5' region of the episome did not always work which can be attributed to the PCR conditions used. However, no integration events were detected as both primer sets for detecting 5' and 3' integration did not amplify a PCR product. This together with the presence of the CDUP ensures that the parasites did not recombine but kept the knockout plasmid episomally. The same PCR results were obtained even after several rounds of drug cycling. In summary, no parasite population with double crossover recombination was obtained neither with the pCC1 vector nor with the pHTK vector, and despite the use of variable drug concentrations and cycling conditions (Table 41).

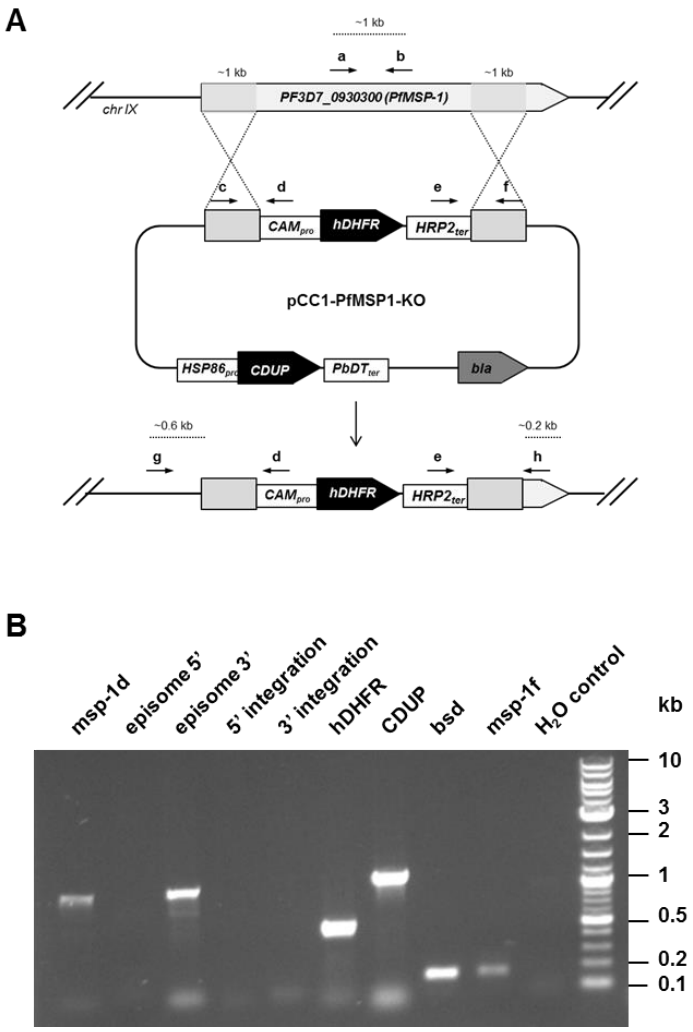

Figure 19 | Knockout strategy for *PfMSP-1D* using the pCC1/pHTK vector system and analysis of transgenic parasites by PCR.

Disruption of the PF3D7_0930300 (*PfMSP-1*) gene in *P. falciparum 3D7 pHBIMFwt* grown in 15 µg/ml blasticidin by double crossover recombination using the pHTK/pCC1 vector system with positive (WR99210) and negative (5-fluorocytosine, ganciclovir) selection.

(A) Design of the knockout plasmids as exemplified for pCC1-PfMSP1-KO. Two 1 kb regions homologous to *Pfmsp-1d* 5' and 3' (light grey) were chosen to flank the positive selection marker cassette. Selection marker cassettes (black boxes) for positive selection encoded hDHFR (pHTK/pCC1 vectors) and for negative selection either TK (pHTK vector) or CDUP (pCC1 vector). Primers used for PCR analysis are shown as black arrows (a-f). *bla*: ampicillin resistance gene; CAM_{pro} and $HSP86_{pro}$, promoters of the *CAM* and *HSP86* genes; *chr IX:* chromosome 9; $HRP2_{ter}$ and $PbDT_{ter}$: terminator regions of the *HRP2* and *PbDHFR-TS* genes.

(B) PCR analysis of genomic DNA from cycled transfectants. Primers were chosen to detect the 5' episome (c+d, 1 kb) and 3' episome (e+f), genomic DNA (*msp-1d*, a+b, 1 kb) as well as integration of the plasmid after recombination along the 5' (g+d, 1 kb) as well as 3' (e+h, 1 kb) fragments. In addition, primers detecting the selection markers CDUP (1 kb), hDHFR (0.5 kb) and blasticidin S deaminase (bsd, 180 bp) were included as well as primers for MSP-1F (*msp-1f*, 180 bp).

3.4.10 Processed MSP-1 binds to erythrocytes

Merozoites are thought to attach to erythrocytes via the interaction of MSP-1 with receptors on the red blood cell surface. However, this interaction has never conclusively been shown, as only MSP-1 fragments have been used in several studies (Boyle et al., 2010; Goel et al., 2003; Nikodem and Davidson, 2000). Thus, the aim was to analyse whether there is a direct interaction of unprocessed or processed MSP-1 with erythrocytes and, if so, whether these interactions can be inhibited. Due to the better availability of full length protein as well as fragments and a panel of antibodies the MAD20 isoform of MSP-1 (MSP-1D) was used.

To assess the ability of the recombinant protein to bind to the host cell, MSP-1D was tested in erythrocyte-binding assays incubating fresh red blood cells with MSP-1D heterodimer that was either unaltered or cleaved with rPfSUB1 overnight (Figure 20 A). Only the processed MSP-1D heterodimer bound to erythrocytes and was eluted with 1.5 M sodium/PBS solution. The assay was repeated with MSP-1D fragments and showed that only MSP-1_{83} and MSP-1_{38} were binding to red blood cells (Figure 20 B).

The erythrocyte binding specificity of the MSP-1D fragments was tested by inhibiting the interaction by applying anti-MSP-1D antibodies (Figure 20 C). Different concentrations of anti-MSP-1D antibodies were tested ranging from 80 µg, 400 µg to 800 µg which corresponds to equimolar, 5- and 10-times the amount of MSP-1D, respectively. While equimolar amounts of antibodies were not sufficient to inhibit erythrocyte binding of processed MSP-1D, 5- and 10-times the concentration of antibodies to MSP-1D specifically inhibited binding to red blood cells confirming the specificity of the interaction.

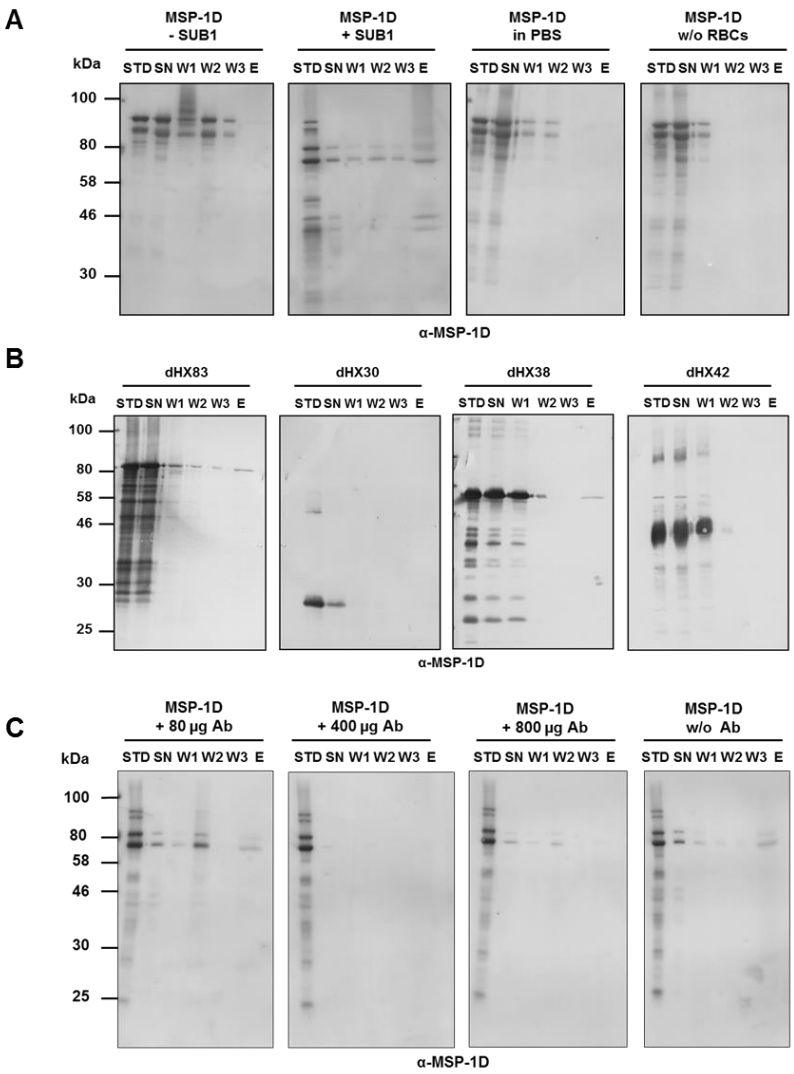

Figure 20 | Binding of MSP-1D to erythrocytes.
Fresh erythrocytes were incubated with MSP-1D heterodimer that was either unprocessed (-SUB1) or cleaved with rPfSUB1 o/n (+SUB1) or with MSP-1D fragments and passed through dibutyl phthalate. Supernatant was taken off and the pellet was washed three times with HTPBS before eluting in 1.5 M NaCl/PBS. All samples were subjected to SDS-PAGE followed by Western blotting. For detection, anti-MSP-1D antibodies were used (rabbit, 1:10,000).
(A) Erythrocyte binding of PfSUB1-processed and unprocessed MSP-1D.
(B) Erythrocyte binding of MSP-1D fragments.
STD: protein standard, SN: supernatant, W1-3: wash 1-3, E: eluate.

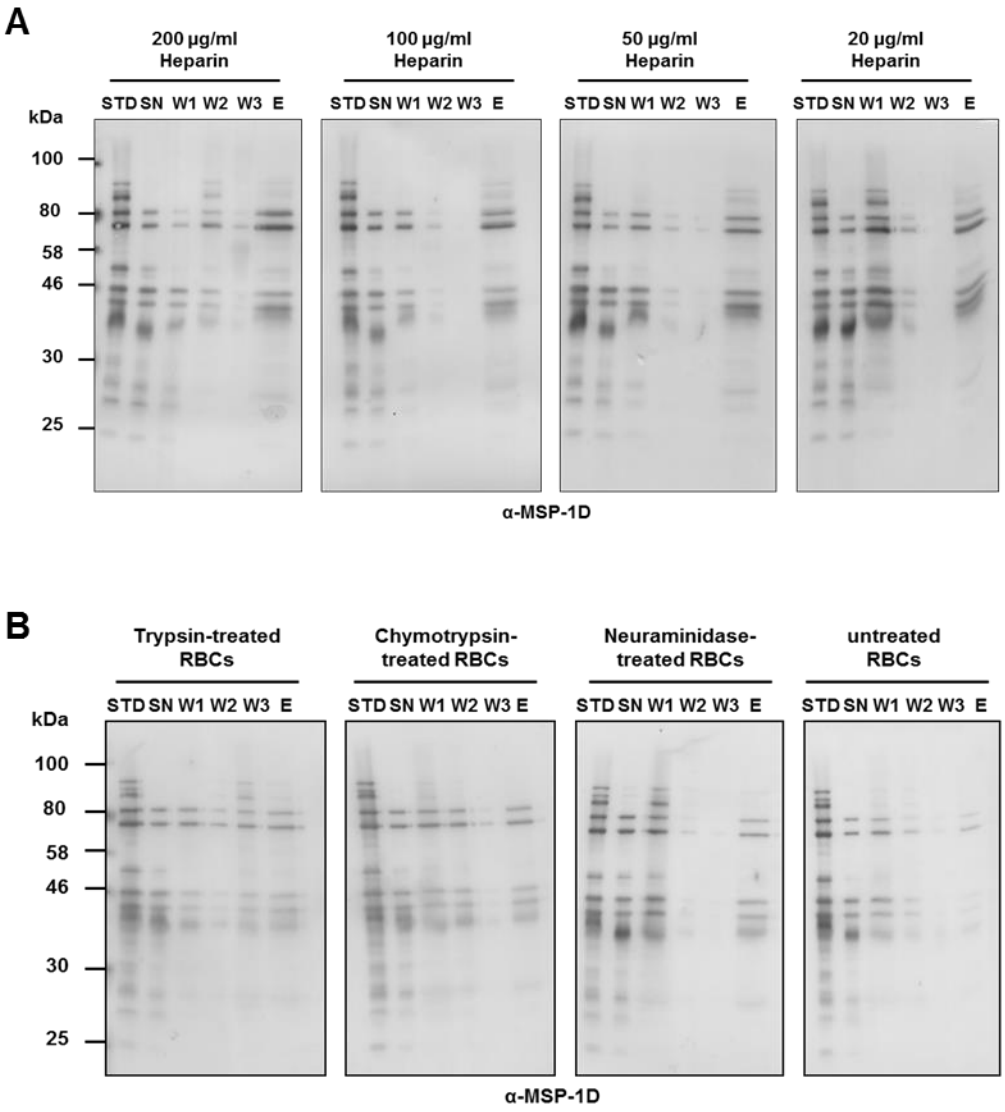

Figure 21 | Erythrocyte binding of MSP-1D is not affected by heparin or enzymatic treatment of red blood cells.

Erythrocytes were incubated with MSP-1D heterodimer that was processed by rPfSUB1 o/n and passed through dibutyl phthalate. Supernatant was taken off and the pellet was washed three times with HTPBS before eluting in 1.5 M NaCl/PBS. All samples were subjected to SDS-PAGE followed by immunoblotting. For detection, anti-MSP-1D antibodies were used (rabbit, 1:10,000). .

(A) Processed MSP-1D was incubated with erythrocytes in the presence of different heparin concentrations.

(B) Erythrocytes were pre-treated with neuraminidase, trypsin or chymotrypsin prior to incubation with MSP-1D.

STD: protein standard, SN: supernatant, W1-3: wash 1-3, E: eluate.

It was previously reported that the binding of MSP-1 to erythrocytes occurs via heparin on the red blood cells (Boyle et al., 2010). Therefore, erythrocyte binding of MSP-1D in the presence of heparin was tested (Figure 21 A). Various different setups were tested: pre-incubating MSP-1D with heparin, red blood cells in presence of heparin, or a mix of all three, heparin, MSP-1D and erythrocytes. Additionally, different concentrations of heparin were used. Nevertheless, all assays equally showed that heparin was not able to inhibit MSP-1D binding to erythrocytes.

In order to narrow down the receptor identity, pre-treatment of red blood cells with several enzymes was performed. Thereby, sialic acid residues as well as protein moieties can be removed from erythrocytes which help to identify the nature of the receptor. Yet, pre-treatment of erythrocytes with trypsin, chymotrypsin and neuraminidase prior to erythrocyte binding assays had no effect on the binding of processed MSP-1D (Figure 21 B).

This is the first study to show the direct binding of full length MSP-1 to erythrocytes. Minimal requirement for this interaction however was prior primary processing of MSP-1. The binding was facilitated via the MSP-1_{83} and MSP-1_{38} fragments and inhibited by specific antibodies. In contrast, enzymatic treatment and heparin addition did not influence the interaction as previously suggested.

4 Discussion

4.1 Cleavage analysis of mutant MSP-1F proteins

In this study, the aim was to unravel the biological significance of primary processing for MSP-1 function. Primary processing of MSP-1 was first observed in 1983 by Freeman and Holder whose findings were later confirmed by other researchers (Blackman et al., 1991; McBride et al., 1982). PfSUB1, the protease carrying out this proteolytic step, was identified thereafter (Blackman et al., 1998). As PfSUB1 has multiple targets, a consensus recognition motif was described allowing for the prediction of further PfSUB1 processing sites within MSP-1 and various proteins of the malaria proteome (Silmon de Monerri et al., 2011) as well as the identification of PfSUB1 inhibitors (Withers-Martinez et al., 2012). The substrate specificity of PfSUB1 was characterised using synthetic peptides and the important amino acids within the recognition motif were mapped (Koussis et al., 2009). Inhibition of protease activity using the specific inhibitor MRT12113 resulted in ablated MSP-1 processing and blocked egress (ED_{50} 180µM) as well as invasion (ED_{50} 25µM) indicating that correct processing of MSP-1 is required for the generation of infective merozoites. Additionally, the order and spatiotemporal regulation of MSP-1 maturation was shown (Child et al., 2010).

Despite this progress, the role of MSP-1 primary processing for the molecular function and interaction of the protein has not been elucidated yet. For this purpose, PfSUB1 cleavage sites within both allelic isoforms of MSP-1 were predicted using the PoPS algorithm and applying the model from Silmon de Monerri et al. (2011). In this work, additional PfSUB1 cleavage sites located at the 83/30 and 38/42 junction were indeed identified (Figure 8). The actual usage of these sites was evaluated by *in vitro* cleavage assays in which mutated recombinant MSP-1 versions were incubated with recombinant PfSUB1 protease in a time-course digestion (Figure 9 and Figure 10). In contrast to earlier mutagenic studies which used synthetic peptides (Koussis et al., 2009), full length MSP-1 was produced and digested. Being a prime vaccine candidate, this

recombinantly produced protein's resemblance to the native MSP-1 complex on the merozoite surface has been thoroughly proven with respect to structure and conformation (Kauth et al., 2003; Kauth et al., 2006). This production technique has also been established under GMP conditions for the generation of a MSP-1 based vaccine. While peptides can easily be accessed by PfSUB1, the overall structure of MSP-1 may play an important role in limiting protease access and thus activity which may in turn regulate the correct spatiotemporal maturation of MSP-1. Together with the recombinant PfSUB1 provided by the laboratory of Prof. M. Blackman as part of a collaboration, this *in vitro* cleavage assay of MSP-1 offers a refined setup reflecting the *in vivo* situation.

Introduction of mutations into predicted cleavage sites and subsequent cleavage analysis revealed that only one site at the 83/30 junction of MSP-1F but two of the three predicted cleavage sites found at the 38/42 junction are indeed substrates of PfSUB1. In addition, another alternative processing site at the 38/42 junction was described earlier (Cooper and Bujard, 1992). Since the studies of Cooper and Bujard (1992), this is the first characterisation of additional cleavage sites within MSP-1. In summary, three redundant cleavage sites were identified at the 38/42 junction suggesting an essential role of this site for MSP-1 function, potentially comparable to a "check-point" during cell cycle progression in other eukaryotes. In case the default site cannot be processed by PfSUB1, two additional cleavage sites compensate for the lack, allowing the parasite to further progress in its life cycle. Alternative usage of cleavage sites was also confirmed by dimethyl labelling of N-termini of PfSUB1-processsed mutant MSP-1F proteins and LC-MS analysis identifying sites 2 and 3 as substrates of PfSUB1 (Figure 11). Besides, our collaboration partners in the laboratory of Prof. M. Blackman at the NIMR in London synthesised peptides based on the additionally identified 38/42 sites, digested them with PfSUB1 and identified the processed products by HPLC. They found a time-dependent cleavage of the peptides beginning with a peptide corresponding to cleavage at site 1 and followed by peptides of the alternative sites 2 and 3. The ordered MSP-1 cleavage and hierarchy of cleavage rates has already been identified for all PfSUB1 cleavage sites within MSP-1

(Child et al., 2010) with the 38/42 junction being the rate-limiting step in primary processing. In addition to the 83/30 and 38/42 cleavage sites, the 30/38 processing site was also successfully rendered refractory to PfSUB1 cleavage by introduction of mutations into the conserved positions of the PfSUB1 recognition sequence allowing for the generation of MSP-1 molecules completely non-cleavable by PfSUB1. In conclusion, I showed that multiple redundant PfSUB1 cleavage sites are present at the 38/42 junction within MSP-1. Using the refined *in vitro* cleavage assay, recombinant MSP-1 was rendered refractory to primary processing. These data strengthen the hypothesis that regulated maturation of MSP-1 is crucial for its function.

4.2 Co-expression of *msp-1f* in *Pf*3D7

MSP-1F was rendered non-cleavable to PfSUB1 *in vitro.* Thus, the question was arising which impact these mutant MSP-1F proteins have *in vivo.* In order to elucidate whether the modified MSP-1 versions remain refractory to PfSUB1 cleavage and investigate its function as well as its effect on parasite fitness, mutant *msp-1f* was expressed in *Pf*3D7 parasites.

Until recently, the most versatile technique for analysing the function of essential genes was the destabilisation domain (DD) system which allows for the down-regulation of protein levels (Armstrong and Goldberg, 2007). As with all systems, the DD system has its limits. The DD tag cannot be inserted into proteins without disturbing their folding, trafficking via the secretory pathway, or their function. So far, only secreted or soluble but no GPI-anchored proteins have been analysed using this system in *P. falciparum.* Therefore, the blasticidin co-selection system was employed in this study. It features comparably small vectors, since a bi-directional promoter, a *var* intron, drives the expression of both the gene of interest as well as the selection marker gene. To overcome the problem of vector instability in *E. coli* due to the high AT-content and the size of *msp-1*, a codon-optimised *msp-1* gene was used (Pan et al., 1999). In this study, *Pf*3D7 parasites were transfected with pHBIMF constructs expressing different variants of the

200 kDa MSP-1 protein in an adjustable manner (Figure 12). These variants were either completely refractory to PfSUB1 cleavage (pHBIMFmutall), mutated in the 38/42 junction (pHBIMFmut38/42) or comprised the wildtype sequence (pHBIMFwt). *Pf*3D7 parasites maintained the different pHBIMF plasmids epsiomally as shown by plasmid rescue and PCR analysis on extracted parasite DNA (Figure 12 B). As a control for regulable expression, *Pf*3D7 parasites expressing renilla luciferase (pHBIRH) were used (Epp et al., 2008). Episome copy numbers were adjusted by adding blasticidin in different concentrations to the culture medium (Figure 12 C) (O'Donnell et al., 2001). Concatamer sizes and thus copy numbers increased with elevated blasticidin concentration. The size of a concatamer is limited to about 90 kb or 9-15 copies of the 6 kb plasmid pDb.Dh.^Db (Williamson et al., 2002). Hence, the vectors used in this study for expressing *msp-1f* (pHBIMF) with a size of 10 kb could reach a maximum of 9 copies per parasite, while the renilla luciferase vector (pHBIRH) with a size of 6 kb could theoretically be expanded to 14 copies per parasite. The copy numbers of pHBIMFwt and pHBIMFmut38/42 with 11 and 7 copies per parasite, respectively, lay indeed within the calculated concatamer size range. On the other hand, the copy number of pHBIRH with 8 copies per parasite could potentially be up-regulated even more by increasing the blasticidin concentration to 20 µg/ml. In contrast, the regulation of pHBIMFmutall copy number was very limited, in fact to only 4 copies per parasite which was also reflected by the transcript numbers (Figure 16). The actual expression of *msp-1f* was investigated for all transgenic parasites by determining the transcript number and calculating the relative expression compared to the endogenous *msp-1d* expression (Figure 16). While the renilla luciferase expression was regulable over a broad range from 13 to 150 % of *msp-1d* expression, the expression of *msp-1fwt* was limited to 37 %. Transcript numbers of the mutant *msp-1f* versions reached only 15 % for MSP-1Fmut38/42 and 10 % for MSP-1Fmutall of MSP-1D expression, respectively. Thus, transgene MSP-1F expression levels did generally not reach the levels of endogenous MSP-1D expression. As the expression of renilla luciferase was adjustable over a wide range, the blasticidin co-selection was demonstrated to be working as intended. Yet, the lower limit of the expression of

MSP-1Fwt indicated that the total amount of MSP-1, both MSP-1F and MSP-1D, which can be expressed and localised to the merozoite surface is limited. Renilla luciferase on the other hand remains in the non-limiting cytosol of the parasite. The approximate number of MSP-1 molecules that can cover the merozoite surface can be calculated assuming that merozoites have an egg-like shape and that the MSP-1 molecule adopts a spherical shape (Erickson, 2009) (Table 42). Thus, approximately 100,000 MSP-1 molecules fit onto the surface of one merozoite. Accordingly, increasing the amount of MSP-1 by co-expression of the heterologous version is limited to this number which is the case for *Pf*3D7 pHBIMFwt 15µ/ml blasticidin with 137 % total MSP-1 expression. The expression of mutant versions with 10 % and 15 % for mutall and mut38/42, respectively, did not reach the MSP-1Fwt expression level indicating that the mutant MSP-1F was not tolerated by the parasite or that they have a deleterious effect on parasite growth. Thus, their expression is limited by the parasite. Due to the continuous culturing of transgenic parasites and treatment with blasticidin selects for "escape mutants" that express enough blasticidin S deaminase to survive the high blasticidin concentrations but produce only low amounts of mutant, probably deleterious MSP-1F. Therefore, transgenic parasites have to be compared with each other, setting *msp-1f*wt expressing parasites as the reference. As the expression levels of mutant *msp-1f* were lower than *msp-1fwt* expression, parasite viability was indeed shown to be affected by mutant MSP-1F.

4.3 Are the MSP-1F versions cleaved *in vivo*?

To address whether the transgenic MSP-1F proteins are processed by PfSUB1 *in vivo*, protein extracts from late schizont stages of all transgenic parasite lines were analysed by Western blotting (Figure 13). As a control, the primary processing of MSP-1D was investigated. Indeed, it occurred normally in all parasite lines showing that PfSUB1 was active. While MSP-1Fwt's processing was as unaltered as in case of the *Pf*FCB1 control, the mutated versions were refractory to proteolytic cleavage *in vivo*. In fact, the primary processing of the

transgenic MSP-1F versions *in vivo* occurred similar to the results obtained from *in vitro* cleavage assays using recombinant MSP-1F proteins. This confirmed that the mutations introduced into PfSUB1 cleavage sites rendered the protein refractory to proteolytic processing as predicted.

The laboratory of Prof. M. Blackman was focussing solely on the 38/42 cleavage junction. They directly inserted mutations into the genomic *msp-1d* of *Pf*3D7 parasites. In accordance with our data, mutation of site 1 led to processing of MSP-1 at the site 2 and mutation of site 1 & 2 led to processing at site 3. However, the mutation of all three sites was repeatedly unsuccessful. Together with the data obtained in this study, we can conclude that correct maturation of MSP-1 is required for parasite infectivity and viability. In particular, the 38/42 cleavage junction with its redundant processing sites seems to have an essential role for the parasite.

4.4 Immunofluorescence analysis

To investigate the cellular fate of MSP-1D and MSP-1F, their localisation was investigated by immunofluorescence analysis of late schizonts using isoform-specific antibodies (Figure 14). Both antibodies showed only low cross-reactivity as tested by staining of the parental parasite lines *Pf*3D7 and *Pf*FCB1 with each of them. All transgenic parasites indeed showed MSP-1D as well as MSP-1F expression with both MSP-1 variants co-localising to the merozoite surface (Figure 14 merge). The signal intensities for MSP-1F were independent of the blasticidin concentration used for culturing and therefore did not allow to draw any conclusions on protein expression in dependency on the blasticidin concentration. As the merged images are highly dependent on the relative signal intensities collected in both channels (MSP-1D and MSP-1F), image processing was required to quantitatively show that both MSP-1 versions co-localise. For this purpose, the Pearson's coefficient was applied using the plugin Coloc2 in Fiji. The values determined for the transgenic parasites were all in the range from 0.8-1 clearly demonstrating the co-localisation of MSP-1D and MSP-1F.

As the merozoite surface was covered with both allelic variants of MSP-1, several questions arose: Are MSP-1D and MSP-1F interacting with each other e.g. dimerising as shown for the MSP-1_{42} fragments (Babon et al., 2007)? This question can be addressed by *in vitro* experiments using gel filtration. As the mutant MSP-1F versions were not processed by PfSUB1 (Figure 13), did these transgenic parasites display a growth defect, either in invasion or egress where MSP-1 is supposed to play a role? The latter questions were answered by investigating the parasite growth of all transgenic parasites.

4.5 Growth analysis and *clag* gene expression

Analysis of parasite growth was investigated by following the parasitemia over 42 h using blood smears and flow cytometry of propidium iodide stained infected erythrocytes. Afterwards, the growth factor was calculated and the significance of differences between the strains was tested by Kruskal-Wallis. The controls *Pf*3D7, *Pf*FCB1 and *Pf*3D7 pHBIRH likewise displayed growth factors of about 7-9 (Figure 17). The same results were obtained for parasites expressing MSP-1Fwt (*Pf*3D7 pHBIMFwt) which were used as a reference for the mutant-MSP-1F expressing parasite lines kept at the same blasticidin concentrations. A significant growth defect was observed for *Pf*3D7 pHBIMFmutall parasites grown in all blasticidin concentrations. In contrast, *Pf*3D7 pHBIMFmut38/42 only grew significantly slower than *Pf*3D7 pHBIMFwt parasites at 2 µg/ml and 15 µg/ml blasticidin (Figure 17 C-F). Taken together, transgenic parasite lines expressing mutant *msp-1f* displayed a small yet significant growth defect indicating that non-cleavable MSP-1F has an impact on parasite viability. This defect is however largely amended by the reduced expression of mutant MSP-1F. During cultivation, parasites were selected to express sufficiently detoxifying amounts of blasticidin S deaminase while keeping the expression of probably deleterious mutant MSP-1F low. Thus, the comparison of transcript and DNA copy numbers of *msp-1fwt* and mutant *msp-1f* offered a much more appropriate readout of the substantial consequences of PfSUB1 cleavage resistance than the growth analysis.

While the DNA copy number of *msp-1fwt* reached 12 copies per parasite, the genes of *msp-1fmut38/42* and *msp-1fmutall* were kept episomally at 6 and 3 copies per parasite, respectively (Figure 12). The same was found for the transcript number of *msp-1f* versions (Figure 16). The expression of *msp-1fwt* was adjustable to 37 % of *msp-1d* expression. However, the mutant *msp-1f* variants were expressed at much lower levels of 15 % for *msp-1fmut38/42* and 10 % *for msp-1fmutall*. The fact that the mutant *msp-1f* versions cannot be up-regulated to the same extent as *msp-1fwt* on both DNA and transcript level, clearly indicates that the expression of mutant *msp-1f* has deleterious effects on parasite growth.

Blasticidin treatment has already been shown to influence parasite growth (Mira-Martinez et al., 2013). Parasites can acquire resistance to blasticidin without the expression of the blasticidin S deaminase by differential expression of *clag 3* genes (Crowley et al., 2011; Mira-Martinez et al., 2013; Nguitragool et al.). Impaired *clag 3* gene expression results in altered nutrient uptake by the ion channel PSAC leading to growth defects. To exclude that the observed growth defect in *Pf*3D7 pHBIMFmut38/42 and *Pf*3D7 pHBIMFmutall parasites did not result from blasticidin treatment and is not an evasion mechanism, the *clag 3* gene expression was monitored (Figure 18). All transgenic parasite lines showed the predominant expression of *clag 3.1* gene, while *clag 3.2* expression was shut down, independent of the blasticidin concentration used for culturing. Besides, parasites could be synchronised by sorbitol treatment which is not applicable in case of impaired PSAC function (Desai, 2014; Mira-Martinez et al., 2013). Thus, parasites should exert normal nutrient uptake by PSAC. This further proved that the observed growth defect was due to impaired MSP-1F processing and not a consequence of hampered nutrient uptake.

4.6 Knockout of *msp-1d*

Knockout of *msp-1* was previously attempted unsuccessfully and led to the conclusion that the gene is essential (O'Donnell et al., 2000). Nevertheless, the MSP-1_{19} fragment with its two EGF-like domains is very conserved among

Plasmodium parasites and can be replaced by sequences from *P. chabaudi* (O'Donnell et al., 2000). In addition, the overall structure of MSP-1D and MSP-1F is conserved as well as the structural motifs responsible for subunit interactions (Kauth et al., 2003). For the generation of the MSP-1 complex *in vitro,* the MSP-1_{42} fragment of the MAD20 prototype could be exchanged by the K1 variant and the heterologous complex was formed as efficiently (Kauth et al., 2003). In order to investigate whether MSP-1F can take over the function of MSP-1D *in vivo*, we attempted to artificially generate diploid parasites and then knockout the endogenous *msp-1d* gene. For this purpose, *Pf*3D7 pHBIMFwt parasites episomally expressing *msp-1f* in an *msp-1d* background were employed and transfected with two knockout constructs. In *P. falciparum*, double homologous crossover recombination is the method of choice for gene replacements or disruptions. The efficiency of obtaining recombined parasites can be enhanced by negative selection against the vector backbone (Duraisingh et al., 2002; Maier et al., 2006). The pHTK and pCC1 vector both comprise enzymes that convert the normally harmless ganciclovir and 5-FC, respectively, into toxic metabolites killing parasites that have not recombined and thus excised the plasmid backbone. For disruption of the *msp-1d* gene, two 1 kb homologous regions from the 5' UTR and 3' region were cloned into the vectors to flank the positive selection marker hDHFR yielding the vectors pHTK-PfMSP1-KO and pCC1-PfMSP1-KO (Figure 19). Besides transgenic *Pf*3D7 pHBIMFwt parasites expressing *msp-1f* wt, the parental *Pf*3D7 parasites were transfected with these constructs as controls. The latter should not yield viable parasites as they do not harbour the heterologous *msp-1f* gene. Unfortunately, upon transfection and several rounds of cycling, no *msp-1d* knockout parasites could be obtained neither with the pHTK nor with the pCC1 vector. Different drug concentrations of 5-FC and ganciclovir up to 12 µM and 20 µM, respectively, were tested based on IC_{50} data from Dr. Sophia Deil (Deil, 2014) and literature data but parasites consistently survived the treatment with negative selection drugs. Prior to transfection, pHTK-PfMSP1-KO and pCC1-PfMSP1-KO plasmids were sequenced revealing no mutations within the negative selection marker cassettes. Thus, parasites were expected to die from treatment with 5-FC or ganciclovir.

The failure of disrupting the *msp-1d* gene in control *Pf*3D7 parasites was expected, as this gene is essential and no co-expressed *msp-1f* was present to substitute the loss of *msp-1d* (O'Donnell et al., 2000). The failure of obtaining recombined *Pf*3D7 pHBIMFwt parasites can be attributed to several potential reasons including vector instability, low transfection efficiency, inappropriate drug on/off cycling periods or suboptimal homology regions. One of the most likely reasons is, however, that the transgene expression was too low to complement for the loss of the endogenous *msp-1d* gene. As mentioned before, the expression of *msp-1f* was determined in *Pf*3D7 pHBIMFwt parasites to indeed only reach 37 % of *msp-1d* expression. Thus, recombinant parasites died within one or two replication cycles. Alternatively, the heterologous MSP-1F version might not be able to complement for MSP-1D function as the variable regions within MSP-1 have important functions for binding to erythrocytes or other proteins e.g. MSP-6, MSP-7 or MSPDBLs and thus parasite viability. In summary, it was not possible to generate parasites with a disrupted *msp-1d* gene locus.

4.7 Erythrocyte binding of MSP-1

Malaria parasites invade red blood cells via different redundant pathways that involve either sialic acid-dependent or sialic acid-independent receptor-ligand interactions (Harvey et al., 2012). The identification of common receptor and ligand molecules on both sites, the host and parasite, will aid vaccine as well as drug development. MSP-1 has long been suggested to mediate initial low affinity attachment to erythrocytes (Boyle et al., 2010; Goel et al., 2003; Nikodem and Davidson, 2000). However, direct evidence is still missing. To investigate the direct interaction of MSP-1 with red blood cells, an erythrocyte binding assay was employed. This study showed that MSP-1 directly interacts with erythrocytes (Figure 20). Yet, only processed MSP-1 but not the MSP-1 heterodimer bound to erythrocytes. This indicated that processing by PfSUB1 induces conformational changes within the MSP-1 molecule leading to the exposure of binding sites that are required for attachment to red blood cells. Indeed, the MSP-1_{83} and MSP-1_{38}

fragments were identified to mediate attachment. Binding was shown to be specific as MSP-1 antibodies efficiently inhibited erythrocyte binding. In contrast, neither heparin nor enzymatic pre-treatment of erythrocytes had an effect on MSP-1 binding (Figure 21). Parasites are able to switch between sialic acid-dependent and independent invasion pathways which can be discriminated by enzymatic treatment of red blood cells. Hence, the binding via MSP-1 might be a conserved mechanism for attachment and invasion used by all parasites, thus widening the opportunities for treatment of malaria.

While earlier studies were solely relying on MSP-1 fragments and only tested the binding to erythrocytes in an indirect manner (Boyle et al., 2010; Goel et al., 2003; Nikodem and Davidson, 2000), this study used full length MSP-1 protein and its naturally occurring processing products to analyse the interaction capabilities with red bloods cells. Using recombinant MSP-1_{38}, 115 amino acids within this fragment were shown to bind to erythrocytes (Nikodem and Davidson, 2000) which is in accordance with our findings. In contrast, Boyle et al. (2010) suggested that MSP-1_{42} binds to heparin on the erythrocyte surface. Upon addition of heparin or heparin-like molecules to the parasite culture, a growth defect was observed. Besides, recombinant MSP-1_{42} bound to heparin beads. The latter experiment was reproduced by our collaboration partners in the laboratory of Prof. M. Blackman, NIMR, London, UK. They found that both unprocessed and processed MSP-1 bound to heparin beads with PfSUB1-processed MSP-1 displaying an 8-10-fold higher affinity than unprocessed protein. Contrary to their findings, we could neither observe a binding of MSP-1_{42} to erythrocytes nor an inhibitory effect of heparin when added to the erythrocyte binding assay. Consequently, we suggest that heparin is not involved in MSP-1 binding to erythrocytes and that it is not mediated via MSP-1_{42}.

Recent data affirm a rather unspecific binding of MSP-1 as well as almost all merozoite surface proteins to heparin (Kobayashi et al., 2013). Moreover, binding of MSP-1_{42} or MSP-1_{33} to heparin occurred with a very low affinity which points to general electrostatic interactions rather than to a specific receptor-ligand interaction. Besides, MSP-1 did not to co-localise with heparin in

immunofluorescence analysis (Kobayashi et al., 2013). Accordingly, inhibition of erythrocyte adsorption and invasion as found by Boyle et al. (2010) did not occur by specifically impeding MSP-1 interaction but rather by blocking all merozoite surface proteins, especially those at the apical tip (Kobayashi et al., 2013).

So far, only one study could visualise and measure the effect of heparin on erythrocyte binding of merozoites by live video microscopy (Crick et al., 2014). In the presence of ~230 µg/ml heparin, merozoite attachment was dramatically reduced by 60 % and the force needed to detach them decreased from 40 pN to 10 pN. However, in the presence of heparin, merozoites were also not able to attach to each other or glass slides, both of which are standard attachment assays. Thus, the authors also excluded a specific receptor-interaction of heparin (Crick et al., 2014).

The identification of the nature of the erythrocyte receptor is very important in terms of drug development. As heparin can be excluded by this study as well as others (Crick et al., 2014; Kobayashi et al., 2013), the receptor identity can be narrowed down using enzymatic treatment of erythrocytes. Pre-treatment of erythrocytes did not affect *Pf*3D7 growth (Boyle et al., 2010). Besides, chymotrypsin treatment of erythrocytes did not fundamentally alter the ability of merozoites to adhere but shortened the time window in which adhesion can take place (Crick et al., 2014). In contrast, the proteinous nature of band 3 as MSP-1 receptor (Goel et al., 2003) should be affected by enzymatic treatment with both chymotrypsin and trypsin leading to either ablated or reduced binding of MSP-1 to erythrocytes. In this study however, trypsin, chymotrypsin and neuraminidase treatment did not affect the binding capacity of processed MSP-1 to red blood cells excluding band 3 as a receptor for MSP-1.

A very recent study suggested that MSP-1 itself is not capable of red blood cell binding but serves as an anchoring platform for proteins involved in initial attachment (Lin et al., 2014). The adaptor proteins MSPDBL1 and MSPDBL2 were identified to bind to the MSP-1 heterodimer as well as to erythrocytes. In our study, the unprocessed MSP-1 heterodimer was also not binding to

erythrocytes. Thus, the hypothesis suggested by Lin et al. was supported and further experiments should be carried out with PfSUB1-processed MSP-1. It is possible that primary processing of MSP-1 induces structural changes enhancing the affinity for both MSPDBLs as well as erythrocytes. Altered protein affinities upon primary processing were already shown in a study from Kauth et al. (2006) where only processed MSP-1 bound MSP-6_{36} and MSP-7_{22}.

The importance of primary processing of MSP-1 for its structural rearrangement and thus its function in attachment as demonstrated in this study is comparable with findings to other microbes such as viruses where proteolytic maturation likewise enables infectivity. For instance, upon budding of the human immunodeficiency virus (HIV) from its host cell, the virion is immature and processing by the viral protease leads to conformational changes in the Gag polyprotein within the particle to produce mature, infectious viruses (Ganser-Pornillos et al., 2008). Accordingly, proteolytic processing might have a similar role of in *P. falciparum*. While, the HIV surface is covered with only one protein that undergoes proteolytic processing during its maturation, *P. falciparum* parasites display many proteins on their surface as well as within their organelles required for invasion that are cleaved by various proteases. Inhibition of PfSUB1 processing by MRT12113 affects many proteins and thus leads to defects in merozoite egress and invasion (Yeoh et al., 2007). On the contrary, this study comprised only cleavage-deficient MSP-1F. This already has tremendous effects on parasite growth demonstrating the importance of correct processing of MSP-1 for parasite viability.

4.8 Outlook

Studies on the merozoite surface protein 1 have been driven by its importance as target of protective immunity and malaria vaccine candidate as well as the need to understand its role during egress and invasion (Babon et al., 2007). In this study, the biological significance of primary processing for MSP-1 function during invasion was investigated.

For this purpose, different versions of MSP-1F that are completely or only partially refractory to PfSUB1 processing *in vitro* and *in vivo* were generated. Using the blasticidin co-selection, *msp-1f* versions were co-expressed in *Pf*3D7 parasites in an adjustable manner (Figure 16). However, the transgene expression could not be raised beyond 37 % of MSP-1D expression. In order to achieve higher expression of *msp-1f* either blasticidin up to 20 µg/ml or a stronger promoter such as ef1α should be used. Besides, the knockout of endogenous *msp-1d* would allow for higher expression rates as the merozoites surface is not covered with endogenously expressed MSP-1D. The latter was attempted, but remained unsuccessful and is discussed in detail below.

Co-expression of both allelic isoforms of MSP-1 was quantified on both DNA and mRNA level by real time PCR. In order to exactly quantify the amount of MSP-1D and MSP-1F protein molecules, different methods could be applied such as quantitative Western blotting, mass spectrometry, 2-D PAGE combined with mass spectrometry (Maaß et al., 2014), microarray-based techniques (Burgin et al., 2014) or new imaging techniques. This would reveal the exact number of MSP-1F molecules on the merozoite surface.

Another interesting question that could be investigated in future studies is whether the different MSP-1 versions interact with each other or form dimers as suggested in earlier studies for MSP-1_{42} (Babon et al., 2007). Therefore, the transgenic parasite lines generated in this study should be analysed with new microscopy techniques (Moerner, 2007) that allow for single-molecule imaging such as stimulated emission depletion (STED) microscopy (Hell and Wichmann, 1994), stochastic optical reconstruction microscopy (STORM) (Rust et al., 2006) or photoactivated localization microscopy (PALM) (Betzig et al., 2006) .

Western Blot analysis of protein extracts from transgenic parasites revealed that mutant MSP-1F is not processed by PfSUB1 *in vivo*, in line with the obtained *in vitro* data. This raised the question whether non-cleavable MSP-1F affects parasite growth, either in invasion or egress. Indeed, analysis of parasite growth revealed a significant growth defect. As these transgenic parasite lines are still

viable they could be used as a tool to dissect, if impaired MSP-1 processing has an impact on egress or invasion. The combination of shaking or flow conditions that mimic the *in vivo* situation with live imaging techniques (Crick et al., 2014; Crick et al., 2013; Glushakova et al., 2005) would allow to analyse the transgenic parasite lines in more detail. Thus, the discrimination between an egress and invasion phenotype may be enabled. Besides, attachment forces of merozoites to erythrocytes can be measured using optical tweezers (Crick et al., 2014). This might reveal, if mutant MSP-1F reduces the binding affinity of merozoites or if it stays at 40 pN as measured for wildtype *Pf*3D7 parasites by Crick et al. (2014).

Unfortunately, knockout of *msp-1d* was not achieved in this study, although parasites were expressing the heterologous *msp-1f* to complement for the loss of the endogenous gene. This indicates that MSP-1F is not able to take over the functions of MSP-1D, as the variable regions might be important for interaction with other molecules and in turn binding to erythrocytes. However, the failure of generating *msp-1d* knockout line could also be attributed to the vector system used for double homologous recombination. Therefore, a very recently developed promising knockout technique could be employed as an alternative approach in future studies. This method has been established in *P. falciparum* in 2014 and is based on the clustered, regularly interspaced, short palindromic repeat (CRISPR)–CRISPR-associated protein (Cas) system (CRISPR-Cas) (Ghorbal et al., 2014).

Another approach to study the effect and function of non-cleavable MSP-1 *in vivo* is to apply the destabilisation domain (DD) system (Armstrong and Goldberg, 2007). Tagging of the endogenous MSP-1D with the DD in *Pf*3D7 pHBIMF parasites would allow the modulation of MSP-1D protein levels and provide insights into the function of episomally expressed MSP-1F. As MSP-1 harbours a signal sequence, a GPI-anchor and several processing sites, the introduction of the DD requires thorough planning. Nevertheless, a proline-rich region within the MSP-1_{33} region was identified where the insertion of the DD is expected to unlikely affect the overall MSP-1 structure. In addition, the DD tag was placed directly in front of the GPI anchor sequence allowing for normal trafficking and

processing by PfSUB1 as well as PfSUB2. These two variants of MSP-1D-DD have already been cloned, but not transfected into *Pf*3D7 pHBIMF parasites due to time limitations (Appendix Figure 28). In order to gain deeper knowledge about the function of episomally expressed *msp-1f* and its mutants, the DD system as well as the CRISPR-Cas9 system may be applied to *Pf*3D7 pHBIMF parasites in future studies.

In this study, primary processing was proven to be a requirement for erythrocyte binding, thus strengthening the hypothesis that MSP-1 is involved in initial attachment. Red blood cell binding was shown to be unaffected by heparin as well as enzymatic treatment suggesting that MSP-1 is a common ligand used by all malaria parasite strains. Using the established erythrocyte binding assay, kinetics and affinity measurements may provide deeper insights into the actual binding affinity of MSP-1 for erythrocytes and the effect of enzymatic treatment or heparin addition. Moreover, MSP-1F (K1 allele) as well as mutant MSP-1 versions, especially the ones that are mutated at the 38/42 cleavage site, should be tested for their ability to bind to erythrocytes. Furthermore, the interaction of MSP-1 with MSP-6_{36} and MSP-7_{22} with the non-cleavable MSP-1F version should be studied *in vitro* using an ELISA-based assay (Lin et al., 2014) that also allows for kinetic studies of protein interactions. These data would reveal whether impaired MSP-1 processing does not only affect erythrocyte binding but also interactions with itself (Babon et al., 2007) or its associated partners such as MSP-6_{36}, MSP-7_{22} and MSPDBLs.

The identification of the MSP-1 receptor has hitherto remained elusive. In the field of virology, the receptor for Hepatitis B virus has recently been identified by a study by Yan et al. (2012) whose approach could be employed for the identification of the erythrocyte receptor in malaria parasites as well. Yan et al. (2012) used a photo-cross linking approach in which the non-proteinogenic amino acid L-photo-leucine (L-2-amino-4,4-azi-pentanoic acid) was activated by ultraviolet light at 365 nm. It yielded a reactive carbene group which irreversible bound to its associated partner and could be precipitated by streptavidin T1 beads. For the identification of the MSP-1 receptor on erythrocytes, one could

grow the parasites in medium containing L-photo-leucine, purify the merozoites and apply them in erythrocyte binding assays or invasion assays as established by Glushakova et al. (2005). The emission of UV light would then cross-link MSP-1 to its receptor. Ultimately, immunoprecipitation and mass spectrometry would allow for the identification of its binding partner.

4.9 Conclusion and Model

Although MSP-1 has been known for several decades, many questions have remained unanswered. During the last couple of years light has shed onto the elucidation of MSP-1 function. In this study, the role of primary processing of MSP-1 has been analysed. I showed that proteolytic cleavage is required for erythrocyte binding. To ensure correct processing, MSP-1 contains several redundant PfSUB1 processing sites. Mutation of these PfSUB1 cleavage sites completely ablated proteolytic processing *in vitro* and *in vivo*. Parasites co-expressing mutant *msp-1* displayed a small yet significant growth defect, further proving the importance of correct MSP-1 maturation for parasite survival.

In conclusion, the data strongly corroborate the hypothesis that PfSUB1 cleavage of MSP-1 is essential for the development of mature and infective merozoites either during egress or invasion. A key functional feature might be the changes in the structural conformation of MSP-1 induced by primary processing that then allow the parasite to attach to erythrocyte, thereby initiating parasite invasion.

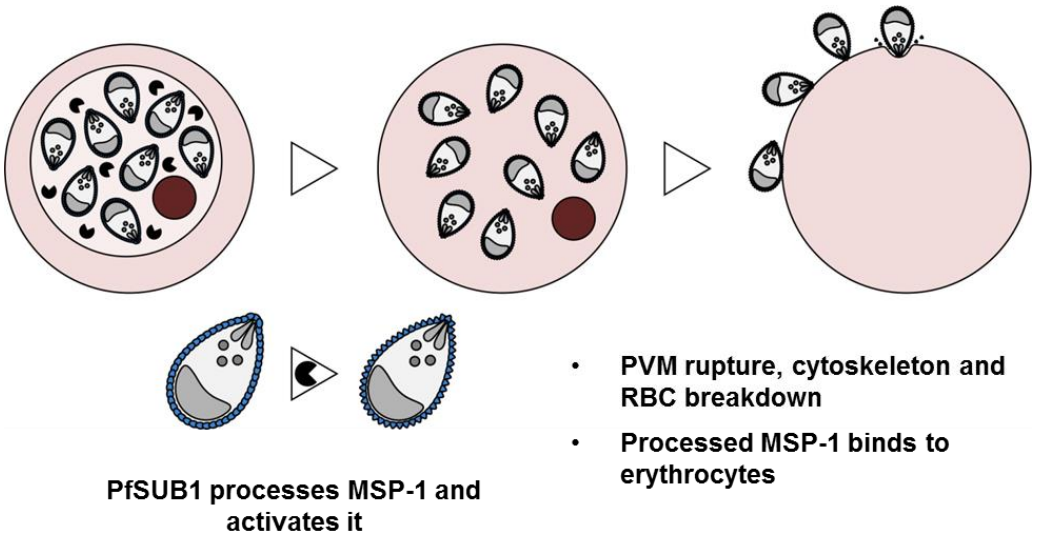

Figure 22 | Working model of MSP-1 function.
Prior to egress, MSP-1 is processed and activated by PfSUB1. Following PVM rupture, the cytoskeleton and membrane of the erythrocyte break down and release merozoites into the bloodstream. These bind to red blood cells via the interaction of MSP-1 with surface receptors to initiate another round of replication.

References

Abkarian, M., Massiera, G., Berry, L., Roques, M., and Braun-Breton, C. (2011). A novel mechanism for egress of malarial parasites from red blood cells. Blood *117*, 4118-4124.

Aikawa, M., Miller, L.H., Johnson, J., and Rabbege, J. (1978). Erythrocyte entry by malarial parasites. A moving junction between erythrocyte and parasite. The Journal of cell biology *77*, 72-82.

Aikawa, M., Miller, L.H., Rabbege, J.R., and Epstein, N. (1981). Freeze-fracture study on the erythrocyte membrane during malarial parasite invasion. The Journal of cell biology *91*, 55-62.

Alonso, P.L., Brown, G., Arevalo-Herrera, M., Binka, F., Chitnis, C., Collins, F., Doumbo, O.K., Greenwood, B., Hall, B.F., Levine, M.M., *et al.* (2011). A research agenda to underpin malaria eradication. PLoS medicine *8*, e1000406.

Alonso, P.L., and Tanner, M. (2013). Public health challenges and prospects for malaria control and elimination. Nature medicine *19*, 150-155.

Andenmatten, N., Egarter, S., Jackson, A.J., Jullien, N., Herman, J.P., and Meissner, M. (2012). Conditional genome engineering in Toxoplasma gondii uncovers alternative invasion mechanisms. Nature methods.

Arastu-Kapur, S., Ponder, E.L., Fonovic, U.P., Yeoh, S., Yuan, F., Fonovic, M., Grainger, M., Phillips, C.I., Powers, J.C., and Bogyo, M. (2008). Identification of proteases that regulate erythrocyte rupture by the malaria parasite Plasmodium falciparum. Nat Chem Biol *4*, 203-213.

Armstrong, C.M., and Goldberg, D.E. (2007). An FKBP destabilization domain modulates protein levels in Plasmodium falciparum. Nature methods *4*, 1007-1009.

Augagneur, Y., Wesolowski, D., Tae, H.S., Altman, S., and Ben Mamoun, C. (2012). Gene selective mRNA cleavage inhibits the development of Plasmodium falciparum. Proceedings of the National Academy of Sciences *109*, 6235-6240.

Babon, J.J., Morgan, W.D., Kelly, G., Eccleston, J.F., Feeney, J., and Holder, A.A. (2007). Structural studies on Plasmodium vivax merozoite surface protein-1. Molecular and biochemical parasitology *153*, 31-40.

Baer, K., Klotz, C., Kappe, S.H., Schnieder, T., and Frevert, U. (2007). Release of hepatic Plasmodium yoelii merozoites into the pulmonary microvasculature. PLoS pathogens *3*, e171.

Baird, J.K. (2005). Effectiveness of antimalarial drugs. The New England journal of medicine *352*, 1565-1577.

Bannister, L.H., Hopkins, J.M., Fowler, R.E., Krishna, S., and Mitchell, G.H. (2000). A brief illustrated guide to the ultrastructure of Plasmodium falciparum asexual blood stages. Parasitol Today *16*, 427-433.

Bergmann-Leitner, E., Duncan, E., and Angov, E. (2009). MSP-1p42-specific antibodies affect growth and development of intra-erythrocytic parasites of Plasmodium falciparum. Malaria journal *8*, 183.

Betzig, E., Patterson, G.H., Sougrat, R., Lindwasser, O.W., Olenych, S., Bonifacino, J.S., Davidson, M.W., Lippincott-Schwartz, J., and Hess, H.F. (2006). Imaging intracellular fluorescent proteins at nanometer resolution. Science *313*, 1642-1645.

Billker, O., Lindo, V., Panico, M., Etienne, A.E., Paxton, T., Dell, A., Rogers, M., Sinden, R.E., and Morris, H.R. (1998). Identification of xanthurenic acid as the putative inducer of malaria development in the mosquito. Nature *392*, 289-292.

Blackman, M.J., Fujioka, H., Stafford, W.H., Sajid, M., Clough, B., Fleck, S.L., Aikawa, M., Grainger, M., and Hackett, F. (1998). A subtilisin-like protein in secretory organelles of Plasmodium falciparum merozoites. The Journal of biological chemistry *273*, 23398-23409.

Blackman, M.J., Heidrich, H.G., Donachie, S., McBride, J.S., and Holder, A.A. (1990). A single fragment of a malaria merozoite surface protein remains on the parasite during red cell invasion and is the target of invasion-inhibiting antibodies. The Journal of experimental medicine *172*, 379-382.

Blackman, M.J., Ling, I.T., Nicholls, S.C., and Holder, A.A. (1991). Proteolytic processing of the Plasmodium falciparum merozoite surface protein-1 produces a membrane-bound fragment containing two epidermal growth factor-like domains. Molecular and biochemical parasitology *49*, 29-33.

Boddey, J.A., and Cowman, A.F. (2013). Plasmodium Nesting: Remaking the Erythrocyte from the Inside Out. Annual Review of Microbiology *67*, 243-269.

Boersema, P.J., Raijmakers, R., Lemeer, S., Mohammed, S., and Heck, A.J.R. (2009). Multiplex peptide stable isotope dimethyl labeling for quantitative proteomics. Nat Protocols *4*, 484-494.

Borrmann, S., and Matuschewski, K. (2011). Protective immunity against malaria by 'natural immunization': a question of dose, parasite diversity, or both? Current opinion in immunology *23*, 500-508.

Boyd, S.E., Garcia de la Banda, M., Pike, R.N., Whisstock, J.C., and Rudy, G.B. (2004). PoPS: a computational tool for modeling and predicting protease specificity. Proceedings / IEEE Computational Systems Bioinformatics Conference, CSB IEEE Computational Systems Bioinformatics Conference, 372-381.

Boyd, S.E., Pike, R.N., Rudy, G.B., Whisstock, J.C., and Garcia de la Banda, M. (2005). PoPS: a computational tool for modeling and predicting protease specificity. Journal of bioinformatics and computational biology *3*, 551-585.

Boyle, M.J., Richards, J.S., Gilson, P.R., Chai, W., and Beeson, J.G. (2010). Interactions with heparin-like molecules during erythrocyte invasion by Plasmodium falciparum merozoites. Blood *115*, 4559-4568.

Burgin, E., Salehi-Reyhani, A., Barclay, M., Brown, A., Kaplinsky, J., Novakova, M., Neil, M.A.A., Ces, O., Willison, K.R., and Klug, D.R. (2014). Absolute quantification of protein copy number using a single-molecule-sensitive microarray. Analyst *139*, 3235-3244.

Carvalho, T.G., Thiberge, S., Sakamoto, H., and Ménard, R. (2004). Conditional mutagenesis using site-specific recombination in Plasmodium berghei. Proceedings of the National Academy of Sciences of the United States of America *101*, 14931-14936.

Chandramohanadas, R., Davis, P.H., Beiting, D.P., Harbut, M.B., Darling, C., Velmourougane, G., Lee, M.Y., Greer, P.A., Roos, D.S., and Greenbaum, D.C. (2009). Apicomplexan parasites co-opt host calpains to facilitate their escape from infected cells. Science *324*, 794-797.

Chang, S.P., Kramer, K.J., Yamaga, K.M., Kato, A., Case, S.E., and Siddiqui, W.A. (1988). Plasmodium falciparum: gene structure and hydropathy profile of the major merozoite surface antigen (gp195) of the Uganda-Palo Alto isolate. Experimental parasitology *67*, 1-11.

Child, M.A., Epp, C., Bujard, H., and Blackman, M.J. (2010). Regulated maturation of malaria merozoite surface protein-1 is essential for parasite growth. Molecular microbiology *78*, 187-202.

Chilengi, R., and Gitaka, J. (2010). Is vaccine the magic bullet for malaria elimination? A reality check. Malaria journal *9 Suppl 3*, S1.

Chitarra, V., Holm, I., Bentley, G.A., Petres, S., and Longacre, S. (1999). The crystal structure of C-terminal merozoite surface protein 1 at 1.8 A resolution, a highly protective malaria vaccine candidate. Molecular cell *3*, 457-464.

Chitnis, C.E. (2001). Molecular insights into receptors used by malaria parasites for erythrocyte invasion. Current opinion in hematology *8*, 85-91.

Clough, B., Paulitschke, M., Nash, G.B., Bayley, P.M., Anstee, D.J., Wilson, R.J., Pasvol, G., and Gratzer, W.B. (1995). Mechanism of regulation of malarial invasion by extraerythrocytic ligands. Molecular and biochemical parasitology *69*, 19-27.

Cogswell, F.B. (1992). The hypnozoite and relapse in primate malaria. Clin Microbiol Rev *5*, 26-35.

Collins, C.R., Hackett, F., Strath, M., Penzo, M., Withers-Martinez, C., Baker, D.A., and Blackman, M.J. (2013). Malaria parasite cGMP-dependent protein kinase regulates blood stage merozoite secretory organelle discharge and egress. PLoS pathogens *9*, e1003344.

Cooper, J.A., and Bujard, H. (1992). Membrane-associated proteases process Plasmodium falciparum merozoite surface antigen-1 (MSA1) to fragment gp41. Molecular and biochemical parasitology *56*, 151-160.

Cortes, A., Benet, A., Cooke, B.M., Barnwell, J.W., and Reeder, J.C. (2004). Ability of Plasmodium falciparum to invade Southeast Asian ovalocytes varies between parasite lines. Blood *104*, 2961-2966.

Cortes, A., Carret, C., Kaneko, O., Yim Lim, B.Y., Ivens, A., and Holder, A.A. (2007). Epigenetic silencing of Plasmodium falciparum genes linked to erythrocyte invasion. PLoS pathogens *3*, e107.

Cox, F. (2010). History of the discovery of the malaria parasites and their vectors. Parasites & Vectors *3*, 5.

Cox, F.E.G. (2002). History of Human Parasitology. Clinical Microbiology Reviews *15*, 595-612.

Crick, A.J., Theron, M., Tiffert, T., Lew, V.L., Cicuta, P., and Rayner, J.C. (2014). Quantitation of malaria parasite-erythrocyte cell-cell interactions using optical tweezers. Biophysical journal *107*, 846-853.

Crick, A.J., Tiffert, T., Shah, S.M., Kotar, J., Lew, V.L., and Cicuta, P. (2013). An automated live imaging platform for studying merozoite egress-invasion in malaria cultures. Biophysical journal *104*, 997-1005.

Crosnier, C., Bustamante, L.Y., Bartholdson, S.J., Bei, A.K., Theron, M., Uchikawa, M., Mboup, S., Ndir, O., Kwiatkowski, D.P., Duraisingh, M.T.*, et al.* (2011). Basigin is a receptor essential for erythrocyte invasion by Plasmodium falciparum. Nature *480*, 534-537.

Crowley, V.M., Rovira-Graells, N., Ribas de Pouplana, L., and Cortes, A. (2011). Heterochromatin formation in bistable chromatin domains controls the epigenetic repression of clonally variant Plasmodium falciparum genes linked to erythrocyte invasion. Molecular microbiology *80*, 391-406.

Deil, S. (2014). New insights into PEXEL-mediated protein export in Plasmodium falciparum: The role of N-terminal acetylation. In Combined Faculties for the Natural Sciences and for Mathematics (Heidelberg: Ruperto-Carola University of Heidelberg).

Desai, S.A. (2014). Why do malaria parasites increase host erythrocyte permeability? Trends Parasitol *30*, 151-159.

Dhingra, V., Rao, K.V., and Narasu, M.L. (1999). Current status of artemisinin and its derivatives as antimalarial drugs. Life Sciences *66*, 279-300.

Duraisingh, M.T., Triglia, T., and Cowman, A.F. (2002). Negative selection of Plasmodium falciparum reveals targeted gene deletion by double crossover recombination. International journal for parasitology *32*, 81-89.

Dvorak, J.A., Miller, L.H., Whitehouse, W.C., and Shiroishi, T. (1975). Invasion of erythrocytes by malaria merozoites. Science *187*, 748-750.

Dvorin, J.D., Martyn, D.C., Patel, S.D., Grimley, J.S., Collins, C.R., Hopp, C.S., Bright, A.T., Westenberger, S., Winzeler, E., Blackman, M.J., *et al.* (2010). A plant-like kinase in Plasmodium falciparum regulates parasite egress from erythrocytes. Science *328*, 910-912.

Engwerda, C.R., and Good, M.F. (2005). Interactions between malaria parasites and the host immune system. Current opinion in immunology *17*, 381-387.

Enserink, M. (2010). Redrawing Africa's malaria map. Science *328*, 842.

Epp, C. (2003). Das Merozoitenoberflächenprotein (MSP)-1 aus Plasmodium falciparum, ein Impfstoffkandidat gegen Malaria: Untersuchungen zur Struktur, Immunogenität und schützenden Wirkung in vitro. In Combined Faculties for the Natural Sciences and for Mathematics (Heidelberg: Ruperto-Carola University of Heidelberg

).

Epp, C., Kauth, C.W., Bujard, H., and Lutz, R. (2003). Expression and purification of Plasmodium falciparum MSP-142: A malaria vaccine candidate. Journal of Chromatography B *786*, 61-72.

Epp, C., Raskolnikov, D., and Deitsch, K.W. (2008). A regulatable transgene expression system for cultured Plasmodium falciparum parasites. Malaria journal *7*, 86.

Erickson, H.P. (2009). Size and shape of protein molecules at the nanometer level determined by sedimentation, gel filtration, and electron microscopy. Biological procedures online *11*, 32-51.

Fairhurst, R.M., Nayyar, G.M., Breman, J.G., Hallett, R., Vennerstrom, J.L., Duong, S., Ringwald, P., Wellems, T.E., Plowe, C.V., and Dondorp, A.M. (2012). Artemisinin-resistant malaria: research challenges, opportunities, and public health implications. The American journal of tropical medicine and hygiene *87*, 231-241.

Farrow, R.E., Green, J., Katsimitsoulia, Z., Taylor, W.R., Holder, A.A., and Molloy, J.E. (2011). The mechanism of erythrocyte invasion by the malarial parasite, Plasmodium falciparum. Seminars in cell & developmental biology *22*, 953-960.

Fidock, D.A., Nomura, T., Talley, A.K., Cooper, R.A., Dzekunov, S.M., Ferdig, M.T., Ursos, L.M., Sidhu, A.B., Naude, B., Deitsch, K.W., *et al.* (2000).

Mutations in the P. falciparum digestive vacuole transmembrane protein PfCRT and evidence for their role in chloroquine resistance. Molecular cell *6*, 861-871.

Freeman, R.R., and Holder, A.A. (1983). Surface antigens of malaria merozoites. A high molecular weight precursor is processed to an 83,000 mol wt form expressed on the surface of Plasmodium falciparum merozoites. The Journal of experimental medicine *158*, 1647-1653.

Frischknecht, F., Baldacci, P., Martin, B., Zimmer, C., Thiberge, S., Olivo-Marin, J.C., Shorte, S.L., and Menard, R. (2004). Imaging movement of malaria parasites during transmission by Anopheles mosquitoes. Cellular microbiology *6*, 687-694.

Ganser-Pornillos, B.K., Yeager, M., and Sundquist, W.I. (2008). The structural biology of HIV assembly. Current Opinion in Structural Biology *18*, 203-217.

Gao, X., Gunalan, K., Yap, S.S., and Preiser, P.R. (2013). Triggers of key calcium signals during erythrocyte invasion by Plasmodium falciparum. Nature communications *4*, 2862.

Gardner, M., Hall, N., Fung, E., White, O., Berriman, M., Hyman, R., Carlton, J., Pain, A., Nelson, K., Bowman, S., *et al.* (2002). Genome sequence of the human malaria parasite Plasmodium falciparum. Nature *419*, 489 - 511.

Garg, S., Agarwal, S., Kumar, S., Yazdani, S.S., Chitnis, C.E., and Singh, S. (2013). Calcium-dependent permeabilization of erythrocytes by a perforin-like protein during egress of malaria parasites. Nature communications *4*, 1736.

Ghorbal, M., Gorman, M., Macpherson, C.R., Martins, R.M., Scherf, A., and Lopez-Rubio, J.-J. (2014). Genome editing in the human malaria parasite Plasmodium falciparum using the CRISPR-Cas9 system. Nat Biotech *32*, 819-821.

Glushakova, S., Humphrey, G., Leikina, E., Balaban, A., Miller, J., and Zimmerberg, J. (2010). New stages in the program of malaria parasite egress imaged in normal and sickle erythrocytes. Current biology : CB *20*, 1117-1121.

Glushakova, S., Lizunov, V., Blank, P.S., Melikov, K., Humphrey, G., and Zimmerberg, J. (2013). Cytoplasmic free Ca2+ is essential for multiple steps in malaria parasite egress from infected erythrocytes. Malaria journal *12*, 41.

Glushakova, S., Mazar, J., Hohmann-Marriott, M.F., Hama, E., and Zimmerberg, J. (2009). Irreversible effect of cysteine protease inhibitors on the release of malaria parasites from infected erythrocytes. Cellular microbiology *11*, 95-105.

Glushakova, S., Yin, D., Gartner, N., and Zimmerberg, J. (2007). Quantification of malaria parasite release from infected erythrocytes: inhibition by protein-free media. Malaria journal *6*, 61.

Glushakova, S., Yin, D., Li, T., and Zimmerberg, J. (2005). Membrane transformation during malaria parasite release from human red blood cells. Current biology : CB *15*, 1645-1650.

Goel, V.K., Li, X., Chen, H., Liu, S.C., Chishti, A.H., and Oh, S.S. (2003). Band 3 is a host receptor binding merozoite surface protein 1 during the Plasmodium falciparum invasion of erythrocytes. Proceedings of the National Academy of Sciences of the United States of America *100*, 5164-5169.

Goldstein, S.T., and Shapiro, C.N. (1997). A recombinant circumsporozoite protein vaccine against malaria. The New England journal of medicine *336*, 1760; author reply 1760-1761.

Greenwood, B.M., Bojang, K., Whitty, C.J., and Targett, G.A. (2005). Malaria. Lancet *365*, 1487-1498.

Guillemin, J. (2001). Miasma, malaria, and method. Molecular interventions *1*, 246-249.

Had2Know.com (2014). Surface Area and Volume of an Egg.

Hakansson, S., Charron, A.J., and Sibley, L.D. (2001). Toxoplasma evacuoles: a two-step process of secretion and fusion forms the parasitophorous vacuole. The EMBO journal *20*, 3132-3144.

Harris, P.K., Yeoh, S., Dluzewski, A.R., O'Donnell, R.A., Withers-Martinez, C., Hackett, F., Bannister, L.H., Mitchell, G.H., and Blackman, M.J. (2005). Molecular identification of a malaria merozoite surface sheddase. PLoS pathogens *1*, 241-251.

Harvey, K.L., Gilson, P.R., and Crabb, B.S. (2012). A model for the progression of receptor-ligand interactions during erythrocyte invasion by Plasmodium falciparum. International journal for parasitology *42*, 567-573.

Hell, S.W., and Wichmann, J. (1994). Breaking the diffraction resolution limit by stimulated emission: stimulated-emission-depletion fluorescence microscopy. Optics letters *19*, 780-782.

Hempelmann, E. (2007). Hemozoin biocrystallization in Plasmodium falciparum and the antimalarial activity of crystallization inhibitors. Parasitology research *100*, 671-676.

Herm-Gotz, A., Agop-Nersesian, C., Munter, S., Grimley, J.S., Wandless, T.J., Frischknecht, F., and Meissner, M. (2007). Rapid control of protein level in the apicomplexan Toxoplasma gondii. Nature methods *4*, 1003-1005.

Hill, D.A., Pillai, A.D., Nawaz, F., Hayton, K., Doan, L., Lisk, G., and Desai, S.A. (2007). A blasticidin S-resistant Plasmodium falciparum mutant with a defective plasmodial surface anion channel. Proceedings of the National Academy of Sciences of the United States of America *104*, 1063-1068.

Hoffman, S.L., Goh, L.M., Luke, T.C., Schneider, I., Le, T.P., Doolan, D.L., Sacci, J., de la Vega, P., Dowler, M., Paul, C., *et al.* (2002). Protection of humans against malaria by immunization with radiation-attenuated Plasmodium falciparum sporozoites. The Journal of infectious diseases *185*, 1155-1164.

Holder, A.A., Lockyer, M.J., Odink, K.G., Sandhu, J.S., Riveros-Moreno, V., Nicholls, S.C., Hillman, Y., Davey, L.S., Tizard, M.L., Schwarz, R.T., *et al.* (1985). Primary structure of the precursor to the three major surface antigens of Plasmodium falciparum merozoites. Nature *317*, 270-273.

Hope, I.A., Mackay, M., Hyde, J.E., Goman, M., and Scaife, J. (1985). The gene for an exported antigen of the malaria parasite Plasmodium falciparum cloned and expressed in Escherichia coli. Nucleic acids research *13*, 369-379.

Ishiguro, J., and Miyazaki, M. (1985). Characterization of blasticidin S-resistant mutants of Saccharomyces cerevisiae. Current genetics *9*, 179-181.

Kauth, C.W., Epp, C., Bujard, H., and Lutz, R. (2003). The merozoite surface protein 1 complex of human malaria parasite Plasmodium falciparum: interactions and arrangements of subunits. The Journal of biological chemistry *278*, 22257-22264.

Kauth, C.W., Woehlbier, U., Kern, M., Mekonnen, Z., Lutz, R., Mucke, N., Langowski, J., and Bujard, H. (2006). Interactions between merozoite surface proteins 1, 6, and 7 of the malaria parasite Plasmodium falciparum. The Journal of biological chemistry *281*, 31517-31527.

Keeley, A., and Soldati, D. (2004). The glideosome: a molecular machine powering motility and host-cell invasion by Apicomplexa. Trends in cell biology *14*, 528-532.

Killick-Kendrick, R. (1978). 1 - Taxonomy, Zoogeography and Evolution. In Rodent Malaria, R. Killick-Kendrick, and W. Peters, eds. (Academic Press), pp. 1-52.

Knecht, D.A., and Dimond, R.L. (1984). Visualization of antigenic proteins on Western blots. Analytical biochemistry *136*, 180-184.

Kobayashi, K., Takano, R., Takemae, H., Sugi, T., Ishiwa, A., Gong, H., Recuenco, F.C., Iwanaga, T., Horimoto, T., Akashi, H., *et al.* (2013). Analyses of interactions between heparin and the apical surface proteins of Plasmodium falciparum. Scientific reports *3*, 3178.

Kolevzon, N., Nasereddin, A., Naik, S., Yavin, E., and Dzikowski, R. (2014). Use of peptide nucleic acids to manipulate gene expression in the malaria parasite Plasmodium falciparum. PloS one *9*, e86802.

Koussis, K., Withers-Martinez, C., Yeoh, S., Child, M., Hackett, F., Knuepfer, E., Juliano, L., Woehlbier, U., Bujard, H., and Blackman, M.J. (2009). A multifunctional serine protease primes the malaria parasite for red blood cell invasion, Vol 28.

Kreidenweiss, A., Hopkins, A.V., and Mordmüller, B. (2013). 2A and the Auxin-Based Degron System Facilitate Control of Protein Levels in Plasmodium falciparum. PloS one *8*, e78661.

Lamarque, M., Besteiro, S., Papoin, J., Roques, M., Vulliez-Le Normand, B., Morlon-Guyot, J., Dubremetz, J.F., Fauquenoy, S., Tomavo, S., Faber, B.W., *et al.* (2011). The RON2-AMA1 interaction is a critical step in moving junction-dependent invasion by apicomplexan parasites. PLoS pathogens *7*, e1001276.

Lamarque, M.H., Roques, M., Kong-Hap, M., Tonkin, M.L., Rugarabamu, G., Marq, J.B., Penarete-Vargas, D.M., Boulanger, M.J., Soldati-Favre, D., and Lebrun, M. (2014). Plasticity and redundancy among AMA-RON pairs ensure host cell entry of Toxoplasma parasites. Nature communications *5*, 4098.

Lew, V.L. (2001). Packaged merozoite release without immediate host cell lysis. Trends Parasitol *17*, 401-403.

Lin, C.S., Uboldi, A.D., Marapana, D., Czabotar, P.E., Epp, C., Bujard, H., Taylor, N.L., Perugini, M.A., Hodder, A.N., and Cowman, A.F. (2014). The Merozoite Surface Protein 1 complex is a platform for binding to human erythrocytes by P. falciparum. Journal of Biological Chemistry.

Lingelbach, K., and Joiner, K.A. (1998). The parasitophorous vacuole membrane surrounding Plasmodium and Toxoplasma: an unusual compartment in infected cells. Journal of cell science *111 (Pt 11)*, 1467-1475.

Lopez, C., Saravia, C., Gomez, A., Hoebeke, J., and Patarroyo, M.A. (2010). Mechanisms of genetically-based resistance to malaria. Gene *467*, 1-12.

Maaß, S., Wachlin, G., Bernhardt, J., Eymann, C., Fromion, V., Riedel, K., Becher, D., and Hecker, M. (2014). Highly precise quantification of protein molecules per cell during stress and starvation responses in Bacillus subtilis. Molecular & Cellular Proteomics.

Maier, A.G., Braks, J.A., Waters, A.P., and Cowman, A.F. (2006). Negative selection using yeast cytosine deaminase/uracil phosphoribosyl transferase in Plasmodium falciparum for targeted gene deletion by double crossover recombination. Molecular and biochemical parasitology *150*, 118-121.

Maier, A.G., Duraisingh, M.T., Reeder, J.C., Patel, S.S., Kazura, J.W., Zimmerman, P.A., and Cowman, A.F. (2003). Plasmodium falciparum erythrocyte invasion through glycophorin C and selection for Gerbich negativity in human populations. Nature medicine *9*, 87-92.

Mayer, D.C., Cofie, J., Jiang, L., Hartl, D.L., Tracy, E., Kabat, J., Mendoza, L.H., and Miller, L.H. (2009). Glycophorin B is the erythrocyte receptor of Plasmodium falciparum erythrocyte-binding ligand, EBL-1. Proceedings of the National Academy of Sciences of the United States of America *106*, 5348-5352.

McBride, J.S., and Heidrich, H.-G. (1987). Fragments of the polymorphic Mr 185 000 glycoprotein from the surface of isolated Plasmodium falciparum merozoites form an antigenic complex. Molecular and biochemical parasitology *23*, 71-84.

McBride, J.S., Walliker, D., and Morgan, G. (1982). Antigenic diversity in the human malaria parasite Plasmodium falciparum. Science *217*, 254-257.

Meissner, M., Breinich, M.S., Gilson, P.R., and Crabb, B.S. (2007). Molecular genetic tools in Toxoplasma and Plasmodium: achievements and future needs. Current opinion in microbiology *10*, 349-356.

Meissner, M., Krejany, E., Gilson, P.R., de Koning-Ward, T.F., Soldati, D., and Crabb, B.S. (2005). Tetracycline analogue-regulated transgene expression in Plasmodium falciparum blood stages using Toxoplasma gondii transactivators. Proceedings of the National Academy of Sciences of the United States of America *102*, 2980-2985.

Ménard, R. (2013). Malaria Methods and Protocols. Springer Science+Business Media, LLC *923*.

Mendis, K., Rietveld, A., Warsame, M., Bosman, A., Greenwood, B., and Wernsdorfer, W.H. (2009). From malaria control to eradication: The WHO perspective. Tropical medicine & international health : TM & IH *14*, 802-809.

Miller, L.H., Hudson, D., Rener, J., Taylor, D., Hadley, T.J., and Zilberstein, D. (1983). A monoclonal antibody to rhesus erythrocyte band 3 inhibits invasion by malaria (Plasmodium knowlesi) merozoites. The Journal of clinical investigation *72*, 1357-1364.

Miller, L.H., McAuliffe, F.M., and Johnson, J.G. (1979). Invasion of erythrocytes by malaria merozoites. Progress in clinical and biological research *30*, 497-502.

Mira-Martinez, S., Rovira-Graells, N., Crowley, V.M., Altenhofen, L.M., Llinas, M., and Cortes, A. (2013). Epigenetic switches in clag3 genes mediate blasticidin S resistance in malaria parasites. Cellular microbiology.

Moerner, W.E. (2007). New directions in single-molecule imaging and analysis. Proceedings of the National Academy of Sciences of the United States of America *104*, 12596-12602.

Morgan, W.D., Birdsall, B., Frenkiel, T.A., Gradwell, M.G., Burghaus, P.A., Syed, S.E., Uthaipibull, C., Holder, A.A., and Feeney, J. (1999). Solution structure of an EGF module pair from the Plasmodium falciparum merozoite surface protein 1. Journal of molecular biology *289*, 113-122.

Morrissette, N.S., and Sibley, L.D. (2002). Cytoskeleton of apicomplexan parasites. Microbiology and molecular biology reviews : MMBR *66*, 21-38; table of contents.

Mota, M.M., and Rodriguez, A. (2004). Migration through host cells: the first steps of Plasmodium sporozoites in the mammalian host. Cellular microbiology *6*, 1113-1118.

Nakato, H., Vivancos, R., and Hunter, P.R. (2007). A systematic review and meta-analysis of the effectiveness and safety of atovaquone proguanil (Malarone)

for chemoprophylaxis against malaria. The Journal of antimicrobial chemotherapy *60*, 929-936.

Nguitragool, W., Bokhari, Abdullah A.B., Pillai, Ajay D., Rayavara, K., Sharma, P., Turpin, B., Aravind, L., and Desai, Sanjay A. Malaria Parasite clag3 Genes Determine Channel-Mediated Nutrient Uptake by Infected Red Blood Cells. Cell *145*, 665-677.

Niang, M., Bei, A.K., Madnani, K.G., Pelly, S., Dankwa, S., Kanjee, U., Gunalan, K., Amaladoss, A., Yeo, K.P., Bob, N.S., *et al.* (2014). STEVOR is a Plasmodium falciparum erythrocyte binding protein that mediates merozoite invasion and rosetting. Cell host & microbe *16*, 81-93.

Nikodem, D.-P., and Davidson, E.-A. (2000). Identification of a novel antigenic domain of Plasmodium falciparum merozoite surface protein-1 that specifically binds to human erythrocytes and inhibits parasite invasion, in vitro. Molecular and biochemical parasitology *108*, 79-91.

O'Donnell, R.A., Freitas-Junior, L.H., Preiser, P.R., Williamson, D.H., Duraisingh, M., McElwain, T.F., Scherf, A., Cowman, A.F., and Crabb, B.S. (2002a). A genetic screen for improved plasmid segregation reveals a role for Rep20 in the interaction of Plasmodium falciparum chromosomes. The EMBO journal *21*, 1231-1239.

O'Donnell, R.A., Freitas-Junior, L.H., Preiser, P.R., Williamson, D.H., Duraisingh, M., McElwain, T.F., Scherf, A., Cowman, A.F., and Crabb, B.S. (2002b). A genetic screen for improved plasmid segregation reveals a role for Rep20 in the interaction of Plasmodium falciparum chromosomes, Vol 21.

O'Donnell, R.A., Hackett, F., Howell, S.A., Treeck, M., Struck, N., Krnajski, Z., Withers-Martinez, C., Gilberger, T.W., and Blackman, M.J. (2006). Intramembrane proteolysis mediates shedding of a key adhesin during erythrocyte invasion by the malaria parasite. The Journal of cell biology *174*, 1023-1033.

O'Donnell, R.A., Saul, A., Cowman, A.F., and Crabb, B.S. (2000). Functional conservation of the malaria vaccine antigen MSP-119across distantly related Plasmodium species. Nature medicine *6*, 91-95.

O'Donnell, R.A., and Blackman, M.J. (2005). The role of malaria merozoite proteases in red blood cell invasion. Current opinion in microbiology *8*, 422-427.

O'Donnell, R.A., Preiser, P.R., Williamson, D.H., Moore, P.W., Cowman, A.F., and Crabb, B.S. (2001). An alteration in concatameric structure is associated with efficient segregation of plasmids in transfected Plasmodium falciparum parasites. Nucleic acids research *29*, 716-724.

Orlandi, P.A., Klotz, F.W., and Haynes, J.D. (1992). A malaria invasion receptor, the 175-kilodalton erythrocyte binding antigen of Plasmodium falciparum

recognizes the terminal Neu5Ac(alpha 2-3)Gal- sequences of glycophorin A. The Journal of cell biology *116*, 901-909.

Pachebat, J.A., Ling, I.T., Grainger, M., Trucco, C., Howell, S., Fernandez-Reyes, D., Gunaratne, R., and Holder, A.A. (2001). The 22 kDa component of the protein complex on the surface of Plasmodium falciparum merozoites is derived from a larger precursor, merozoite surface protein 7. Molecular and biochemical parasitology *117*, 83-89.

Pan, W., Ravot, E., Tolle, R., Frank, R., Mosbach, R., Turbachova, I., and Bujard, H. (1999). Vaccine candidate MSP-1 from Plasmodium falciparum: a redesigned 4917 bp polynucleotide enables synthesis and isolation of full-length protein from Escherichia coli and mammalian cells. Nucleic acids research *27*, 1094-1103.

Petersen, I., Eastman, R., and Lanzer, M. (2011). Drug-resistant malaria: molecular mechanisms and implications for public health. FEBS letters *585*, 1551-1562.

Pino, P., Sebastian, S., Kim, E.A., Bush, E., Brochet, M., Volkmann, K., Kozlowski, E., Llinas, M., Billker, O., and Soldati-Favre, D. (2012). A tetracycline-repressible transactivator system to study essential genes in malaria parasites. Cell host & microbe *12*, 824-834.

Pradel, G., and Frevert, U. (2001). Malaria sporozoites actively enter and pass through rat Kupffer cells prior to hepatocyte invasion. Hepatology *33*, 1154-1165.

Pradel, G., Garapaty, S., and Frevert, U. (2002). Proteoglycans mediate malaria sporozoite targeting to the liver. Molecular microbiology *45*, 637-651.

Pradel, G., Garapaty, S., and Frevert, U. (2004). Kupffer and stellate cell proteoglycans mediate malaria sporozoite targeting to the liver. Comparative hepatology *3 Suppl 1*, S47.

Prommana, P., Uthaipibull, C., Wongsombat, C., Kamchonwongpaisan, S., Yuthavong, Y., Knuepfer, E., Holder, A.A., and Shaw, P.J. (2013). Inducible Knockdown of Plasmodium</italic> Gene Expression Using the glmS</italic> Ribozyme. PloS one *8*, e73783.

Ramasamy, R. (1998). Molecular basis for evasion of host immunity and pathogenesis in malaria. Biochimica et biophysica acta *1406*, 10-27.

Retief, F., and Cilliers, L. (2006). Periodic pyrexia and malaria in antiquity. South African medical journal = Suid-Afrikaanse tydskrif vir geneeskunde *96*, 684, 686-688.

Richard, D., MacRaild, C.A., Riglar, D.T., Chan, J.A., Foley, M., Baum, J., Ralph, S.A., Norton, R.S., and Cowman, A.F. (2010). Interaction between Plasmodium falciparum apical membrane antigen 1 and the rhoptry neck protein

complex defines a key step in the erythrocyte invasion process of malaria parasites. The Journal of biological chemistry *285*, 14815-14822.

Rozen, S., and Skaletsky, H. (2000). Primer3 on the WWW for general users and for biologist programmers. Methods Mol Biol *132*, 365-386.

Rudolph, R., and Lilie, H. (1996). In vitro folding of inclusion body proteins. FASEB journal : official publication of the Federation of American Societies for Experimental Biology *10*, 49-56.

Rust, M.J., Bates, M., and Zhuang, X. (2006). Sub-diffraction-limit imaging by stochastic optical reconstruction microscopy (STORM). Nat Meth *3*, 793-796.

Sakamoto, H., Takeo, S., Maier, A.G., Sattabongkot, J., Cowman, A.F., and Tsuboi, T. (2012). Antibodies against a Plasmodium falciparum antigen PfMSPDBL1 inhibit merozoite invasion into human erythrocytes. Vaccine *30*, 1972-1980.

Salmon, B.L., Oksman, A., and Goldberg, D.E. (2001). Malaria parasite exit from the host erythrocyte: a two-step process requiring extraerythrocytic proteolysis. Proceedings of the National Academy of Sciences of the United States of America *98*, 271-276.

Salvador, A., Hernandez, R.M., Pedraz, J.L., and Igartua, M. (2012). Plasmodium falciparum malaria vaccines: current status, pitfalls and future directions. Expert review of vaccines *11*, 1071-1086.

Sanchez, C.P., Stein, W., and Lanzer, M. (2003). Trans stimulation provides evidence for a drug efflux carrier as the mechanism of chloroquine resistance in Plasmodium falciparum. Biochemistry *42*, 9383-9394.

Schechter, I., and Berger, A. (1967). On the size of the active site in proteases. I. Papain. Biochemical and biophysical research communications *27*, 157-162.

Schrader, F.C., Barho, M., Steiner, I., Ortmann, R., and Schlitzer, M. (2012). The antimalarial pipeline--an update. International journal of medical microbiology : IJMM *302*, 165-171.

Schwartz, L., Brown, G.V., Genton, B., and Moorthy, V.S. (2012). A review of malaria vaccine clinical projects based on the WHO rainbow table. Malaria journal *11*, 11.

Sharma, P., and Chitnis, C.E. (2013). Key molecular events during host cell invasion by Apicomplexan pathogens. Current opinion in microbiology *16*, 432-437.

Shio, M.T., Kassa, F.A., Bellemare, M.J., and Olivier, M. (2010). Innate inflammatory response to the malarial pigment hemozoin. Microbes and infection / Institut Pasteur *12*, 889-899.

Silmon de Monerri, N.C., Flynn, H.R., Campos, M.G., Hackett, F., Koussis, K., Withers-Martinez, C., Skehel, J.M., and Blackman, M.J. (2011). Global

identification of multiple substrates for Plasmodium falciparum SUB1, an essential malarial processing protease. Infection and immunity *79*, 1086-1097.

Sinden, R. (1997). Infection of mosquitoes with rodent malaria. In The Molecular Biology of Insect Disease Vectors, J. Crampton, C.B. Beard, and C. Louis, eds. (Springer Netherlands), pp. 67-91.

Sinden, R.E., and Billingsley, P.F. (2001). Plasmodium invasion of mosquito cells: hawk or dove? Trends Parasitol *17*, 209-212.

Singh, B., Lee, K., Matusop, A., Radhakrishnan, A., Shamsul, S., Cox-Singh, J., Thomas, A., and Conway, D. (2004). A large focus of naturally acquired Plasmodium knowlesi infections in human beings. Lancet *363*, 1017 - 1024.

Singh, S., Soe, S., Weisman, S., Barnwell, J.W., Perignon, J.L., and Druilhe, P. (2009). A conserved multi-gene family induces cross-reactive antibodies effective in defense against Plasmodium falciparum. PloS one *4*, e5410.

Stafford, W.H., Blackman, M.J., Harris, A., Shai, S., Grainger, M., and Holder, A.A. (1994). N-terminal amino acid sequence of the Plasmodium falciparum merozoite surface protein-1 polypeptides. Molecular and biochemical parasitology *66*, 157-160.

Stafford, W.H., Gunder, B., Harris, A., Heidrich, H.G., Holder, A.A., and Blackman, M.J. (1996). A 22 kDa protein associated with the Plasmodium falciparum merozoite surface protein-1 complex. Molecular and biochemical parasitology *80*, 159-169.

Stoute, J.A., Slaoui, M., Heppner, D.G., Momin, P., Kester, K.E., Desmons, P., Wellde, B.T., Garcon, N., Krzych, U., and Marchand, M. (1997). A preliminary evaluation of a recombinant circumsporozoite protein vaccine against Plasmodium falciparum malaria. RTS,S Malaria Vaccine Evaluation Group. The New England journal of medicine *336*, 86-91.

Straimer, J., Lee, M.C.S., Lee, A.H., Zeitler, B., Williams, A.E., Pearl, J.R., Zhang, L., Rebar, E.J., Gregory, P.D., Llinas, M.*, et al.* (2012). Site-specific genome editing in Plasmodium falciparum using engineered zinc-finger nucleases. Nat Meth *9*, 993-998.

Sturm, A., Amino, R., van de Sand, C., Regen, T., Retzlaff, S., Rennenberg, A., Krueger, A., Pollok, J.M., Menard, R., and Heussler, V.T. (2006). Manipulation of host hepatocytes by the malaria parasite for delivery into liver sinusoids. Science *313*, 1287-1290.

Sturm, A., Graewe, S., Franke-Fayard, B., Retzlaff, S., Bolte, S., Roppenser, B., Aepfelbacher, M., Janse, C., and Heussler, V. (2009). Alteration of the parasite plasma membrane and the parasitophorous vacuole membrane during exo-erythrocytic development of malaria parasites. Protist *160*, 51-63.

Tanabe, K., Mackay, M., Goman, M., and Scaife, J.G. (1987). Allelic dimorphism in a surface antigen gene of the malaria parasite Plasmodium falciparum. Journal of molecular biology *195*, 273-287.

Tham, W.H., Healer, J., and Cowman, A.F. (2012). Erythrocyte and reticulocyte binding-like proteins of Plasmodium falciparum. Trends Parasitol *28*, 23-30.

Trucco, C., Fernandez-Reyes, D., Howell, S., Stafford, W.H., Scott-Finnigan, T.J., Grainger, M., Ogun, S.A., Taylor, W.R., and Holder, A.A. (2001). The merozoite surface protein 6 gene codes for a 36 kDa protein associated with the Plasmodium falciparum merozoite surface protein-1 complex. Molecular and biochemical parasitology *112*, 91-101.

Turschner, S., and Efferth, T. (2009). Drug resistance in Plasmodium: natural products in the fight against malaria. Mini reviews in medicinal chemistry *9*, 206-2124.

Tuteja, R. (2007). Malaria — an overview. FEBS Journal *274*, 4670-4679.

Vaishnava, S., and Striepen, B. (2006). The cell biology of secondary endosymbiosis--how parasites build, divide and segregate the apicoplast. Molecular microbiology *61*, 1380-1387.

van Agtmael, M.A., Eggelte, T.A., and van Boxtel, C.J. Artemisinin drugs in the treatment of malaria: from medicinal herb to registered medication. Trends in Pharmacological Sciences *20*, 199-205.

Weber, J.L., Leininger, W.M., and Lyon, J.A. (1986). Variation in the gene encoding a major merozoite surface antigen of the human malaria parasite Plasmodium falciparum. Nucleic acids research *14*, 3311-3323.

Westerfeld, N. (2002). Herstellung rekombinanter Vaccinia-Viren als Träger des Oberflächenproteins MSP1 aus Plasmodium falciparum und ihre Charakterisierung in Hinsicht auf einen Malaria-Impfstoff In Combined Faculties for the Natural Sciences and for Mathematics (Heidelberg: Ruperto-Carola University of Heidelberg).

White, N.J. (2014). Malaria: a molecular marker of artemisinin resistance. Lancet *383*, 1439-1440.

WHO (2009). World Health Statistics.

WHO (2013). World Malaria Report 2013.

WHO (2014). Tables of malaria vaccine projects globally.

Wickramarachchi, T., Cabrera, A.L., Sinha, D., Dhawan, S., Chandran, T., Devi, Y.S., Kono, M., Spielmann, T., Gilberger, T.W., Chauhan, V.S., *et al.* (2009). A novel Plasmodium falciparum erythrocyte binding protein associated with the merozoite surface, PfDBLMSP. International journal for parasitology *39*, 763-773.

Wilkins, M.R., Gasteiger, E., Bairoch, A., Sanchez, J.C., Williams, K.L., Appel, R.D., and Hochstrasser, D.F. (1999). Protein identification and analysis tools in the ExPASy server. Methods Mol Biol *112*, 531-552.

Williams, T.N. (2006). Human red blood cell polymorphisms and malaria. Current opinion in microbiology *9*, 388-394.

Williamson, D.H., Janse, C.J., Moore, P.W., Waters, A.P., and Preiser, P.R. (2002). Topology and replication of a nuclear episomal plasmid in the rodent malaria Plasmodium berghei. Nucleic acids research *30*, 726-731.

Winograd, E., Clavijo, C.A., Bustamante, L.Y., and Jaramillo, M. (1999). Release of merozoites from Plasmodium falciparum-infected erythrocytes could be mediated by a non-explosive event. Parasitology research *85*, 621-624.

Withers-Martinez, C., Carpenter, E.P., Hackett, F., Ely, B., Sajid, M., Grainger, M., and Blackman, M.J. (1999). PCR-based gene synthesis as an efficient approach for expression of the A+T-rich malaria genome. Protein engineering *12*, 1113-1120.

Withers-Martinez, C., Saldanha, J.W., Ely, B., Hackett, F., O'Connor, T., and Blackman, M.J. (2002). Expression of recombinant Plasmodium falciparum subtilisin-like protease-1 in insect cells. Characterization, comparison with the parasite protease, and homology modeling. The Journal of biological chemistry *277*, 29698-29709.

Withers-Martinez, C., Suarez, C., Fulle, S., Kher, S., Penzo, M., Ebejer, J.P., Koussis, K., Hackett, F., Jirgensons, A., Finn, P.*, et al.* (2012). Plasmodium subtilisin-like protease 1 (SUB1): insights into the active-site structure, specificity and function of a pan-malaria drug target. International journal for parasitology *42*, 597-612.

Woehlbier, U., Epp, C., Hackett, F., Blackman, M.J., and Bujard, H. (2010). Antibodies against multiple merozoite surface antigens of the human malaria parasite Plasmodium falciparum inhibit parasite maturation and red blood cell invasion. Malaria journal *9*, 77.

Woehlbier, U., Epp, C., Kauth, C.W., Lutz, R., Long, C.A., Coulibaly, B., Kouyate, B., Arevalo-Herrera, M., Herrera, S., and Bujard, H. (2006). Analysis of antibodies directed against merozoite surface protein 1 of the human malaria parasite Plasmodium falciparum. Infection and immunity *74*, 1313-1322.

Yamaguchi, H., Yamamoto, C., and Tanaka, N. (1965). Inhibition of protein synthesis by blasticidin S. I. Studies with cell-free systems from bacterial and mammalian cells. Journal of biochemistry *57*, 667-677.

Yamauchi, L.M., Coppi, A., Snounou, G., and Sinnis, P. (2007). Plasmodium sporozoites trickle out of the injection site. Cellular microbiology *9*, 1215-1222.

Yan, H., Zhong, G., Xu, G., He, W., Jing, Z., Gao, Z., Huang, Y., Qi, Y., Peng, B., Wang, H., *et al.* (2012). Sodium taurocholate cotransporting polypeptide is a functional receptor for human hepatitis B and D virus. eLife *1*, e00049.

Yeoh, S., O'Donnell, R.A., Koussis, K., Dluzewski, A.R., Ansell, K.H., Osborne, S.A., Hackett, F., Withers-Martinez, C., Mitchell, G.H., Bannister, L.H., *et al.* (2007). Subcellular discharge of a serine protease mediates release of invasive malaria parasites from host erythrocytes. Cell *131*, 1072-1083.

Zong, S., Kron, M.W., Epp, C., Engler, T., Bujard, H., Kochanek, S., and Kreppel, F. (2011). DeltaE1 and high-capacity adenoviral vectors expressing full-length codon-optimized merozoite surface protein 1 for vaccination against Plasmodium falciparum. The journal of gene medicine *13*, 670-679.

Appendix

A1 Mutation of cleavage junctions in MSP-1F

Table 35 | Overview of mutations of cleavage sites within MSP-1F
Upper two panels display wildtype amino acids and nucleotide sequence, respectively. Mutations introduced are indicated in the title of the respective sequences. The two lower panels show mutated nucleotide and amino acid sequences. Mutated amino acids and nucleotides are marked in red.

83/30

Mut D/G

K	T	E	G	Q	S	D	N	S	E
AAA	ACT	GAA	GGA	CAG	TCA	GAT	AAC	TCC	GAG
AAA	ACT	GAA	GAC	CAG	TCA	GGT	AAC	TCC	GAG
K	T	E	D	Q	S	G	N	S	E

Mut G/T

K	T	E	G	Q	S	D	N	S	E
AAA	ACT	GAA	GGA	CAG	TCA	GAT	AAC	TCC	GAG
AAA	GGT	GAA	ACA	CAG	TCA	GAT	AAC	TCC	GAG
K	G	E	T	Q	S	D	N	S	E

30/38

Mut KK

E	V	S	A	N	D	D	T	S	H
GAA	GTG	AGC	GCT	AAC	GAC	GAC	ACC	TCT	CAC
GAA	AAG	AGC	AAG	AAC	GAC	GAC	ACC	TCT	CAC
E	K	S	K	N	D	D	T	S	H

Mut DD

E	V	S	A	N	D	D	T	S	H
GAA	GTG	AGC	GCT	AAC	GAC	GAC	ACC	TCT	CAC
GAA	GAT	AGC	GAT	AAC	GAC	GAC	ACC	TCT	CAC
E	D	S	D	N	D	D	T	S	H

Mut VA

E	V	S	A	N	D	D	T	S	H
GAA	GTG	AGC	GCT	AAC	GAC	GAC	ACC	TCT	CAC
GAA	GCG	AGC	GTT	AAC	GAC	GAC	ACC	TCT	CAC
E	A	S	V	N	D	D	T	S	H

Mut AD

E	V	S	A	N	D	D	T	S	H
GAA	GTG	AGC	GCT	AAC	GAC	GAC	ACC	TCT	CAC
GAA	GTG	AGC	GAT	AAC	GAC	GCC	ACC	TCT	CAC
E	V	S	D	N	D	A	T	S	H

38/42 site 1

Mut KK

V	V	T	G	E	A	V	T	P	S
GTG	GTC	ACC	GGT	GAG	GCT	GTC	ACT	CCT	TCC
GTG	AAG	ACC	AAG	GAG	GCT	GTC	ACT	CCT	TCC
V	K	T	K	E	A	V	T	P	S

Mut DD

V	V	T	G	E	A	V	T	P	S
GTG	GTC	ACC	GGT	GAG	GCT	GTC	ACT	CCT	TCC
GTG	GAC	ACC	AAG	GAT	GCT	GTC	ACT	CCT	TCC
V	D	T	D	E	A	V	T	P	S

38/42 site 2

Mut KK

P	I	F	G	E	S	E	E	D	Y
CCT	ATC	TTC	GGC	GAG	AGC	GAG	GAG	GAC	TAC
CCT	AAG	TTC	AAG	GAG	AGC	GAG	GAG	GAC	TAC
P	K	F	K	E	S	E	E	D	Y

Mut DD

P	I	F	G	E	S	E	E	D	Y
CCT	ATC	TTC	GGC	GAG	AGC	GAG	GAG	GAC	TAC
CCT	GAC	TTC	GAC	GAG	AGC	GAG	GAG	GAC	TAC
P	D	F	D	E	S	E	E	D	Y

Mut EG

P	I	F	G	E	S	E	E	D	Y
CCT	ATC	TTC	GGC	GAG	AGC	GAG	GAG	GAC	TAC
CCT	ATC	TTC	GAA	GGG	AGC	GAG	GAG	GAC	TAC
P	I	F	E	G	S	E	E	D	Y

Mut GI

P	I	F	G	E	S	E	E	D	Y
CCT	ATC	TTC	GGC	GAG	AGC	GAG	GAG	GAC	TAC
CCT	GGC	TTC	ATC	GAG	AGC	GAG	GAG	GAC	TAC
P	G	F	I	E	S	E	E	D	Y

Mut SG

P	I	F	G	E	S	E	E	D	Y
CCT	ATC	TTC	GGC	GAG	AGC	GAG	GAG	GAC	TAC
CCT	ATC	TTC	TCC	GAG	GGC	GAG	GAG	GAC	TAC
P	I	F	S	E	G	E	E	D	Y

38/42 site 3

Mut LL (P2P4)

I	T	T	S	Q	N	V	D	D	E
ATT	ACC	ACA	TCT	CAG	AAC	GTC	GAC	GAT	GAG
ATT	CTC	ACA	TTG	CAG	AAC	GTC	GAC	GAT	GAG
I	L	T	L	Q	N	V	D	D	E

Mut LL (P1P2)

I	T	T	S	Q	N	V	D	D	E
ATT	ACC	ACA	TCT	CAG	AAC	GTC	GAC	GAT	GAG
ATT	ACC	ACA	TTG	TCG	AAC	GTC	GAC	GAT	GAG
I	T	T	L	L	N	V	D	D	E

38/42 site 4

Mut KK

H	V	G	A	E	S	N	T	I	T
CAT	GTC	GGA	GCC	GAG	TCC	AAT	ACA	ATT	ACC
CAT	GTC	AAA	AAA	GAG	TCC	AAT	ACA	ATT	ACC
H	V	K	K	E	S	N	T	I	T

Mut DED

H	V	G	A	E	S	N	T	I	T
CAT	GTC	GGA	GCC	GAG	TCC	AAT	ACA	ATT	ACC
CAT	GAT	GAG	GAC	GAG	TCC	AAT	ACA	ATT	ACC
H	D	E	D	E	S	N	T	I	T

Mut VV

H	V	G	A	E	S	N	T	I	T
CAT	GTC	GGA	GCC	GAG	TCC	AAT	ACA	ATT	ACC
CAT	GTC	GTT	GTC	GAG	TCC	AAT	ACA	ATT	ACC
H	V	V	V	E	S	N	T	I	T

A2 MSP-1 and its fragments

Table 36 | Fragment weights of MSP-1 before and after processing by PfSUB1. Molecular weights were calculated using ExPASy (Wilkins et al., 1999).

Fragment	MW [kDa]
MSP-1F	187.6
MSP-$1F_{83}$	80.5
MSP-$1F_{30}$	23.7
MSP-$1F_{38}$	40.2
MSP-$1F_{42}$	43.2
MSP-1_{42}*	44.9
MSP-1_{42}**	46.7
MSP-1_{42}***	47.6
MSP-1D	195.7
MSP-$1D_{83}$	82.5
MSP-$1D_{30}$	21.6
MSP-$1D_{38}$	46.3
MSP-$1D_{42}$	45.3

***cleaved at site 4

** cleaved at site 3 (Cooper and Bujard, 1992)

*cleaved at site 2

Table 37 | List of protein fragments identified by LC-MS in MSP-1Fmut38/42_1_KK and PfSUB1-digested MSP-$1F_{42}$ fragment after dimethyl labelling according to (Boersema et al., 2009).
The ratio of medium/light reflects the specific enrichment of protein fragments in MSP-1Fmut38/42_1_KK (medium) over MSP-1_{42*} (light). All fragments above a ratio of 10 are predominantly found in MSP-1Fmut38/42_1_KK, while fragments with a ratio below 1 are found in MSP-1_{42*}.

aa positions	sequence	medium/light	light	medium
1-12	sEEDYDDLGQVk	0.153	1.315E6	2.013E5
15-28	eAVTPSVIDNILSk	119.358	3.337E6	3.982E8
29-46	IENEYEVLYLkPLAGVYR			
29-46	iENEYEVLYLkPLAGVYR	101.483	4.719E6	4.789E8
29-46	IENEYEVLYLkPLAGVYR			
79-89	nVLESDLIPYk	87.700	3.924E6	3.442E8
113-121	fLSSYNYIk	104.519	3.004E6	3.139E8
166-178	yLPFLNNIETLYk	77.926	3.312E6	2.581E8
166-178	YLPFLnNIETLYk			
166-178	YLPFLNnIETLYk			
195-201	vLNYTYEkSn			
228-249	nNNFVGIADLSTDYNHNNLLTk			
228-249	nNNFVGIADLSTDYNHNNLLTk	0.075	2.692E6	2.013E5
228-249	nNNFVGIADLSTDYNHNNLLTk	0.216	9.338E5	2.013E5
228-249	nNNFVGIADLSTDYnHNnLLTk	0.168	1.196E6	2.013E5
250-262	fLSTGmVFENLAk	62.102	5.202E6	3.231E8
250-262	FLSTGmVFEnLAk			
288-297	qcPQNSGcFR	3.100	2.291E6	7.101E6
288-297	qcPqNSGcFR	0.300	6.233E6	1.868E6
288-297	qcPQNSGcFR	0.300	6.233E6	1.868E6
351-373	ITcEcTkPDSYPLFDGIFcSSSN			
	HVLqNFSVFFNk			
	HVLQnFSVFFNk			
	kPASTHVGAESNTITTSQ			
	LFEnILSLGk			
	nLNnSLk			
	nLnNSLk			
	NSLNDESkR			
	TVLSNLLDGNLQGMLnISQH			
	TVLSNLLDGNLQGMLnISQH			
	TVLSNLLDGNLQGMLNISqH			
	TVLSNLLDGNLQGMLNISqH			

Table 38 | List of protein fragments identified by LC/MS in MSP-1Fmut38/42_2_KK and PfSUB1-digested MSP-1_{42**} after dimethyl labelling according to Boersema et al. (2009).
The ratio of Medium/Light reflects the specific enrichment of protein fragments in MSP-1Fmut38/42_2_KK (medium) over MSP-1_{42**} (light). All fragments above a ratio of 10 are predominantly found in MSP-1Fmut38/42_2_KK while fragments with a ratio below 1 are found in MSP-1_{42**}. In-gel labelling identified the N-terminus of the MSP-1_{42**} fragment at the Cooper and Bujard cleavage site NDDEVDDVIVPK.

aa positions	sequence	medium/light	light	medium
1	mNDDTSHSTNLNNSLk		4.615E4	1.435E7
2	nDDTSHSTNLNNSLk	116.389	1.532E4	1.783E6
2	mNDDTSHSTNLNNSLkLFENILSLGk	23.618	1.532E4	3.619E5
27	nkNIYQELIGQk	300.000	1.532E4	4.665E7
29	nIYQELIGQk	226.453	1.236E6	2.799E8
39	sSENFYEk	300.000	1.030E6	5.421E8
47	iLkDSDTFYNESFTNFVk	300.000	1.532E4	3.352E8
50	dSDTFYNESFTNFVk	300.000	1.532E4	7.266E6
65	skADDINSLNDESk	300.000	2.218E5	8.544E7
67	aDDINSLNDESk	300.000	1.532E4	2.123E7
67	aDDINSLNDESkR	300.000	1.532E4	5.018E7
81	kLEEDINk	28.801	1.532E4	4.413E5
82	lEEDInkLk	94.782	1.532E4	1.452E6
82	lEEDINk		1.003E5	3.116E7
91	kTLQLSFDLYNk	263.620	1.532E4	4.039E6
92	tLQLSFDLYNkYk	300.000	1.532E4	1.769E8
92	tLQLSFDLYNk	133.135	1.971E6	2.624E8
132	eQLESkLNSLNNPk	177.537	1.532E4	2.720E6
136	lSYLSSGLHHLIAELk	140.016	1.532E4	2.145E6
138	lNSLNNPk	300.000	1.532E4	5.930E6
146	hVLQNFSVFFNk	300.000	1.532E4	1.410E8
146	hVLQNFSVFFNkk	300.000	1.532E4	1.114E7
159	kEAEIAETENTLENTk	288.464	1.532E4	4.420E6
160	eAEIAETENTLENTk	181.763	1.532E4	2.785E6
182	gLVkYYnGESSPLk	300.000	1.532E4	4.996E6
186	yYNGESSPLk	300.000	4.332E5	2.608E8
196	tLSEESIQTEDNYASLENFk	300.000	1.532E4	1.362E8
196	tLSEESIQTEDNYASLENFkVLSk	300.000	1.532E4	1.174E7
224	lkDNLNLEk	300.000	1.532E4	4.616E7
226	dNLNLEk		3.765E4	1.000E7
255	nkNYTGNSPSENNTDVNNALESYk	174.476	1.532E4	2.673E6
257	nYTGNSPSENNTDVNNALESYkk	300.000	1.532E4	6.588E7

aa positions	sequence	medium/light	light	medium
257	nYTGNSPSENNTDVNNALESYk	283.365	1.532E4	4.342E6
269	kFLPEGTDVATVVSESGSDTLEQSQPk	172.624	1.532E4	2.645E6
270	fLPEGTDVATVVSESGSDTLEQSQPk	300.000	1.532E4	1.212E8
270	fLPEGTDVATVVSESGSDTLEqSQPk	71.044	1.532E4	1.089E6
353	tkEAVTPSVIDNILSk	0.896	1.024E8	9.176E7
355	eAVTPSVIDNILSk	0.355	6.285E8	2.234E8
369	iENEYEVLYLkPLAGVYR	0.414	7.348E8	3.041E8
405	eNFkNVLESDLIPYk	4.356	6.271E5	2.731E6
409	nVLESDLIPYkDLTSSNYVVk	0.618	5.392E7	3.331E7
409	nVLESDLIPYk	0.227	3.369E8	7.661E7
420	dLTSSNYVVkDPYk	0.243	2.978E7	7.237E6
451	dkFLSSYNYIk	0.407	3.470E7	1.412E7
453	fLSSYNYIkDSIDTDINFANDVLGYYk	272.046	1.532E4	4.168E6
453	fLSSYNYIk	0.215	2.009E8	4.323E7
476	sDLDSIk	0.003	7.752E7	1.532E4
305	kPASTHVGAESNTITTSQNVDDEVDDVIIVPk	300.000	1.532E4	2.213E7
16	IFENILSLGk	300.000	1.465E6	7.064E8
159	eAEIAETENTLENTkILLk	123.729	1.532E4	1.896E6
390	qLENNVmTFNVNVkDILNSR	89.138	1.230E6	1.096E8
534	vLNYTYEkSNVEVk	65.347	1.532E4	1.001E6
494	yINDkQGENEk	47.378	1.532E4	7.259E5
126	ITLLkEQLESk	38.041	1.532E4	5.829E5
626	kQcPQNSGcFR	35.843	3.848E5	1.379E7
561	IADFkk	31.565	2.176E6	6.868E7
602	tVLSNLLDGNLQGmLNISQHQcVkk	25.330	1.836E6	4.651E7
499	qGENEkYLPFLNNIETLYk	17.569	3.737E6	6.565E7
713	tIQDkLADFk	10.480	1.766E6	1.851E7
602	tVLSNLLDGNLQGmLNISQHQcVk	2.209	1.380E8	3.049E8
689	kITcEcTkPDSYPLFDGIFcSSSN	1.664	1.934E7	3.219E7
518	tVNDkIDLFVIHLEAk	1.393	5.658E8	7.879E8
567	nNNFVGIADLSTDYNHNNLLTk	1.087	2.865E8	3.115E8
337	fkESEEDYDDLGQVk	1.007	8.658E7	8.721E7
646	cLLNYkQEGDk	0.966	1.535E6	1.483E6
713	fLSTGmVFENLAk	0.817	4.336E8	3.541E8
690	iTcEcTkPDSYPLFDGIFcSSSN	0.809	2.300E8	1.861E8
534	vLNYTYEk	0.690	1.460E9	1.007E9
389	kQLENNVmTFNVNVk	0.657	2.292E7	1.507E7
486	sDLDSIkk	0.519	9.759E7	5.061E7

aa positions	sequence	medium/light	light	medium
389	qLENNVmTFNVNVk	0.516	2.372E8	1.225E8
550	eLNYLk	0.389	3.399E8	1.323E8
484	ykSDLDSIk	0.371	2.218E7	8.225E6
339	eSEEDYDDLGQVk	0.328	5.282E7	1.733E7
505	yLPFLNNIETLYk	0.240	3.699E7	8.884E6
646	cLLNYk	0.217	1.445E8	3.130E7
461	dSIDTDINFANDVLGYYk	0.163	2.675E8	4.356E7
523	iDLFVIHLEAk	0.137	9.283E7	1.270E7
657	cVENPNPTcNENnGGcDADAk	0.118	1.269E7	1.498E6
566	kNNNFVGIADLSTDYnHNNLLTk	0.039	3.928E5	1.532E4
548	ikELNYLk	0.016	9.436E5	1.532E4
627	qcPQNSGcFR	0.003	4.761E7	1.532E4
652	qEGDkcVENPNPTcnENNGGcDADAk	0.003	7.431E6	1.532E4
215	vLSkLEGk		3.281E5	7.787E7

A3 Loading control for protein extracts from transgenic parasites

Protein extracts from all transgenic parasites as well as *Pf*3D7 and *Pf*FCB1 were prepared from synchronous cultures of late schizonts and equal protein amounts were analysed by Western blotting. As a loading control AMA1 was used in this study. AMA1 is a very abundant micronemal protein that undergoes proteolytic processing similar to MSP-1. Thus AMA-1 can be detected as an 83 kDa protein and a 66 kDa protein band. As shown in Figure 23, AMA1 is present in all transgenic parasite lines in equal amounts. As extracts from *Pf*3D7 and *Pf*FCB1 were loaded in much smaller amounts, AMA1 is barely detectable.

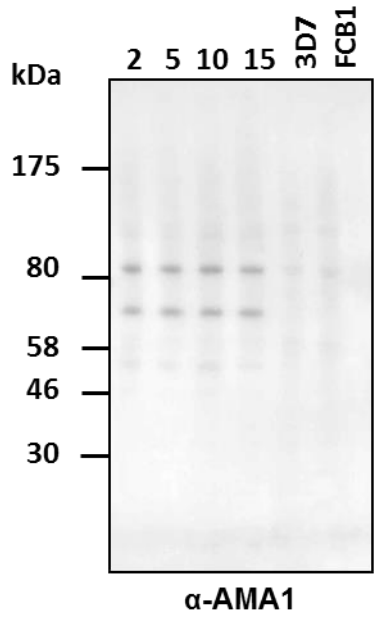

Figure 23 | Western Blot analysis of transgenic parasites via anti-AMA1 antibody.
Protein extracts from control parasites *Pf*3D7 and *Pf*FCB1 as well as transgenic parasites *Pf*3D7 pHBIMFwt grown in the presence of 2-15µg/ml blasticidin were subjected to SDS PAGE and subsequent Western blotting. As loading control Western Blot was probed with anti-AMA1 antibody (rabbit, 1:5,000).

A4 Absolute quantification of copy number and transcription

Table 39 | Primers and DNA template used for standard curves.

gene (primer)	template DNA
msp-1d	3D7, pARL5'KO
msp-1f (f83)	pHBIMFmutaII
actin (p100)	3D7
bsd (bsd3)	pHBIMFmutaII
renilla luciferase (renilla)	pHBIRH
fructose-1,6-bisphosphatase (P61)	3D7
clag 3.1	3D7
clag 3.2	3D7

Table 40 | Calculation of copy numbers and DNA concentrations used for standard curves.
The copy number can be calculated using the following formula:
number of copies = amount[ng]*6.022*10^{23}/(length[bp]*10^{9}*650) (1bp=650 Da)

DNA	pHBIMF mutaII	pARL5'KO -GFP	3D7	pHBIRH
length [bp]	**10368**	**5912**	**2.33E+07**	**6318**
copy number			**amount [ng]**	
10	1.12E-07	6.38E-08	2.51E-04	6.89E-08
100	1.12E-06	6.38E-07	2.51E-03	6.89E-07
1000	1.12E-05	6.38E-06	2.51E-02	6.89E-06
10,000	1.12E-04	6.38E-05	2.51E-01	6.89E-05
100,000	1.12E-03	6.38E-04	2.51E+00	6.89E-04
1,000,000	1.12E-02	6.38E-03	2.51E+01	6.89E-03
10,000,000	1.12E-01	6.38E-02	2.51E+02	6.89E-02
100,000,000	1.12E+00	6.38E-01	2.51E+03	6.89E-01
original concentration [ng/µl]	177	149.5	40	3334
dilution factor	100	100	1	1000
V for 10 wells with 10^{7} copies [µl]	6.32	4.27	62.9	0.207

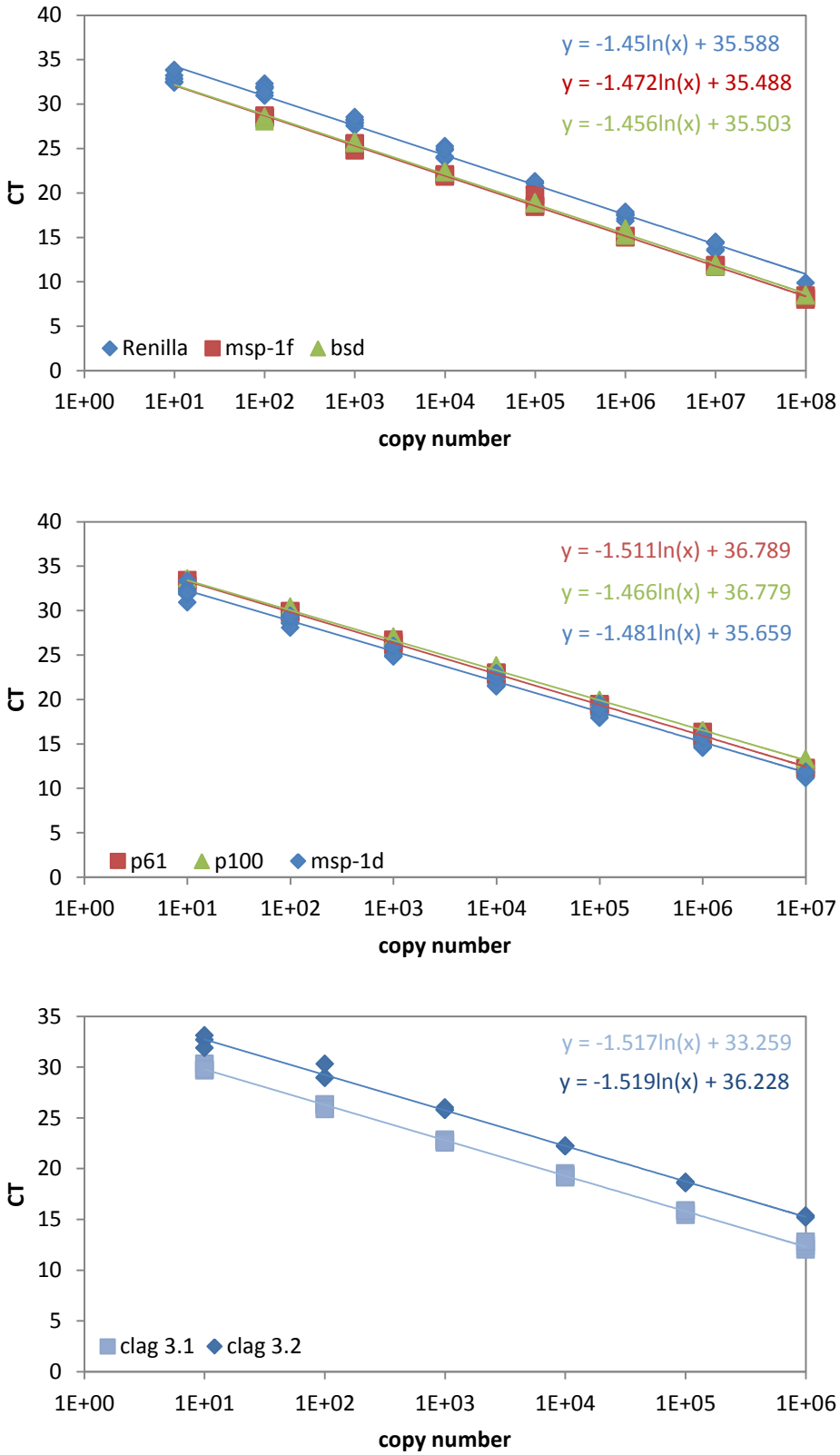

Figure 24 | qRT-PCR standard curves for absolute quantification of DNA copy numbers and transcript numbers.
The standard curve for *msp-1d* was generated by combining the data obtained from standard curves with gDNA and pARL 5'KO.

A5 Knockout of *msp-1d*

Table 41 | Cycling of transfectants to acquire knockout of *PfMSP-1D* via double crossover recombination

Summary of different attempts to gain knockout parasites using the pHTK/pCC vector system. Parasites were either directly (cycle no. 0) subjected to negative selection (5-FC or ganciclovir) or cultured in absence of the positive selection drug (WR) for at least three weeks prior to reapplication of the first drug and subsequent negative selection drug (cycle no. 1). In order to reinforce loss of episomes, parasites were cycled for a second round off the positive selection drug (cycle no. 2). The reappearance periods after drug application varied from0 days to 6-22 days) to no recovery at all (-). Prior to and after negative selection, genomic DNA was collected from the parasites and analysed by PCR.

Parental strain	construct	Positive selection (+conc.)	Cycle no.	Reappearance after 1st drug exposure (days)	Duration OFF 1st drug (days)	Negative selection drug (+conc.)	Reappearance after 2nd drug exposure (days)
3D7 pHBIMF wt 10 µg/ml	pCC1-PfMSP1D-KO	WR (5nM) 26022013	0 1 1 1 2	11 2 2 2 2	21 - - - -	- 5-FC (500nM) 5-FC (1µM) 5-FC (6µM) 5-FC (12µM)	- Parasites did not die from 5-FC
3D7 pHBIMF wt 15 µg/ml	pCC1-PfMSP1D-KO	WR (5nM)	0 0 0	2 2 2	- - 10	5-FC (1µM) 5-FC (6µM) -	Parasites did not die from 5-FC
3D7	pHTK-PfMSP1D-KO	WR (5nM)	0 1 2	8 2 10	21 0 22	- ganciclovir (20µM) ganciclovir (20µM)	- Parasites did not die from ganciclovir
3D7	pCC1-PfMSP1D-KO	WR (5nM)	0 1 2	8 2 10	21 0 22	- 5-FC (1µM) 5-FC (1µM)	- Parasites did not die from 5-FC
3D7 pHBIMF wt 15 µg/ml	pHTK-PfMSP1D-KO	WR (5nM)	0 1 2	6 2 10	21 0 22	- ganciclovir (20µM) ganciclovir (20µM)	- 3 Parasites did not die from ganciclovir
3D7 pHBIMF wt 15 µg/ml	pCC1-PfMSP1D-KO	WR (5nM)	0 1 2	6 2 10	21 0 22	- 5-FC (1µM) 5-FC (1µM)	- Parasites did not die from 5-FC

A6 Surface coverage with MSP-1

Table 42 | Calculation of MSP-1 molecule number on the merozoite surface.

Object	formula	result
MSP-1	sphere	
molecular weight		200 kDa
volume	1.212*Mw †	242.4 nm
diameter	(V/PI*6)^(1/3)	7.7 nm
cross-section area	PI*d^2/4	47.0 nm^2
merozoite	egg-like ellipsoid	
dimensions	equatorial radius	0.5 µm
	short polar radius	0.6 µm
	long polar radius	0.9 µm
surface area	see equation below	4.2 µm
amount of MSP-1 on surface	surface/MSP-1 cross-section	90181 molecules

†(Erickson, 2009)

Scheme of an egg-like ellipsoid used for calculation merozoite surface area:

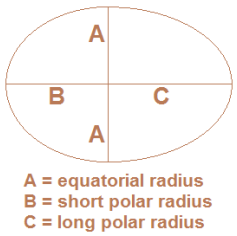

Equation for calculating the merozoite surface area (Had2Know.com, 2014):

$$A = 2\pi a^2 + \pi a\left(\frac{b^2}{\sqrt{b^2 - a^2}}\cos^{-1}\left(\frac{a}{b}\right) + \frac{c^2}{\sqrt{c^2 - a^2}}\cos^{-1}\left(\frac{a}{c}\right)\right)$$

A7 Vector maps

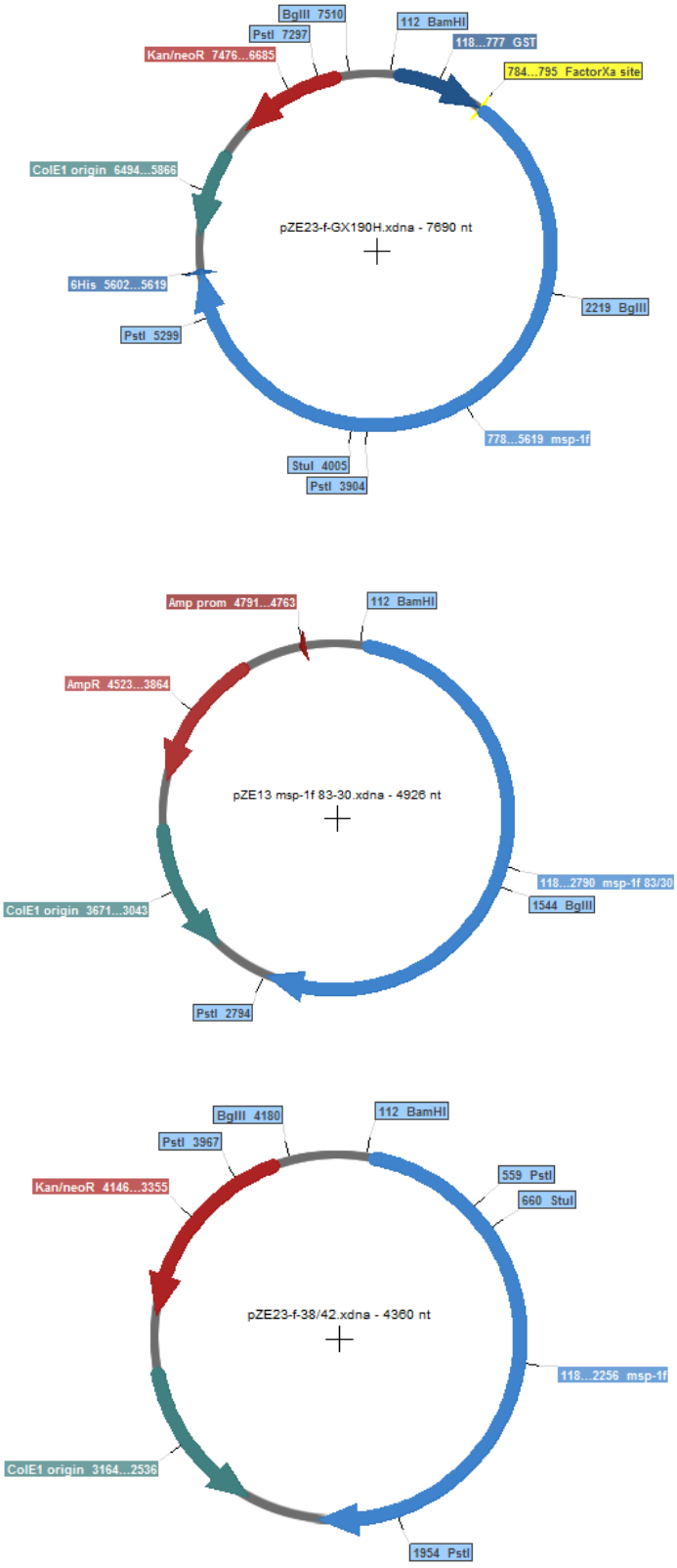

Figure 25 | *E. coli* expression vectors.

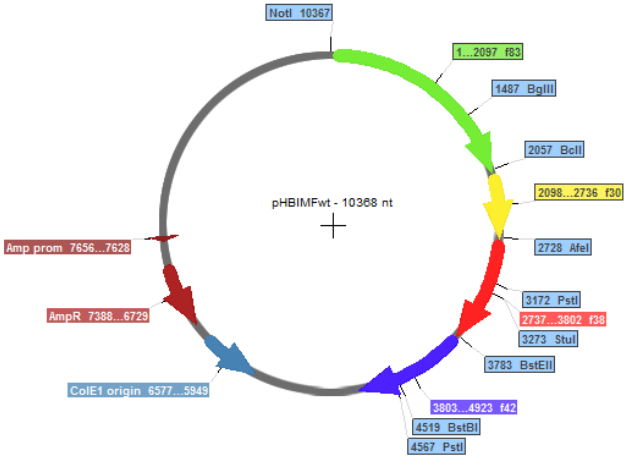

Figure 26 | *P. falciparum* expression vector.

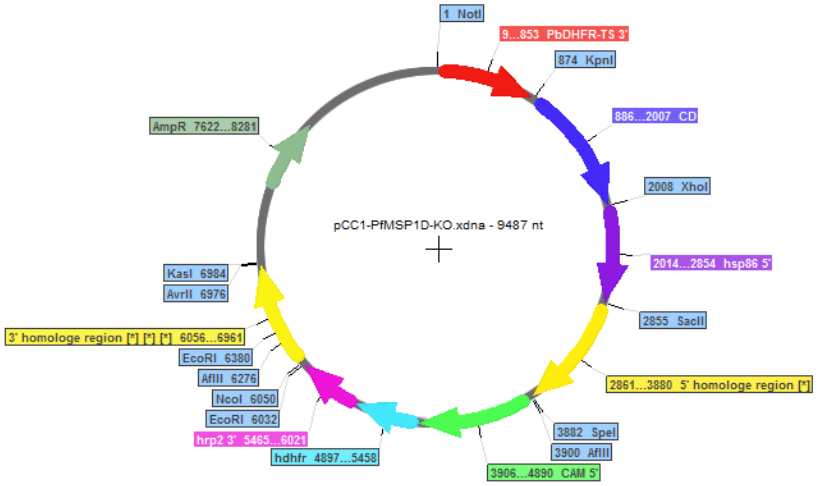

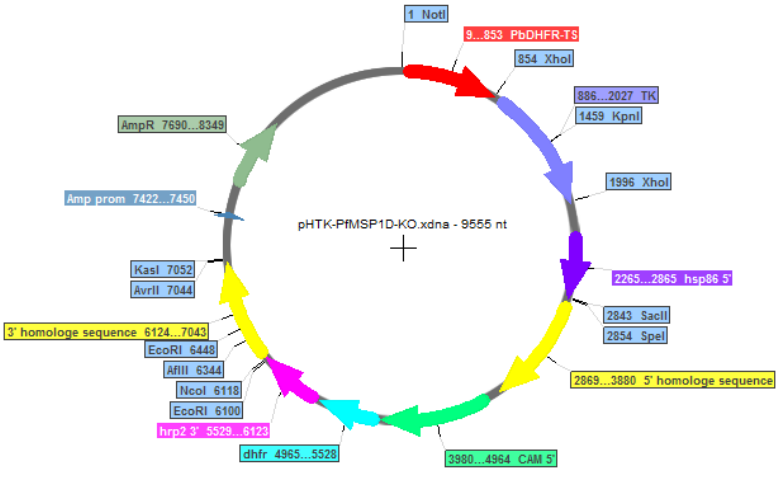

Figure 27 | *P. falciparum* knockout vectors.

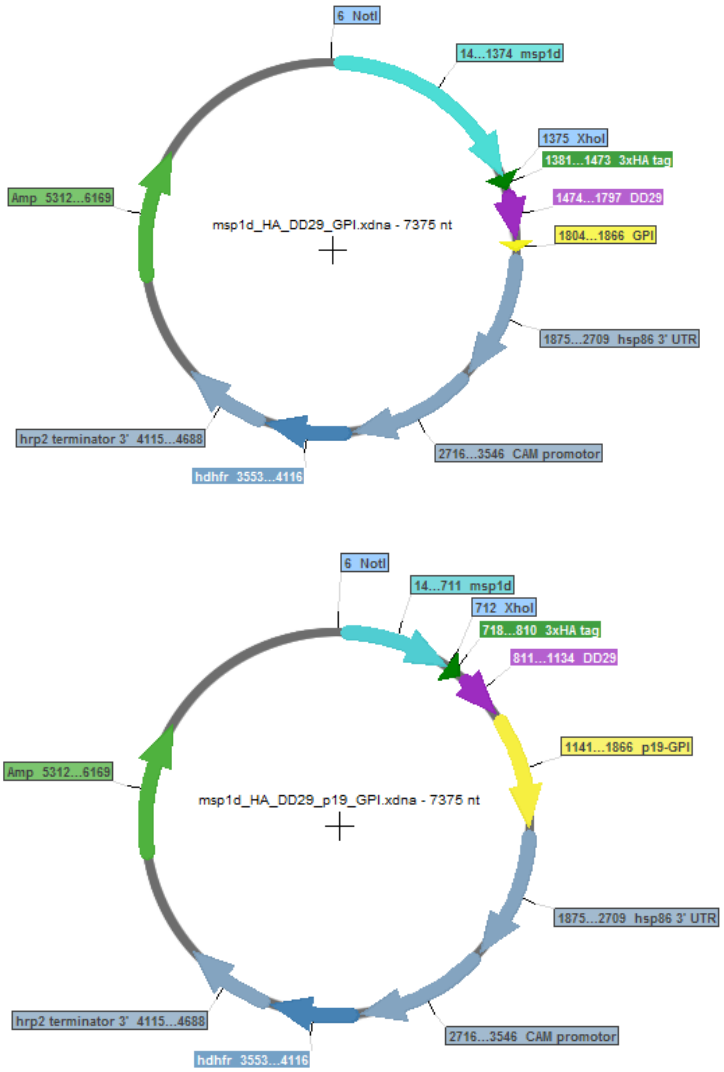

Figure 28 | *P. falciparum* knockdown vectors.